2010

Hindbrain Serotonin Neurons Activate 5-HT1A Receptors in the Nucleus Tractus Solitarius (NTS) to Modulate Sympathetic and Ventilatory Recovery Following Hypotensive Hemorrhage

Ling-Hsuan Kung
Loyola University Chicago

LOYOLA UNIVERSITY CHICAGO

HINDBRAIN SEROTONIN NEURONS ACTIVATE 5-HT_{1A} RECEPTORS IN THE NUCLEUS TRACTUS SOLITARIUS (NTS) TO MODULATE SYMPATHETIC AND VENTILATORY RECOVERY FOLLOWING HYPOTENSIVE HEMORRHAGE

A DISSERTATION SUBMITTED TO

THE FACULTY OF THE GRADUATE SCHOOL

IN CANDIDACY FOR THE DEGREE OF

DOCTOR OF PHILOSOPHY

PROGRAM IN NEUROSCIENCE

BY

LING-HSUAN KUNG (THERESA)

CHICAGO, ILLNOIS

DECEMBER 2010

ACKNOWLEDGEMENT

I give my deep thanks to my advisor, Dr. Karie E Scrogin, for her wonderful mentorship throughout my Ph.D. education. I am extremely grateful for her guidance all along my dissertation studies. She encouraged me to make great progress not only in scientific research, but also in every aspect of my life.

I sincerely thank my committee members, Dr. Edward Neafsey, Dr. Lydia DonCarlos, Dr. Mary Druse-Manteuffel and Dr. Caron Dean-Bernhoft, for their constant support and thoughtful input.

I also give thanks to the people in my laboratory. It was a great pleasure to work with Dr. Ruslan Tiniakov, Dr. Nichole Dudek, Dr. Marcus Henze, Jaimee Glasgow, Jaime Vantrease and Anna Ruszaj. They provided me with a wonderful scientific environment and inspired my research. I am also grateful to the faculty, staff, and students of the neuroscience program and the Graduate School of Loyola University Chicago for their constant support.

Finally, I would like to thank my family and friends especially my uncle, Kao-Der Kung, my mother, Feng-I Kung, my husband, Fei Han, and my son, Nathan Han, for their unconditional love and encouragement.

Dedicated to My Mother, Uncle and My Husband

TABLE OF CONTENTS

LIST OF TABLES

LIST OF FIGURES

LIST OF ABBREVIATIONS

5,7-DHT	5,7-dihydroxytryptamine
5-HT-ir	serotonin immunoreactive/ immunoreactivity
8-OH-DPAT	8-hydroxy-2-*n*-di[propylamino] tetralin
ACTH	adrenocorticotropic hormone
ANG II	angiotensin II
ANP	atrial natriuretic peptide
AOI	area of interest
AP	area postrema
BE	base excess
BRS	baroreflex sensitivity
BP	blood pressure
BP SDNN	standard deviation of blood pressure between normal beats
CPG	central pattern generator
CO_2	carbon dioxide
ComNTS	commissural subnucleus of the nucleus tractus solitarius
CRH	corticotrophin-releasing hormone
CVLM	caudal ventrolateral medulla
DAB	3, 3'–diaminobenzadine tetrahydrochloride
DBP	diastolic blood pressure

dEMG	diaphragmatic EMG
DLH	D,L-homocysteic acid
DMX	dorsal motor nucleus
DR	dorsal raphe
EPI	epinephrine
FIO_2	fraction of inspired oxygen
GABA	γ-Aminobutyric acid
HR	heart rate
HF	high frequency
IBI	interbeat interval
IML	intermediolateral cell column
iv.	intravenous
KCN	potassium cyanide
LF	low frequency
MAP	mean arterial pressure
MAP_{50}	mean arterial pressure at mid-range
MBP	mean blood pressure
MR	median raphe
MVI	minute ventilation index
NA	nucleus ambiguus
NE	norepinephrine
NPY	neuropeptide Y

NTS	nucleus tractus solitarius
$PaCO_2$	arterial blood CO_2 pressure
PaO_2	arterial blood O_2 pressure
Pb	barometric pressure
p-CPA	p-chlorophenylalanine
PNMT	phenylethanolamine-N-methyltransferase
PPY	parapyramidal region
Pwv	water vapor pressure
RAAS	renin-angiotensin-aldosterone system
RM	raphe magnus
RO	raphe obscurus
RP	raphe pallidus
RR	respiratory rate
RSNA	renal sympathetic nerve activity
RTN	retrotrapezoid nucleus
RVLM	rostroventrolateral medulla
SBP	systolic blood pressure
SDNN	standard deviation of blood pressure between normal beats
SUB	subependymal region
TV	tidal volume
TPH	tryptophan hydroxylase
TPH-ir	tryptophan hydroxylase immunoreactive/ immunoreactivity

TH	tyrosine hydroxylase
TH-ir	tyrosine hydroxylase immunoreactive/ immunoreactivity
vlPAG	ventrolateral periaqueductal gray
VL-LPBN	ventrolateral aspect of the lateral parabrachial nucleus
Y	instantaneous gain

CHAPTER I

INTRODUCTION

Overview of Project

Significance

Trauma is the fifth overall leading cause of death in the United States according to the most recent report from the National Center of Vital Statistics released in April 2009 (Heron et al., 2009). The "Leading Causes of Death Report" for the year 2006 indicates that trauma is also the leading cause of death of young people between the ages of 1 to 44 years (WISQARS, 2009). For example, motor vehicle death was responsible for 55.7% of all unintentional injury deaths of individuals between the ages of 20 to 30 in the year 2006. Most such deaths result either from the initial blood loss or from secondary reperfusion injury following resuscitation (Cocchi et al., 2007; Sauaia et al., 1995; Takasu et al., 2005).

The cardiovascular response to blood loss is complex and multiphasic (Figure 1). At the beginning of blood loss, arterial pressure is maintained primarily through a primary compensatory response characterized by increased sympathetic-mediated vascular resistance (Chalmers et al., 1967; Cornish et al.,

1988; Evans et al., 1993b; Schadt and Ludbrook, 1991). After significant blood loss (in human ~20% to 30%; ~14% in rats), this primary compensatory response is reversed, resulting in a sympatholytic response which is characterized as hypotension, bradycardia and sympathoinhibition (Hasser and Schadt, 1992; Ludbrook and Ventura, 1994, , 1996). The cumulative effect is similar to fainting, with a hemodynamic character reminiscent of vasovagal syncope. Such a response is often referred to as the syncopal response (Sander-Jensen et al., 1987). If blood loss continues, circulatory shock develops as a consequence of inadequate perfusion of the peripheral tissue (Haljamae, 1984). During development of circulatory shock, a secondary compensatory response develops as sympathetic activity is slowly re-established to regain normal perfusion pressure. This is the stage at which patients are normally seen in the emergency room or at the scene of a trauma. Failure to resuscitate patients adequately during this phase can lead to decompensation, which is characterized by a cascade of metabolic events that leads to loss of proper vasoconstrictor function, circulatory collapse and eventually death (Chaudry et al., 1990).

Currently, the standard treatment for hypovolemic shock includes rapid and massive volume resuscitation. This has remained the gold standard of treatment over the last 65 years despite the significant pathology associated with its use. Catecholamines, including epinephrine (EPI), norepinephrine (NE) and dopamine, as well as other vasoconstrictors such as vasopressin are also used to raise perfusion pressure in patients in circulatory shock (Balogh et al., 2003a;

Balogh et al., 2003b; Garrison et al., 2004; Peitzman et al., 1995). There are major disadvantages to the use of either volume resuscitation or vasoconstrictor treatments. Either treatment alone may not be sufficient to increase perfusion pressure, and both can exacerbate reperfusion injury (Greenway and Lawson, 1966; Martel et al., 2002; Meier-Hellmann et al., 1997). Both treatments also require technical training and close monitoring to apply safely to patients. Therefore, adequate treatment is often delayed, resulting in prolonged ischemia, which can, in turn, worsen reperfusion injury. Alternative therapies that can be applied quickly with minimal training and do not exacerbate reperfusion injury are needed to improve patient outcomes after severe hemorrhage.

We recently found that intravenous (iv.) injection of the 5-HT_{1A}-receptor agonist, 8-hydroxy-2-*n*-di[propylamino] tetralin (8-OH-DPAT), increases systemic perfusion pressure in rats subjected to hypovolemic shock by stimulation of sympathetic-mediated increases in venous tone. The drug does not increase total peripheral resistance, indicating that the pressor effect (i.e., increased blood pressure) of the drug is mediated almost exclusively by increased cardiac output (Tiniakov and Scrogin, 2006). 8-OH-DPAT also improves acid-base balance in animals subjected to hemorrhagic shock prior to volume restitution (Tiniakov et al., 2007). These data suggest that serotonergic agonists may be a promising alternative to the vasoconstrictors currently used in resuscitation from hypovolemic shock. However, the location of the 5-HT_{1A} receptor population that mediates this response is not known. Activation of 5-HT_{1A} receptors by the

administration of 8-OH-DPAT in the vicinity of the dorsal hindbrain surface rapidly re-establishes normal perfusion pressure following blood loss in unanaesthetized rats (Scrogin, 2003). These findings suggest the possibility that 5-HT_{1A} receptor agonists may act in the dorsomedial hindbrain where arterial baroreceptor and peripheral chemoreceptor afferents terminate to mediate their beneficial effects during hypovolemia. Prior studies indicate that caudal raphe serotonin neurons are activated by hemorrhage. In preliminary studies we found that lesion of these neurons also attenuated the secondary compensatory phase following hemorrhage. It is not known whether endogenous serotonin released during hemorrhage acts on 5-HT_{1A} receptors to produce a compensatory hemodynamic response to blood loss. Studies performed in this dissertation investigated the cardiovascular effects of endogenous serotonin and 5-HT_{1A}-receptor agonists in hemorrhaged rats in an effort to better determine the mechanisms of the potential benefits of serotonin manipulation in hypovolemic shock.

Main Hypothesis

In this project, several studies were performed to test the following OVERALL HYPOTHESIS: *Hindbrain serotonergic neurons activate 5-HT_{1A} receptors in the nucleus tractus solitarius (NTS) to facilitate sympathetic and respiratory recovery following hypotensive hemorrhage*. The following specific aims were pursued to test this hypothesis.

Specific Aim 1: To test the hypothesis that caudal medullary serotonergic neurons facilitate sympathetic recovery after acute hypotensive hemorrhage in conscious rats.

Rationale: We and others have shown that serotonergic neurons of the ventrolateral periaqueductal gray (vlPAG), raphe obscurus (RO), raphe magnus (RM) and its lateral extension around the parapyramidal region (PPY) are activated selectively by hypotensive hemorrhage (Dean and Woyach, 2004; Ruszaj et al., 2006). To determine if serotonin neurons in these regions influence hemodynamic responses to hemorrhage, we selectively lesioned serotonin nuclei activated by hypotensive hemorrhage and showed that the lesions attenuated the secondary compensatory recovery of blood pressure (BP) and heart rate (HR) following hypotensive hemorrhage (Ruszaj et al., 2006). However, it was not known if these serotonergic nuclei contributed to the secondary compensatory recovery of HR and arterial pressure by augmenting sympathetic recovery. Moreover, it was not known whether the effects of serotonin on these hemodynamic parameters were accompanied by altered blood gases. To test this, we examined sympathetic recovery during the secondary compensatory phase as well as changes in blood gases after hypotensive hemorrhages in rats subjected to selective lesion of caudal medullary serotonergic neurons in the RO, RM, and PPY. Given recent evidence that caudal medullary serotonergic neurons are important in central

chemoreception and that central chemoreceptors may be activated by hemorrhage (Richerson, 2004), we also determined whether the lesion interfered with sympathetic and ventilatory responses to central chemoreflex stimulation.

Experiment:

A) It was determined if selective destruction of caudal medullary serotonergic neurons activated by hypotensive hemorrhage attenuates sympathetic and ventilatory recovery after hypotensive hemorrhage.

B) It was determined if selective destruction of caudal medullary serotonergic neurons attenuates sympathetic and ventilatory responses to central chemoreflex stimulation.

Specific Aim 2: To test the hypothesis that 5-HT_{1A}-receptor agonists act on receptors expressed on non-serotonergic cells to accelerate sympathetic recovery after hypotensive hemorrhage in conscious rats.

Rationale: We have found that 5-HT_{1A}-receptor agonists accelerate sympathetic recovery during the secondary compensatory phase of hypotensive hemorrhage (Scrogin, 2003). 5-HT_{1A} receptors are found on non-serotonergic cells where they act as post-synaptic targets of serotonin neurons. They are also found on serotonergic neurons where they act as autoreceptors to hyperpolarize

the serotonin cell membrane. Previous studies indicate that depletion of serotonin prevents the sympatholytic and depressor (decreased blood pressure) responses to hemorrhage (Elam et al., 1985). Therefore, it is possible that 5-HT_{1A}-receptor agonists reverse the sympatholytic response to hemorrhage by inhibiting endogenous serotonin release. To test this, we examined the effect of systemic 5-HT_{1A}-receptor agonist administration in rats subjected to serotonin lesion in order to eliminate 5-HT_{1A} autoreceptors. It was reasoned that if 5-HT_{1A}-receptor agonists stimulate sympathetic recovery by inhibiting serotonin neurons, then lesion of serotonin neurons should prevent or attenuate the sympatholytic phase of hemorrhage and a 5-HT_{1A}-receptor agonist should not further augment sympathetic recovery during the secondary compensatory phase.

Experiments:

A) It was determined if global destruction of serotonergic neurons attenuates the sympatholytic response following recovery of hypotensive hemorrhage.

B) It was determined if global destruction of serotonin neurons attenuates the sympathoexcitatory response to 5-HT_{1A} receptor agonist in rats subjected to hypotensive hemorrhage.

Specific Aim 3: To test the hypothesis that serotonergic neurons activate 5-HT_{1A} receptors in the NTS to stimulate recovery of sympathetic activity after hypotensive hemorrhage in conscious rats.

Rationale: Prior work has shown that 5-HT_{1A}-receptor agonists injected into the cisterna magna produce a very rapid and robust increase in sympathetic activity in animals subjected to hypotensive hemorrhage. These data suggest that activation of 5-HT_{1A} receptors near the dorsal surface of the caudal hindbrain contributes to the sympathoexcitatory effect of 8-OH-DPAT in hypovolemic rats (Scrogin, 2003). We have also shown that the full sympathoexcitatory effect of 8-OH-DPAT is dependent upon intact sinoaortic afferents that carry arterial baroreceptor and peripheral chemoreceptor afferents and project to the NTS (Osei-Owusu and Scrogin, 2004). The caudal NTS is the projection site of arterial baroreceptor and peripheral chemosensory afferents, and both the arterial baroreflex and chemoreflex are engaged by hypotensive hemorrhage. A high density of serotonergic nerve terminals has been observed within the commissural subnucleus of the NTS (comNTS) where cardiovascular and chemosensory afferents terminate (Manaker and Verderame, 1990). Recent work has shown that glutamatergic input to the ventrolateral aspect of the lateral parabrachial nucleus (VL-LPBN) is necessary for sympathetic-mediated recovery of BP following hypotensive hemorrhage (Blair and Mickelsen, 2006). The NTS provides the majority of glutamatergic input to the VL-LPBN, suggesting that the

NTS may also play a critical role in recovery of perfusion pressure following hypotensive hemorrhage.

It is not known if serotonin nerve terminals within the NTS contribute to sympathetic recovery during the secondary compensatory phase of acute hypotensive hemorrhage in conscious rats. Studies in this aim addressed this question by determining if selective lesion of serotonergic projections to NTS regions that receive arterial baroreceptor and peripheral chemoreceptor afferent innervation influenced sympathetic recovery following hemorrhage. Because both the baroreflex and the peripheral chemoreflex are engaged during hypotensive hemorrhage, additional studies were conducted to determine if the same lesion of serotonin nerve terminals in the NTS influenced arterial baroreflex or peripheral chemoreflex sensitivity.

Experiments:

A.1) It was determined if destruction of serotonin nerve terminals in the NTS attenuated sympathetic recovery after hypotensive hemorrhage.

A.2) It was determined if destruction of serotonin nerve terminals in the NTS inhibited peripheral chemoreceptor sensitivity.

A.3) It was determined if destruction of serotonin nerve terminals in the NTS inhibited arterial baroreflex sensitivity (BRS).

B) Attempts were made to determine whether pharmacological blockade of 5-HT_{1A} receptors in the NTS blocked sympathetic recovery after hypotensive hemorrhage.

C) Attempts were made to determine whether pharmacological blockade of 5-HT_{1A} receptors in the NTS prevented the sympathoexcitatory effect of systemically administered 5-HT_{1A}-receptor agonist after hypotensive hemorrhage.

CHAPER II

REVIEW OF RELATED LITERATURE

A. Current treatment for hemorrhagic shock

Hypovolemic shock result from inadequate perfusion of peripheral organs such that the physiologic needs of the tissue is not met. The current treatment for hemorrhagic shock includes infusion of a large volume of fluid such as lactated Ringer's solution or isotonic saline as early and as rapidly as possible (Stern, 2001). The aim of this treatment strategy is to rapidly restore intravascular volume to maintain vital organ perfusion. However, studies suggest that aggressive fluid resuscitation alone may be harmful (Leppaniemi et al., 1996). For instance, rapid fluid resuscitation can lead to sudden tissue re-oxygenation after ischemia, which can generate inflammatory responses that contribute to organ damage and failure.

Due to the numerous sequelæ associated with aggressive volume resuscitate, an alternative treatment that combines lower-volume resuscitation with whole blood or blood substitutes, and/ or colloid solutions to raise intravascular volume and perfusion pressure to subnormal levels has recently gained favor (Hess and Thomas, 2003; Leppaniemi et al., 1996; Repine et al., 2006; Stern, 2001). Unfortunately, blood products are not always readily

available outside the hospital or on the battlefield. Hemoglobin-based oxygen carriers have been shown to enhance tissue perfusion and reduce oxygen debt, and improve resuscitation outcomes in animals. Although experimental studies indicate that administration of the bovine hemoglobin-based oxygen carrier, HBOC-21, in hemorrhagic shock is effective and improves outcome, the potential toxic effects of the treatment such as vasoconstriction and acute renal failure have reduced enthusiasm for its clinical use (Alayash, 1999; Arnaud et al., 2005; Fitzpatrick et al., 2005; Moore et al., 2004).

Therapeutic hypothermia has also been used as an adjuvant treatment to low-volume infusion of whole blood. This method can protect the organism against the ischemic effects of hemorrhage. Investigators found that lactate levels were significantly lower in hypothermia-treated animals subjected to hypovolemic shock suggesting an improved balance of tissue oxygen supply and demand (Prueckner et al., 2001; Takasu et al., 2000). Wladis et al. reported that hypothermia slowed HR and induced a further reduction of cardiac output and cardiac work in hemorrhaged animals (Wladis et al., 2001). Nevertheless, hypothermic treatment did not change mortality during hemorrhage.

Another controversial treatment is the use of vasoconstrictor agents to help raise perfusion pressure. Dopamine, dobutamine, NE and vasopressin have all been used to treat hypovolemic shock (Hamed et al., 1983; Kellum and Pinsky, 2002; Neiberger and Passmore, 1979). Complications of these

vasoconstrictor agonists are related to excessive arterial vasoconstriction and exacerbation of organ ischemia (Kellum and Pinsky, 2002).

No one resuscitation treatment strategy has been found to improve outcomes beyond the protocols established decades ago. Therefore, new novel methodologies are needed. Such methods should be easy to implement and increase perfusion pressure without further exacerbating end organ ischemia.

B. Autonomic response to hemorrhage

Progressive blood loss in conscious animals produces a complex multiphasic response of the autonomic nervous system (Figure 1). At the beginning of blood loss, arterial pressure is well maintained primarily through unloading of baroreceptors, which reduces cardiac vagal drive and increases sympathetic drive (Chalmers et al., 1967; Cornish et al., 1988; Evans et al., 1992; Schadt and Ludbrook, 1991). This phase is called the primary compensatory phase. After a significant amount of blood loss (~20% to 30% in human; ~15% in unanaesthetized rats) these compensatory responses suddenly decline, resulting in decreased sympathetic outflow and a rapid fall in BP (Hasser and Schadt, 1992; Ludbrook and Ventura, 1996). This response, similar in hemodynamic character to vasovagal syncope, is also called the sympatholytic phase (Sander-Jensen et al., 1987). This is a transient phase that is thought to protect cerebral perfusion by promoting a posture in which the head lies at the same level as the

heart, thereby reducing the perfusion pressure needed to deliver blood to the brain (Van Lieshout et al., 2003). If blood loss does not cease after vasovagal syncope, circulatory shock develops as a consequence of reduced peripheral organ perfusion (Haljamae, 1984). The beginning of circulatory shock is characterized by a slow rise of sympathetic activity and HR. Therefore, this phase is called the secondary compensatory phase. If blood loss continues to progress, vascular permeability eventually increases, vascular reactivity declines, and sympathetic activation is no longer able to maintain pressure. This fourth phase is known as decompensation and is extremely difficult to treat.

The mechanisms that contribute to the different phases of circulatory shock are not known but remain an active area of investigation. As a consequence important reflex mechanisms have been found to contribute to the various phases of shock, but the triggers that activate and terminate these responses are not well understood.

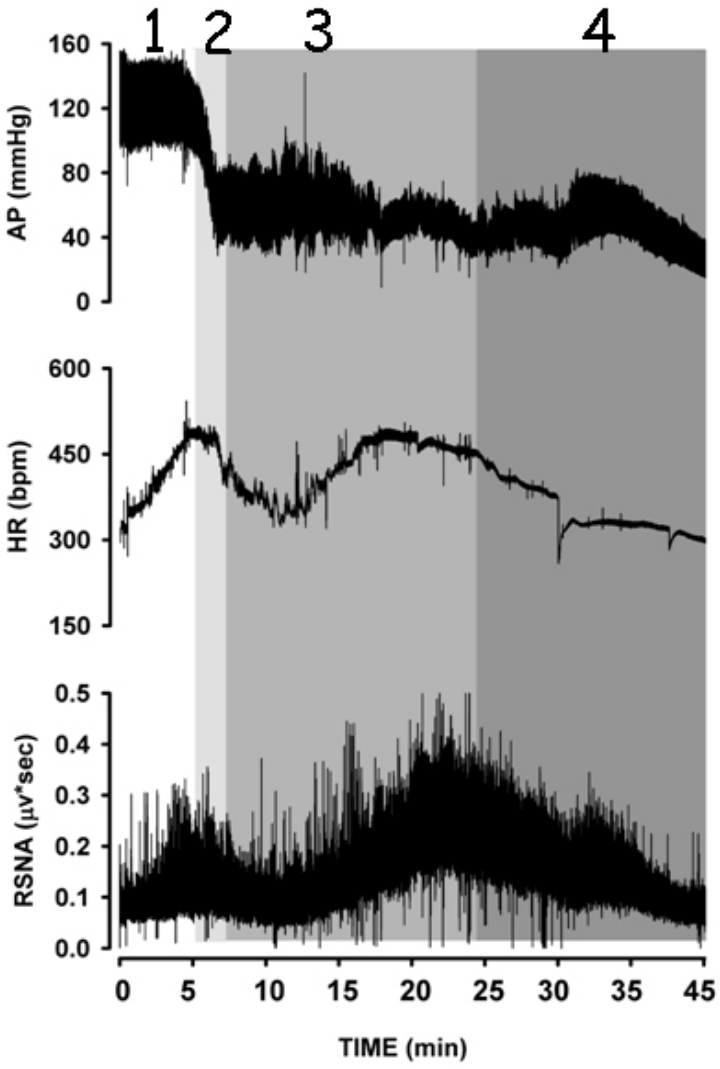

Figure 1: The hemodynamic responses to hemorrhage initiated at time 0 in a conscious rat. 1. Primary compensatory phase, 2. Sympatholytic phase, 3. Secondary compensatory phase, and 4. Decompensation. Arterial pressure (AP), heart rate (HR), renal sympathetic nerve activity (RSNA)

C. Overview of baro-, chemo- and cardiopulmonary reflexes during hypotensive hemorrhage

Baro- and chemo reflexes are a dual system of sensors and neural reflexes that control mean arterial pressure (MAP). The primary sensors of the arterial baroreceptors are stretch receptors located on the vascular walls of the carotid sinuses and aortic arch. During the primary compensatory phase, blood volume reductions reduce tension on the vascular wall. As a consequence baroreceptors are unloaded stretch is reduced, leading to a series of feedback responses that result in increased sympathetic mediated vascular constriction, increased HR and consequently increased BP.

Peripheral chemoreceptor activation may also play a role in maintaining BP. Baroreceptor unloading results in increased sympathetic drive which can then reduce blood flow to peripheral chemoreceptors in the carotid bodies of the carotid sinus. Peripheral chemoreceptors sense a decrease in tissue PaO_2, which in turn elicits a chemoreflex response that includes increased sympathetic activity and ventilation.

Another set of baroreceptors, the so called low-pressure cardiopulmonary baroreceptors, are located in the pulmonary artery and the atria. Stretch of these receptors depends largely on the blood volume returned to the heart or the venous return. These mechanoreceptors detect the “fullness” of the circulation and further control the circulating volume of blood. During hypotensive hemorrhage there is less distention of the atria. In an effort to correct a low or

reduced effective circulating volume these receptors also stimulate the renin-angiotensin-aldosterone system (RAAS) to promote sodium retention through communication with the adrenal medulla. Increased sympathetic activity to the kidney reduces renal blood flow and stimulates renin release leading to reduced sodium excretion.

Other hormones involved in BP control during hemorrhage include vasopressin and atrial natriuretic peptide (ANP). Neural input from the medullary brainstem stimulates the paraventricular nucleus of the hypothalamus to signal the posterior pituitary to increase secretion of vasopressin, which in turn circulates to the kidney to inhibit water exertion, and to the vasculature to promote vasoconstriction. Atrial natriuretic peptide is synthesized and stored by atrial myocytes and is normally released in response to stretch of low-pressure volume sensors. Atrial natriuretic peptide circulates to the kidney to promote natriuresis (Na^+ excretion). Thus, the reduced effective circulating volume that develops during hemorrhage inhibits the release of ANP and reduces Na^+ excretion. By executing all these hormonal or neuronal pathways, cardiopulmonary receptors help to control circulating blood volume and thus cardiac output.

Central pathways in control of baroreflex

Arterial BP is maintained within relatively strict limits by an important homeostatic reflex mechanism, the arterial baroreflex or arterial baroreceptor reflex. When arterial BP is elevated, the reflex is activated and inhibits sympathetic output and thus causes BP to decrease. Likewise, when arterial BP decreases, baroreceptors are unloaded, leading to increased sympathetic activity and a BP rise.

Anatomy of the arterial baroreflex

Stretch receptors located in the aortic arch and carotid sinus monitor the degree of vessel wall stretching, which is directly related to the pressure in the carotid arteries. Both aortic arch and carotid sinus regions serve as pressure/stretch sensors and are thus called the baroreceptors (Heymans, 1968). Action potentials are generated by stretch, and the greater the stretch, the greater the frequency of action potentials generated.

As shown in Figure 2, stretch in the carotid sinus and aortic arch generates action potentials that travel through the glossopharyngeal and vagus nerves, respectively, to the caudal NTS in the medulla. Second order NTS neurons that receive afferent input from the baroreceptors send excitatory glutamatergic fibers to the caudal ventrolateral medulla (CVLM). The CVLM

sends inhibitory γ-Aminobutyric acid (GABA) projections to the rostroventrolateral medulla (RVLM). An anatomical study using combined anterogradely- and retrogradely transported tracers demonstrated that terminals originating from cell bodies within the CVLM were contiguous with bulbospinal neurons in the RVLM (Li et al., 1992). The bulbospinal neurons in the RVLM, in turn, send excitatory glutamatergic projections to the sympathetic preganglionic neurons in the intermedio-lateral cell column of thoracic and upper lumbar segments of the spinal cord which activate the sympathetic neurons that control vasoconstriction and HR. Therefore, when baroreceptors are activated by increased BP, the NTS activates the CVLM, which in turn inhibits the RVLM, thus reducing the sympathetic outflow to the heart, arterioles and veins. The NTS also sends excitatory projections to the nucleus ambiguus (NA), which houses the parasympathetic motor neurons that project to the heart. Thus, parasympathetic outflow to the heart is increased during increased baroreceptor stretch. Similarly, a decrease in baroreceptor firing rate results a decrease in parasympathetic drive to the heart.

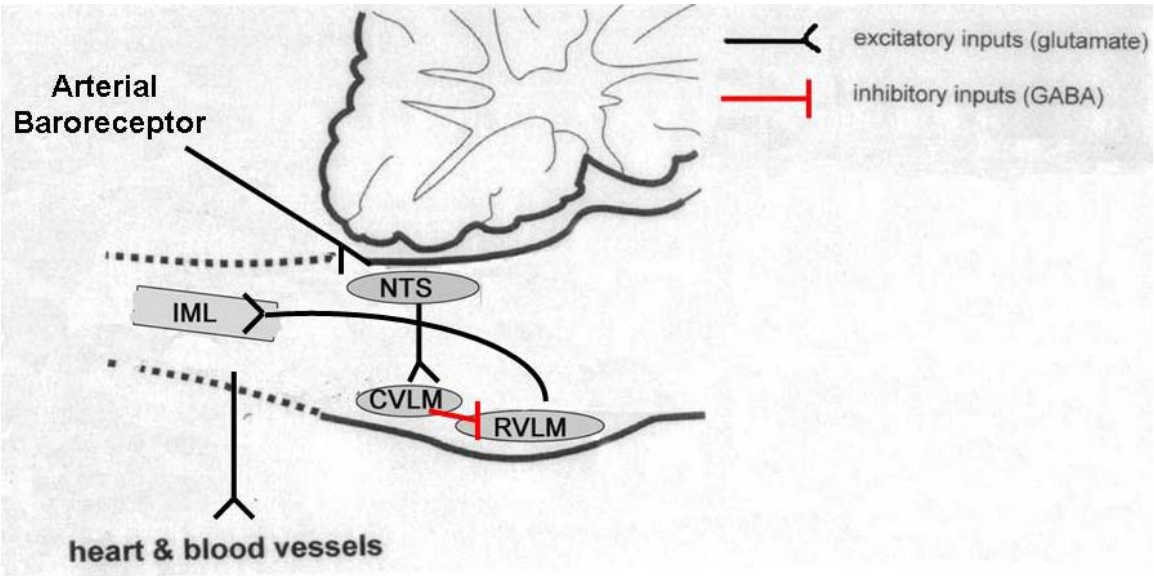

Figure 2: Central pathway of the arterial baroreflex. Arterial baroreceptors innervate the NTS. Excitatory projections from the NTA project to the CVLM. Inhibitory GABAergic neurons in the CVLM inturn inhibit the RVLM to modulate sympathetic drive to the heart and blood vessels. NTS: nucleus tractus solitarius; CVLM : caudal ventral lateral medulla ; RVLM : rostroventrolateral medulla ; IML: intermediolateral cell collumn

Peripheral chemoreflex

Peripheral chemoreceptors primarily respond to reduced arterial blood oxygen and increased blood pH and act accordingly to increase or decrease ventilation. In addition, peripheral chemoreceptors also detect arterial carbon dioxide (CO_2) levels ($PaCO_2$) However, CO_2 is primarily detected by central chemoreceptors, since these receptors appear to be more sensitive to changes in arterial blood CO_2 levels then are peripheral chemoreceptors.

The peripheral chemoreceptors are located in a collection of cells known as the aortic and carotid bodies, which are located on the arch of the aorta and the sinus of the carotid artery, respectively. The carotid body is composed of several cell types, one of which, the glomus cell, can activate nerve fibers that join the glossopharyngeal nerve. The aortic glomus cells activate nerves that travel through the vagus nerve. The carotid bodies have an extraordinarily high blood flow and small arteriovenous differences in PO_2, PCO_2 and pH indicate that the blood flow is in high excess of metabolic demand. Glomus cells are the chemosensitive cells that detect changes in arterial PO_2 and PCO_2 or pH. They stimulate afferent nerves to increase their firing rate in response to low arterial PO_2 or pH and high arterial PCO_2. Signals from carotid and aortic bodies are sent to the comNTS via the glossopharyngeal and vagus nerves. The comNTS then integrates signals from both sets of afferent nerves and appropriately modulates respiration patterns and sympathetic activity.

Moreira and colleagues (2006) have proposed a model that explains how peripheral chemoreceptor activation increases ventilation and sympathetic activity. Specifically, a subset of cells of the comNTS sends excitatory projections directly to the RVLM to produce an overall increase in pre-sympathetic neuronal activity during hypoxia (Figure 3). More recently Takakura and colleagues used an anterograde tracer and immunohistochemistry methods to demonstrate that hypoxia activates comNTS glutamatergic neurons that innervate the retrotrapezoid nucleus (RTN), a nucleus containing pH sensitive neurons that may integrate peripheral and central chemoreception (Takakura et al., 2006). In addition, the comNTS is thought to innervate and activate a ventilatory central pattern generator (CPG) in the pre-Bötzinger complex located at the caudal pole of the CVLM (Figure 4). When excited by the comNTS, the CPG increases excitatory input to respiratory motor neurons in the spinal cord, and at the same time produces oscillations of inhibitory input to the pre-sympathetic neurons of the RVLM that then become entrained to respiration. As a consequence, hypoxia increases ventilation and sympathetic activity; and the increase in sympathetic activity develops a pronounced ventilatory rhythm.

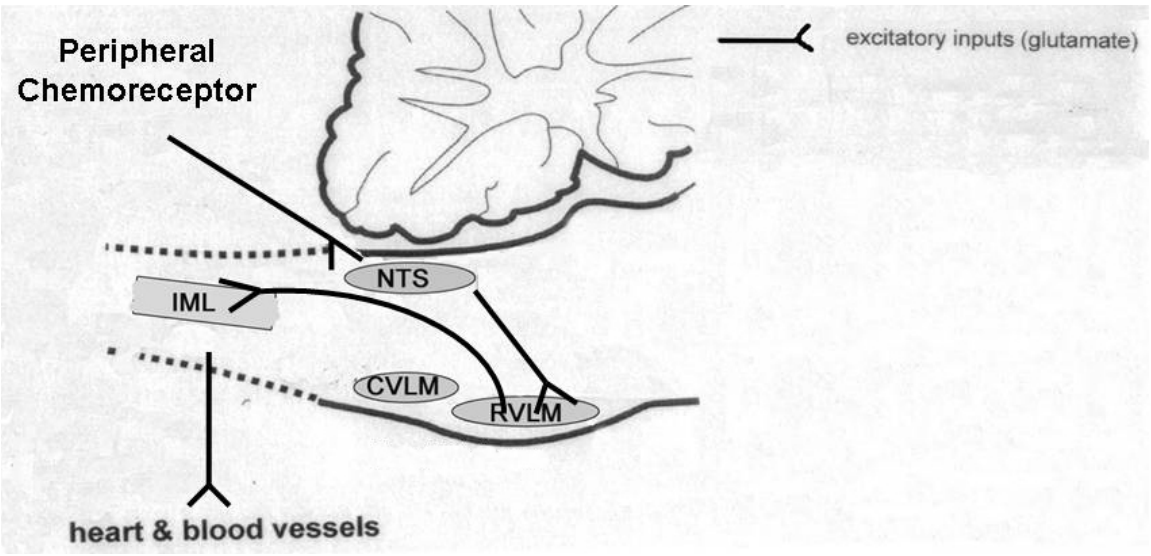

Figure 3: Illustration of central pathway of peripheral chemoreflex activation of sympathetic drive during hypoxia or decreased pH. Peripheral chemoreceptors convey their information to neurons in the NTS which directly activate the RVLM to mediate sympathetic out flow to the heart and blood vessels. NTS: nucleus tractus solitarius; CVLM : caudalventrolateral medulla ; RVLM : rostralventrolateral medulla ; IML: intermediolateral cell collumn

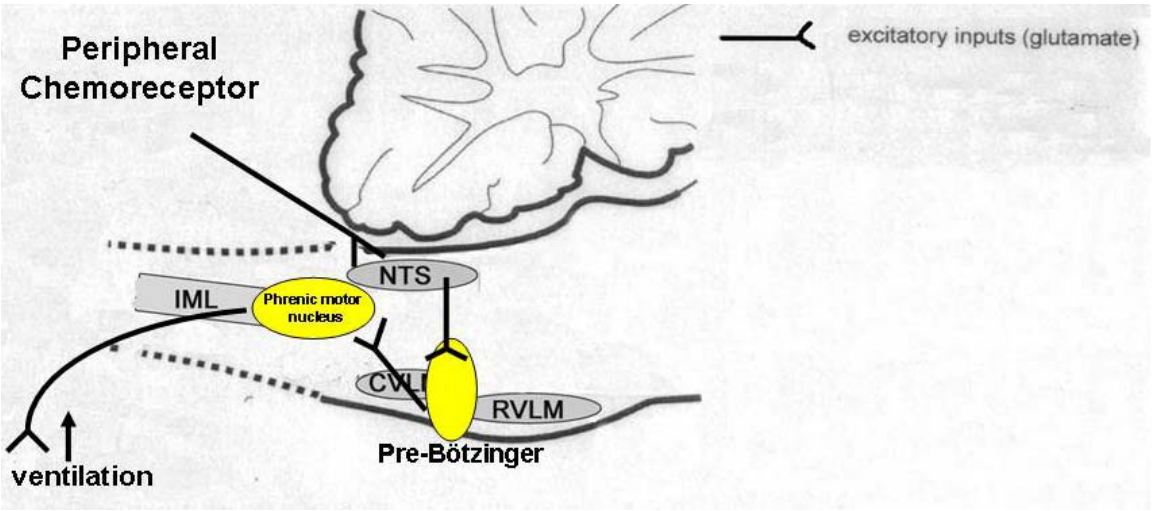

Figure 4: Illustration of central pathway of peripheral chemoreflex activation of ventilation during hypoxia or decreased pH. Peripheral chemoreceptor afferents convey their information to neurons in the NTS which directly innervate and activate cells of the Pre-Bötzinger complex. The Pre-Bötzinger complex activates the phrenic motor nucleus that, in turn, contracts the diaphragm to increase ventilation. NTS: nucleus tractus solitarius; CVLM : caudalventrolateral medulla ; RVLM : rostralventrolateral medulla ; IML: intermediolateral cell collumn

Central chemoreflex

In contrast to peripheral chemoreceptors which primarily sense low PaO2, the central chemoreceptors mainly sense low pH in the brain, which generally reflects a high arterial PCO_2. Arterial CO_2 can readily diffuse across the blood brain barrier where it acidifies brain tissue and thereby stimulates the central chemoreceptors to modulate breathing and increase sympathetic activity.

The exact location of central chemoreceptors is not well understood. Over the years, researchers have identified several potential sites in the central nervous system. Evidence suggests that they are located on the ventral medullary surface. Applying acidic solutions to the RVLM or CVLM leads to a prompt increase in ventilation (Loeschcke et al., 1963). Moreover, focally cooling these areas to 20°C to reversibly inhibit neurons blunts the ventilatory response to respiratory acidosis (Loeschcke, 1982). These earlier studies led to the widespread acceptance that the ventral lateral medulla was the sole location of central respiratory chemoreceptors. More recently, studies have shown other possible locations of central chemoreceptors. These include the NTS, locus coeruleus, cells of the mid-line medullary raphe, the rostral aspect of the ventral respiratory group (the pre-Bötzinger complex) and the RTN (Ballantyne and Scheid, 2001; Gray et al., 2001; Nattie and Li, 2002a, 2002b; Putnam, 2001; Richerson, 2004). Data from Moreira and colleagues suggest that increased CO_2 may stimulate sympathetic drive by directly exciting pre-sympathetic neurons of

the RVLM that may be intrinsically sensitive to pH. Alternatively or in addition, RVLM neurons may receive excitatory input from neighboring RTN pH- sensitive cells. The CPG is also thought to be pH sensitive. Therefore, an increase in CO_2 may lead to increased sympathetic activity with a prominent ventilatory rhythm due to the simultaneous increase in activity of the pre-sympathetic RVLM cells and concurrent rhythmic inhibitory input from the respiratory CPG (Moreira et al., 2006).

In addition, serotonin neurons have been found to play a prominent role in chemoreception in awake animals. Serotonergic medullary raphe neurons are good candidates for central chemoreception because of their location. A subset of medullary raphe neurons are located very close to the basilar artery, the major artery perfusing the brainstem (Bradley et al., 2002). Many serotonergic neurons lie close to the vessel walls and may actually partially penetrate the walls and get close enough to the vessel lumen to detect $PaCO_2$ (Richerson, 2004). Using patch-clamp recordings from *in vitro* brain slices, it was shown that neurons within the medullary raphe nuclei are intrinsically sensitive to increased CO_2 (Richerson, 1995). Furthermore, primary neuronal cultures isolated from the medullary raphe could be differentiated based on their response to CO_2 (Wang et al., 1998). Those cells stimulated by CO_2 were found to be serotonergic, while those inhibited by CO_2 did not appear to contain serotonin (Wang et al., 2001). Evidence from *in vivo* experiments supports the hypothesis the medullary

serotonergic neurons are central chemoreceptors. For example, inhalation of CO_2 increases c-Fos expression in cells of the medullary raphe of cats (Larnicol et al., 1994). It was later confirmed that CO_2-activated neurons in the medulla of rats expressed serotonin and tryptophan hydroxylase (TPH) (Haxhiu et al., 2001; Johnson et al., 2003). Also adult rats subjected to a neonatal lesion of the medullary serotonergic neurons showed elevated PaCO2 under eucapnic conditions and a blunted ventilatory response to increased CO_2 (Mueller et al., 1984, , 1985). Also, 8-OH-DPAT microdialyzed into the medullary raphe of adult rats to selectively suppress serotonin neuron activity resulted in a substantial attenuation of the ventilatory response to hypercapnia. In addition, selective lesion of the medullary raphe serotonergic neurons using microinjections of the toxin saporin conjugated to antibodies against the serotonin transporter also caused depression of ventilatory responses to inhaled CO_2 (Messier et al., 2004; Nattie et al., 2004). Collectively, these data indicate that medullary serotonergic neurons are either central respiratory chemoreceptors or are involved in the processing of chemoreceptor input (Figure 5).

There is a high concentration of serotonin immunoreactive (5-HT-ir) nerve terminals within the main respiratory nuclei. These include the NA, the NTS, Bötzinger complex, pre-Bötzinger complex, phrenic motor nucleus, and the hypoglossal nucleus (Holtman, 1988; Jacobs and Azmitia, 1992; Voss et al., 1990; Zhan et al., 1989). The specific pathways by which serotonin augments

central chemoreflex function is are still not yet clear. However, the serotonin projections to the pre-Bötzinger complex suggest that activation of serotonin cells during acidosis may augment ventilation in some way (Figure 6).

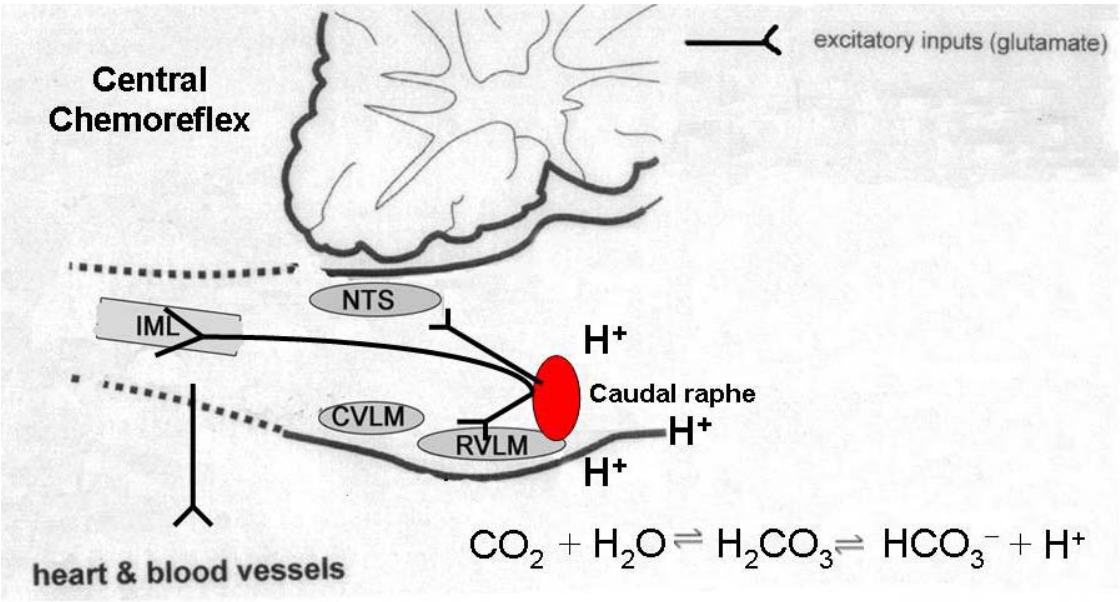

Figure 5: Illustration of central pathway of central chemoreflex to increase sympathetic drive during blood loss. Acid is generated in the peripheral tissue due to anaerobic metabolism during blood loss. Hydrogen ions are converted to CO_2 which readily cross the blood brain barrier. Caudal serotonin raphe neurons sense the change in pH and CO_2 and activate multiple nuclei including the nucleus tractus solitarius (NTS), rostroventrolateral medulla (RVLM) and intermediolateral cell column (IML) in the spinal cord to increase sympathetic activity. Caudal ventrolateral medulla (CVLM).

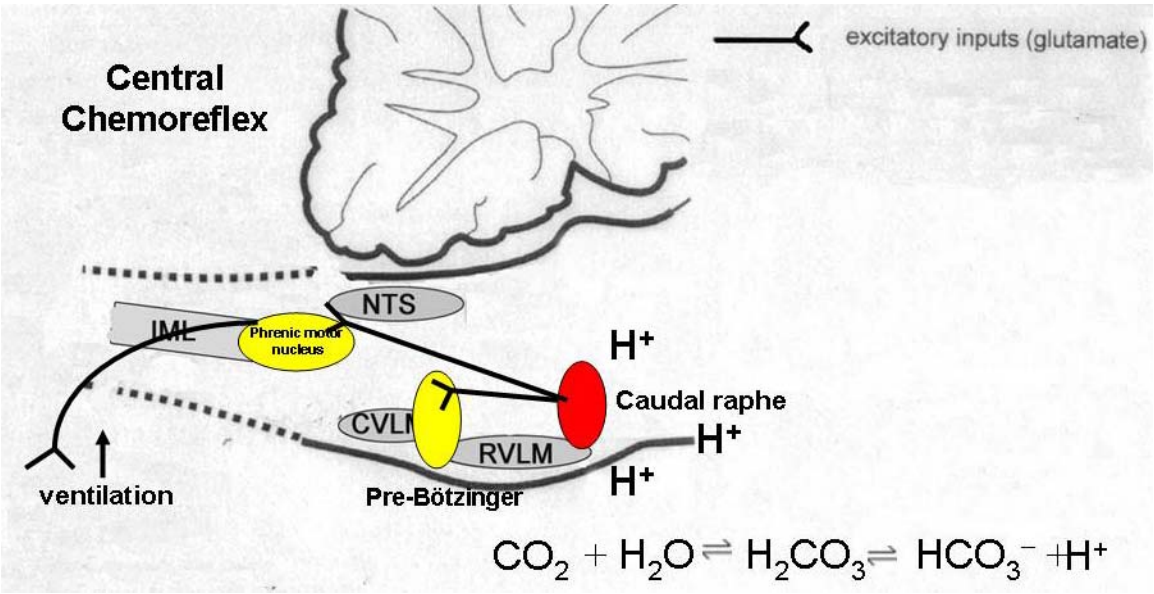

Figure 6: Illustration of central pathway of central chemoreflex in the ventilatory response to blood loss. Peripheral tissue generates acid due to anaerobic metabolism during blood loss. Protons were converted to CO_2 where readily passes the blood brain barrier. Caudal serotonin raphe neurons sense changes in pH and CO_2, and may activate multiple respiratory nuclei including the pre-Bötzinger and phrenic motor nucleus to increase ventilation.

Cardiopulmonary reflex

Cardiopulmonary receptors are low pressure baroreceptors found in the atria and pulmonary vessels that are involved with the regulation of blood volume. Stretch of the receptors sends signals to the ventro lateral subnucleus of the NTS via non-myelinated and myelinated vagal afferent fibers (Berger, 1979; Kalia and Welles, 1980). Activation of these receptors decreases sympathetic drive to the kidney and increases sympathetic drive to the sinus node to increase HR (Bishop et al., 1983; Fox et al., 1977). The primary purpose of the cardiopulmonary reflex is to regulate volume. It does so through changes in long-term fluid regulation and so may be less important in the acute response to hemorrhage.

D. Hormonal response to hemorrhage

A number of hormones are released during hemorrhage. They include catecholamines and vasoactive peptides such as ANGII (Mathai et al., 1997; Stocker et al., 2001), neuropeptide Y (NPY) (Qureshi et al., 1998), vasopressin (Laycock et al., 1979), and stress hormones including adrenocorticotropic hormone (ACTH), corticosterone (cortisol in human), and oxytocin (Kadekaro et al., 1990; Kasting and Wilkinson, 1987).

Catecholamines, including EPI and NE, are released by chromaffin cells of the adrenal medulla into the bloodstream. Norepinephrine and EPI act on $ß_1$-adrenergic receptors on cardiomyocytes to increase cardiac contractility. Both

EPI and NE also stimulate α-adrenergic receptors of vascular smooth muscle to produced arterial and venous vasoconstriction. Sympathetic increases that develop during the primary compensatory phase of hemorrhage lead to an increase in plasma EPI and NE, and the amount of hormone released is correlated to the amount of blood loss. Low volume hemorrhage leads to little or no change in hormone responses, while more severe blood loss leads to a near 2000 fold increase in EPI (Bereiter et al., 1984; Darlington et al., 1986; Dempsher and Gann, 1983). In conscious rats or anesthetized dogs and cats it is hypothesized that baroreceptors must be unloaded before hemorrhage can elicit an adrenocorticotropin hormone (ACTH) response (Darlington et al., 1986; Munzner et al., 1981). Adrenocorticotropin hormone is derived from pro-opiomelanocortin in the anterior pituitary gland. Anterior pituitary secretion of ACTH is dependent on stimulation of corticotrophin-releasing hormone (CRH) and vasopressin. Circulating ACTH, in turn, acts on melanocortin-2 receptors on the adrenal cortex to stimulate the production and release of glucocorticoid hormones (cortisol in human and corticosterone in rats). The melanocortin-2 receptor is coupled to a heterotrimeric G protein and stimulates adenyly cyclase. This resulting increase in cAMP activates PKA, which phosphorylates a variety of proteins. As a result important proteins are activated, such as the P-450 enzymes that are needed for cortisol synthesis. The hemodynamic effect of cortisol is an increase in BP and tissue perfusion during the secondary compensatory phase of hemorrhage, which is thought to result from increased

sensitivity to NE (Haggendal et al., 1976; Hellman et al., 1982). Adrenocorticotropin hormone also stimulates the synthesis of NE. In addition, cortisol circulates to the adrenal medulla where it regulates phenylethanolamine-N-methyltransferase (PNMT) in chromaffin cells. Phenylethanolamine-N-methyltransferase is the rate limiting enzyme in EPI production. The stress of hemorrhage that is sensed and propagated by the CRH-ACTH-cortisol axis sustains the EPI response as well.

Vasopressin has been reported to be secreted immediately during the primary compensatory phase of hemorrhage in rats (Kadekaro et al., 1990; Kasting, 1988). Plasma levels of vasopressin also increase during unloading of the baroreceptors at this phase of hemorrhage (Laycock et al., 1979; Quail et al., 1987). Vasopressin maintains BP following hemorrhage through activation of V_1 receptors located in arterial vascular smooth muscle where it causes vasoconstriction and increased peripheral resistance (Johnson et al., 1988). In addition, circulating vasopressin may influence autonomic regulation during hemorrhage through both V_1 and V_2 receptors in the brainstem. Peuler et al. reported that vasopressin contributes to the sympatholytic responses observed after hypotensive hemorrhage (Peuler et al., 1990). Several reports have also shown that vasopressin exerts cardio-stimulatory and vasodilatory actions via the V_2 receptor (Brooks and Hatton, 1991; Liard, 1988, , 1990). Fujisawa et al. reported that in conscious rats hemorrhage increased the plasma vasopressin concentration more than 50-fold (Fujisawa et al., 1994). Vasopressin, via V_1

receptors, contributes to BP recovery after hemorrhage both peripherally and centrally (Johnson et al., 1988). Others have noted that specific brain regions including the area postrema (AP) and NTS are potential sites of action of vasopressin. Specifically, the drug promotes exaggerated sympathoinhibition during vasopressin-mediated hypertension, an effect which is attenuated after AP lesion (Undesser et al., 1985). Fujisawa and others observed that inhibition of V_1 receptors attenuated BP recovery in hemorrhaged rabbits. Blockade of V_2 receptors did not affect the BP response but prolonged the sympatholytic response (Brizzee et al., 1991; Fujisawa et al., 1994).

An important hormone system, the RAAS, regulates BP through direct vasoconstriction and fluid balance during the secondary compensatory phase of hemorrhage. When blood volume is low, renin secreted from kidney converts angiotensinogen to angiotensin I, which is, in turn, converted to ANG II, by angiotensin converting enzyme. ANG II also acts on the adrenal cortex to cause release of aldosterone, which causes the proximal tubules of the kidneys to increase the reabsorption of sodium, which ultimately results in enhanced water re-absorption. During hypotensive hemorrhage, RAAS activity increases, resulting in elevated levels of ANG II and production of aldosterone. As a result BP is increased by vasoconstriction (Averill et al., 1983; DeMaria et al., 1989; Essadki and Atkinson, 1981). Angiotensin II type I receptor blockers given during hemorrhage exaggerate the depressor response to blood loss (Francis et al., 2004).

Neuropeptide Y is a potent nonadrenergic vasoconstrictor peptide, and virtually all adrenergic neurons and a subset of A1 noradrenergic cells express NPY (Everitt et al., 1984; Sawchenko et al., 1985). Neuropeptide Y is present in sympathetic nerves that innervate blood vessels, heart, brain, adrenal medulla, and the gut (Zukowska-grojec and Walestedt, 1993). This peptide helps to maintain BP during stress via direct vasoconstrictor actions on selected vascular beds, and works with other vasoactive agents synergistically (McDermott et al., 1993). Morris and colleagues reported that NE and EPI plasma concentrations doubled immediately after the start of hemorrhage and climbed even higher after 30 minutes. However, NPY was only doubled by 10 minutes after hemorrhage and remained elevated for 1hr afterwards (Morris et al., 1987). Though endogenous NPY has no role in maintaining BP under normal physiological conditions, it surely contributes to BP recovery following hemorrhage possibly via post-synaptic Y_1 receptors (Qureshi et al., 1998).

E. Overview of central serotonergic system

Anatomy

The serotonin system in the brain arises from specific nuclei mainly situated in the mid-line of the brainstem and midbrain. Nine cell groups (B1-B9) have been identified with a high density of serotonergic cell bodies (Dahlstrom and Fuxe, 1964). They include more rostral cell groups in the mid-brain known

as the dorsal (DR-B7) and median raphe (MR-B8). Extensions of these nuclei are found more caudally in the pons as well (B5 and B6 respectively). These serotonin cell groups project rostrally to many different regions in the forebrain including the hypothalamus, thalamus, hippocampus, striatum, and cortex (van de Kar and Lorens, 1979). Serotonin cell groups located in the vlPAG project to the central nucleus of the amygdaloid complex and thalamus (Chen et al., 1992; Li et al., 1990). Midbrain raphe nuclei that project throughout the forebrain are associated with arousal, anxiety, aggression and control of cerebral blood flow (Hendricks et al., 2003; Saper et al., 2001; Underwood et al., 1995).

Three prominent midline raphe nuclei are located more caudally and project within the medulla and down to the spinal cord. These include the RM, and a more ventral group raphe pallidus (RP), and a caudal mid-line group, the RO. The RM also contains bilateral cells that extend around the pyramidal tracts and comprise the so called PPY. Bago and colleagues also found that serotonergic neurons of the midline caudal raphe nuclei project to the RVLM, with a minor contribution also coming from the DR and vlPAG (Bago et al., 2002). They further found that after microinjection of the 5-HT_{1A}-receptor antagonist, WAY-100635, into the pressor region of RVLM the sympatholytic response to hemorrhage was delayed and attenuated while renal sympathetic nerve activity (RSNA) was increased and maintained above baseline. These findings led to the conclusion that serotonin acts on 5-HT_{1A} receptors expressed by pre-sympathetic RVLM neurons to promote the sympatholytic phase of hypotensive hemorrhage.

Interestingly, activation of the vlPAG elicits sympathoinhibition, which is mediated, in part, through neurons in the caudal mid-line medulla (Bago and Dean, 2001; Dean, 2005). We and others found that serotonin neurons in the RM, PPY and vlPAG are activated during the secondary compensatory phase of hemorrhage in conscious rats (Bago et al., 2002; Ruszaj et al., 2006). These findings led to speculation that vlPAG neurons activated by hemorrhage may stimulate midline serotonergic neurons to inhibit the RVLM during hemorrhage.

Another important group of serotonin neurons is found along the extent of the ventral surface on the subependymal layer of the region lateral to the bottom of the pyramidal tract, hereafter referred to as subependymal region (SUB). The SUB cell groups, especially its serotonergic component, project directly to the intermediolateral cell column (IML). These cells are also activated by hypotensive hemorrhage. Such neurons probably function as pre-sympathetic cells, although their sympathetic targets and function are not well defined (Jansen et al., 1995).

Together the caudal hindbrain cell groups have been implicated in gating pain, modulating ventilation, and cardio-vascular control, as well as regulating sympathetic drive in the control of BP and thermogenesis (Jacobs and Azmitia, 1992; Jacobs and Fornal, 1997; Lovick, 1997; Mason, 2001).

The NTS is one of the major projection sites of serotonin neurons. Such projections originate from the caudal raphe nuclei (RM, RO, RP and PPY), the DR (Schaffar et al., 1988; Steinbusch, 1981; Thor and Helke, 1987), and

peripherally from the nodose ganglia which house the cell bodies of vagal sensory afferent nerves (Gaudin-Chazal et al., 1982; Nosjean et al., 1990; Thor et al., 1988). The densest region of serotonin immunoreactive (5-HT-ir) terminals is located in portions of the commissural and dorsomedial band of the parvocellular subdivision of the NTS. The remainder of the commissural, lateral and medial subdivisions has a moderate density of serotonin nerve terminals. Only occasional fibers are observed in the ventrolateral subnucleus and the remainder of the parvocellular subdivisions of the NTS (Maley and Elde, 1982).

The rostral serotonin nuclei (B5-B9) give rise to almost all ascending fibers, whereas the caudal groups (B1-B4), give rise to the majority of descending fibers (Aitken and Tork, 1988; Bowker et al., 1981). Serotonin fibers and a high density of terminals are found throughout the gray matter of most spinal cord segments. The caudal raphe have also been shown to project to the sympathetic pre-ganglionic neurons of the IML cell column, where they are important in stimulating sympathetic drive to brown adipose tissue to promote thermogenesis (Loewy, 1981; Loewy and McKellar, 1981).

Co-transmitters

Although serotonin is the primary neurotransmitter produced in serotonergic neurons, several co-transmitters of serotonergic neurons have been identified. In 1984, Ottersen and Storm-Mathisen first reported that serotonin-containing neurons of the rat and mouse brainstems were immunopositive for glutamate (Ottersen and Storm-Mathisen, 1984). Later evidence from several reports showed that the same cell populations were also immunopositive for a glutamate biosynthetic enzyme (Kaneko and Hicks, 1990). A separate group also reported glutamate-like immunoreactivity in serotonin neurons of rat and monkey brains (Nicholas et al., 1992). In addition, evidence suggests that glutamate can be released as a co-transmitter together with serotonin *in vitro* (Johnson, 1994).

Thyrotropin-releasing hormone and substance P are two major co-transmitters that co-exist with serotonin in raphe neurons that project to the spinal cord and within the brainstem (Hokfelt et al., 1975; Lighton et al., 1984; Thor and Helke, 1989; Thor et al., 1988). Thyrotropin-releasing hormone and serotonin are co-depleted by the 5-HT neurotoxin 5,7-dihydroxytryptamine (5,7-DHT). Injection of TRH and serotonin evoke similar motoric and behavioral abnormalities, i.e. strong responses in both extensor and flexor muscles of the hind limbs, increased body temperature, and induction of the “wet dog shake” phenomenon in rats (Bedard et al., 1979; Bedard and Pycock, 1977; Hensel, 1973; Wei et al., 1975). Thor and Helke used double labeling techniques to

identify serotonin- and substance P-containing projections from raphe nuclei to the NTS (Thor and Helke, 1987). A subsequent study revealed that serotonin and substance P are colocalized in the NTS, the dorsal motor nucleus of the vagus (DMX), and AP, and a similar fiber density of both are found in the ventral horn of the cervical spinal cord and the hypoglossal nucleus. Considerably fewer serotonin and substance P double-labeled varicosities are found in the NTS compared to ventral horn and hypoglossal nucleus. In the NTS only 5% of the serotonin immunoreactive varicosities contain substance P, while less than 1% of the substance P-immunoreactive varicosities also contained serotonin immunoreactivity in the NTS (Thor et al., 1988). Varicosities that contain both serotonin and substance P are not likely from the nodose or petrosal ganglia. Instead they appear to derive from PPY, RO, RP and MR (Thor and Helke, 1987, , 1989; Thor et al., 1988).

Serotonin receptors

Currently, a total of four major families of 5-HT receptors with at least 14 subtypes are known (Hoyer et al., 1994). They include G protein-coupled receptors of the $5HT_1$, $5HT_2$, $5\text{-}HT_4$, $5\text{-}ht_5$, $5\text{-}ht_6$, and $5\text{-}HT_7$ receptor families and ligand-gated ion channels of the receptor $5HT_3$ receptor family. These receptors have distinct distributions and mediate a wide range of cellular responses.

The $5HT_1$ receptor family includes 5-HT_{1A}, 5-HT_{1B}, 5-HT_{1D}, 5-HT_{1E}, 5-HT_{1F} receptors. 5-HT_{1A} receptors are coupled to inhibitory G proteins and inhibit adenylyl cyclase. The $5HT_{1A}$ receptors are serotonin autoreceptors expressed on the cell body and dendrites of serotonin cells. $5HT_{1A}$ receptors are also located on non-serotonergic cells. Upon activation, $5HT_{1A}$ receptors hypopolarize cell membranes by opening K^+ channels or by decreasing calcium influx via voltage-gated calcium channels (Albert et al., 1996; Barnes and Sharp, 1999). The 5-HT_3 receptors are ligand-gated ion channels located primarily on peripheral neurons and depolarize membranes by opening of a non-selective cation channel. Many of the 14 identified serotonin receptor subtypes have been found in the NTS. A high density of 5-HT_{1A}, 5-HT_{1B} receptors, 5-HT_{2A}, 5-HT_{2C}, 5-HT_3, 5-ht_{5A} and 5-HT_7 receptors have been found in the NTS (Manaker and Verderame, 1990; Oliver et al., 2000; Pompeiano et al., 1994; Ramage and Villalon, 2008; Steward et al., 1993). Application of serotonin to the NTS evokes falls in BP and HR (Laguzzi et al., 1984) or elevations in BP (Merahi et al., 1992). The 5-HT_{1A} and 5-HT_2 receptors are thought to be involved in the hypotensive effect of serotonin in the NTS (Itoh and Bunag, 1991), while the hypertension seems to involve 5-HT_3 receptors (Merahi et al., 1992). It has been suggested that activation of 5-HT_{1A} receptors in the NTS stimulates ventilation in rats after spinal cord injury (Teng et al., 2003) and in intact cats and rats (Garner et al., 1989; Mendelson et al., 1990). It has also been demonstrated in anaesthetized rats that synaptic transmission of vagal afferent inputs to the NTS, including

those from non-myelinated cardiopulmonary afferents, can be increased by activation of 5-HT_3 receptors (Jeggo et al., 2005). 5-HT_7 receptors are also involved in the neurotransmission of vagal afferent input into the NTS in anaesthetized rats (Oskutyte et al., 2009).

Major functions of serotonin

Central serotonin has been implicated in appetitive behaviors, neuroendocrine function, emotion, cognition, autonomic responses, thermoregulation, and motoric behaviors (Currie and Coscina, 1998; Jorgensen, 2007; Morrison et al., 1999). However, its cardiovascular effects are less well documented. A dose-dependent increase in BP has been observed after unilateral application of serotonin into the NTS in anesthetized rats (Wolf et al., 1981). Serotonin antagonists significantly attenuate this presser effect, while fluoxetine, a serotonin uptake inhibitor, significantly enhances the magnitude of the pressor response (Wolf et al., 1981). Lambert and colleagues also reported that serotonin injected into the 3rd ventricle in anesthetized rats produced a rise in BP coincident with a sympathetically mediated reduction in HR and ventilation (Lambert et al., 1978).

F. Serotonin and the 5HT $_{1A}$ receptor in hemorrhage

The amino acid L-tryptophan is the precursor for the synthesis of serotonin. Initially L-tryptophan is transported from the interstitium into neurons and is converted to 5-hydroxytryptophan by the enzyme TPH. Aromatic L-amino acid decarboxylase is a soluble pyridoxal-5'-phosphate-dependent enzyme, which then converts 5-hydroxytryptophan to serotonin. The product of serotonin breakdown by monoamine oxidase is 5-Hydroxyindoleacetic acid, which is excreted in the urine. Global depletion of serotonin with p-chlorophenylalanine (p-CPA), an inhibitor of TPH, attenuates the hypotensive, bradycardic and sympatholytic effects of hemorrhage in the anesthetized cat. Intravenous administration of the non-selective 5HT-receptor antagonist, methysergide, was also found to reverse the hypotensive response to blood withdrawal (Elam et al., 1985). Similar results have also been observed in chloralose-anesthetized rats (Morgan et al., 1988). Central administration of methysergide also prevented the fall of BP in rabbits subjected to caval vein occlusion (Evans et al., 1992). More recent studies by Dean and Bago showed that injection of the 5HT$_{1A}$-receptor antagonist, WAY-100635 directly into the pressor area of RVLM delayed and attenuated the fall in BP during the sympatholytic phase of hemorrhage in anesthetized rats (Dean and Bago, 2002). Together, these results suggested that endogenous serotonin acts on 5-HT$_{1A}$ receptors in the RVLM to cause the bradycardic and sympatholytic responses to hemorrhage. Our lab and others have investigated which

serotonin cell groups are activated by hypotensive hemorrhage by determining which of these cell groups express the immediate early gene c-FOS in response to blood withdrawal (Bago et al., 2002; Ruszaj et al., 2006). We have found that specific serotonin cell groups, including the vlPAG, RO, PPY and SUB expressed c-Fos after exposure to hypotensive hemorrhage, but not after hypotension alone in the awake rat (Ruszaj et al., 2006). Together, the existing data suggested that the vlPAG, RO, PPY or SUB mediate the sympatholytic phase of hypotensive hemorrhage. However, this view remains controversial, since significant serotonin depletion fails to attenuate the sympatholytic response in unanaesthetized rabbits (Evans et al., 1992).

We and others have also found that the selective 5-HT_{1A}-receptor agonist, 8-OH-DPAT, mimics the cardiovascular effects of methysergide in unanaesthetized hypovolemic cats and rats (Evans et al., 1993b; Scrogin et al., 2000). The ability of methysergide and 8-OH-DPAT to delay and attenuate the sympatholytic responses to hemorrhage was blocked by systemic administration of the selective 5-HT_{1A}-receptor antagonist, WAY-100635 (Scrogin et al., 2000). Additional evidence indicates that systemic administration of the partial 5-HT_{1A} agonist buspirone, or 8-OH-DPAT, can reverse the sympatholytic response to hemorrhage (Osei-Owusu and Scrogin, 2004). 8-OH-DPAT also stimulates sympathetic-dependent increases in venous tone, improves blood gases, and increases cardiac output as well as renal perfusion in conscious rats subjected to hypovolemic shock (Tiniakov and Scrogin, 2006). Thus, activation of 5-HT_{1A}

receptors by exogenous serotonin agonists produces sympathoexcitatory effects that are hemodynamically beneficial in hypovolemic shock.

Our laboratory also found that the 5-HT_{1A}-receptor agonist 8-OH-DPAT is more potent in restoring BP and sympathetic activity in hemorrhaged-rats when administered into the 4^{th} cerebral ventricle compared to injections in to more rostral parts of the cerebroventricular system (Scrogin, 2003). This led us to speculate that 8-OH-DPAT acts on receptors located near the dorsal surface of the medulla to reverse the sympatholytic responses to hemorrhage. Autoradiographic and electrophysiological studies have demonstrated a significant expression of functional 5-HT_{1A} receptors near the dorsomedial surface of the medulla in the NTS (Thor et al., 1992a, 1992b). The full sympathoexcitatory effect of 5-HT_{1A}-receptor agonists is dependent on intact sinoaortic afferents that carry arterial baroreceptor and peripheral chemosensory afferents to the NTS (Osei-Owusu and Scrogin, 2006). Together the data suggest that serotonin or 5-HT_{1A}-receptor agonists may act on receptors that facilitate sympathetic responses elicited by arterial baroreceptors or peripheral chemoreceptors to induce recovery of sympathetic activity during the secondary compensatory phase of hemorrhage.

G. Serotonin in central chemoreflex function

Please refer to the central chemoreflex section (page 25).

H. Serotonin in peripheral chemoreflex function

There is a dense serotonergic fiber projection from the caudal raphe nuclei (RM, RO, RP and PPY) to the comNTS where peripheral chemoreceptor afferents terminate (Schaffar et al., 1988; Steinbusch, 1981; Thor and Helke, 1987). The caudal NTS also contains a high density of various serotonin receptors subtypes including $5HT_{1A}$, $_{1B}$, $_{2}$, $_{3,}$ and $_{7}$ receptors (Manaker and Verderame, 1990; Pazos et al., 1985; Pratt et al., 1990; Ramage and Villalon, 2008). In the NTS, $5HT_{1A}$ receptors appear to be distributed in areas associated with the coordination of swallowing, respiration, and cardiovascular function, while $5HT_{1B}$ sites appear preferentially distributed in areas of the NTS associated with gastrointestinal, hepatic, pancreatic, and cardiovascular function (Thor et al., 1992a). Little is known about the role of serotonin in modulating responses to hypoxia. Studies suggest that serotonergic RO neurons that project to the NTS inhibit the cardiovagal or bradycardic component of the peripheral chemoreflex by releasing serotonin in the NTS, which, in turn activates $5HT_3$ receptors (Weissheimer and Machado, 2007). However, the same receptors do not appear to modulate the ventilatory or sympathetic component of the reflex (Nosjean et al., 1995; Sevoz et al., 1997). More recent work by Taylor et al. has shown that suppression of the caudal raphe serotonergic neurons has no effect on ventilatory response to hypoxia in awake rat (Taylor et al., 2005). In addition, activation of chemoresponsive single units in the NTS during chemoreceptor

afferent activation was suppressed when the RM was stimulated (Perez and Ruiz, 1995). Together, these findings suggest that caudal serotonin raphe neurons either do not influence peripheral chemoreception or possibly inhibit sensitivity to hypoxia.

Studies in this dissertation will more carefully explore the role of endogenous serotonin and exogenous 5-HT_{1A} receptors in the control of ventilation and sympathetic activity during hemorrhage and during the activation of reflex pathways that are normally engaged during hemorrhage.

CHAPTER III

Serotonin neurons of the caudal raphe nuclei contribute to sympathetic recovery following the hypotensive hemorrhage

Abstract

Caudal medullary serotonergic neurons positively modulate sympathetic recovery after acute hypotensive hemorrhage in conscious rats. Serotonin is thought to contribute to the sympatholytic syncopal-like response that develops during severe blood loss by inhibiting pre-sympathetic neurons of the RVLM. Previously, we determined that serotonergic neurons of the RO, RM, PPY, SUB and vlPAG region are activated by hypotensive hemorrhage, but not hypotension alone. To determine if caudal hindbrain cells contribute to the sympatholytic response to blood loss, they were targeted for destruction with a selective serotonin neurotoxin. We found that lesion of caudal hindbrain serotonergic cells sufficient to produce greater than 80% loss of serotonin nerve terminal immunoreactivity in the RVLM did not affect the sympatholytic response, but instead accelerated the RSNA fall during blood loss, attenuated the recovery of RSNA during the secondary compensatory phase of hemorrhage, and exaggerated metabolic acidosis. Hindbrain serotonin lesion also attenuated

ventilatory and sympathetic responses to stimulation of central chemoreceptors but increased spontaneous arterial BRS and decreased BP variability. Together, the data indicate that serotonin cells of the caudal hindbrain contribute to the secondary compensatory response following blood loss that helps to maintain oxygenation of peripheral tissue in the unanaesthetized rats. This effect may be related to facilitation of the chemoreflex response to acidosis.

Introduction

Progressive hemorrhage leads to a complex, multiphasic autonomic response, the origins of which are not well understood. The initial sympathetic activation that accompanies mild blood loss during the primary compensatory phase is mediated by arterial baroreceptor unloading and is quite likely augmented by cardiopulmonary reflex activation (Osei-Owusu and Scrogin, 2006; Quail et al., 1987; Schreihofer et al., 1994). After significant blood loss, these compensatory responses suddenly abate, resulting in a sympatholytic response that is characterized by rapid sympathetic withdrawal and cardiac vagal activation (Barcroft and Edholm, 1945; Osei-Owusu and Scrogin, 2006; Schadt and Ludbrook, 1991). If blood loss continues, autonomic compensation is slowly re-established, eventually culminating in tachycardia and sympathoexcitation (Tiniakov and Scrogin, 2006). However, if severe hypovolemia persists much beyond the point of maximal sympathetic activation, the vasculature becomes

unresponsive to catecholamines leading to a decompensation that is difficult to treat (Liu et al., 2003).

Several lines of evidence suggest that serotonin release in the central nervous system contributes to the early sympathetic withdrawal that accompanies significant blood loss in the sympatholytic phase. For instance, the hypotensive response to hemorrhage is delayed and attenuated in anesthetized animals subjected to global serotonin depletion with systemic administration of the tryptophan hydroxylase inhibitor, p-CPA (Blum and Spath, 1986; Elam et al., 1985; Morgan et al., 1988). In accord, systemic administration of the broad-spectrum serotonin receptor antagonist, methysergide, rapidly reverses the hypotensive response to blood loss and improves survival of anesthetized cats subjected to severe hemorrhage (Elam et al., 1985). More recently it was found that unilateral injection of the 5-HT_{1A}-receptor antagonist, WAY-100635, in the pressor region of the RVLM attenuated and delayed the sympatholytic response to blood loss in anesthetized rats (Dean and Bago, 2002). Together, these findings suggest that a sympatholytic effect of 5-HT_{1A} receptor activation in the RVLM mediates the sympathoinhibitory hemodynamic response to severe hemorrhage.

However, this view remains controversial since significant serotonin depletion fails to produce an observable delay or attenuation of the depressor response in unanaesthetized rabbits subjected to central hypovolemia via caval vein occlusion (Evans et al., 1992). Moreover, both systemic and

intracerebroventricular administration of serotonin 5-HT_{1A}-receptor agonists, including the potent full 5-HT_{1A}-receptor agonist 8-OH-DPAT, mimics the ability of methysergide to delay the onset of the sympatholytic response to blood loss in conscious rats (Scrogin et al., 2000). The ability of either methysergide or 8-OH-DPAT to delay hypotension is prevented by prior treatment with WAY-100635. As such, the effect of methysergide is most likely due to an agonist action on 5-HT_{1A} receptors, rather than blockade of endogenous serotonin. More recent evidence indicates that systemic administration of partial and full 5-HT_{1A}-receptor agonists can rapidly reverse the sympatholytic response to hemorrhage and dramatically improve blood gases in animals subjected to hypovolemic shock (Osei-Owusu and Scrogin, 2004; Tiniakov and Scrogin, 2006). Thus, studies in unanaesthetized animals call into question the role of endogenous serotonin in the sympatholytic response to hemorrhage. In fact, they suggest that serotonin receptor activation may instead contribute to the secondary sympathetic compensatory phase of hypotensive hemorrhage.

However, it is possible that a redundant, non-serotonergic pathway that is normally suppressed during anesthesia contributes to the depressor response in unanaesthetized rats. Alternatively, it is possible that in prior studies that utilized unanaesthetized models serotonin depletion was not sufficient to affect the sympatholytic response. To further address these possibilities, we determined whether targeted destruction of serotonergic nuclei that are normally activated by hypotensive hemorrhage is required for normal sympathetic responses to

hemorrhage in unanaesthetized rats. Indices of BRS were also assessed to determine the effect of lesion on baroreflex integrity. Measures of central chemoreflex sensitivity were also performed to provide functional evidence of serotonin depletion based on recent evidence demonstrating the importance of ventromedial medullary serotonin cells on arterial PCO_2 detection in conscious animals (Dias et al., 2007).

Methods

Animals

Male Sprague-Dawley rats (300 - 350 g, Harlan, Indianapolis, IN) were acclimated to the housing facility while given *ad libitum* access to food and water at least 1 wk prior to surgery. The facility was maintained at a constant temperature of 22 ± 2 °C with a light/dark cycle of 12:12 hrs. All experiments were approved by the Institutional Animal Care and Use committee and were conducted in accordance with the Guide for the Care and Use of Laboratory Animals as adopted and promulgated by the US National Institutes of Health.

Surgery

Neurotoxin studies: major caudal hindbrain serotonin nuclei were initially targeted for selective serotonin lesion based on outcomes from our previous c-Fos study which showed that serotonin neurons of the RO, RM, RP, PPY, SUB, vlPAG nuclei expressed c-FOS in response to hypotensive hemorrhage

(Glasgow et al., 2009; Ruszaj et al., 2006). All rats were pre-treated with the dopamine and NE re-uptake blocker, nomifensine (15 mg/kg in 20% β-cyclodextran), at least 30 min prior to neurotoxin injection to prevent toxin-induced destruction of noradrenergic and dopaminergic cells. Rats were anesthetized with sodium pentobarbital (65 mg/kg, i.p.) and placed in a stereotaxic apparatus. The incisor bar was placed 11 mm below the level of the interaural cavity. The back of the skull was exposed and a portion of the occipital bone was removed to expose the brainstem. The occipital membrane was incised and a micropipette injector (O.D. ~20 μm) was centered at the caudal tip of calamus scriptorus. Injections of either 5,7-dihydroxytryptamine (5,7-DHT; 5 mM in 0.1% ascorbic acid) or vehicle (0.1% ascorbic acid) were made in three rostro-caudal planes: 1.9, 2.9, and 3.9 mm rostral to the caudal end of calamus scriptorus. Three 200-nl injections were made 3 mm below the dorsal surface of the brainstem (relative to calamus scriptorus) at each rostro-caudal plane, 1.1 mm to the left and right of the midline and at the midline, for a total of 9 injections targeted to the ventromedial serotonergic cell groups of the caudal brainstem in each rat. The neck muscle and skin were closed in separate layers.

Two weeks later, all rats were re-anesthetized with sodium pentobarbital (65 mg/kg, i.p.) and implanted with vascular catheters one day prior to the experiment (Figure 7). In these studies, catheters were placed bilaterally in the femoral arteries to enable direct measurement of arterial pressure and simultaneous arterial blood withdrawal. A third catheter was placed unilaterally in

the femoral vein for drug injections. Catheters were externalized at the nape of the neck and secured with sutures. During the same surgery, dual recording electrode leads were placed around a renal sympathetic nerve fiber bundle and against the abdominal side of the diaphragm to enable recording of RSNA and diaphragmatic EMG (dEMG), respectively (Figure 8). The electrode connector was externalized through the subcutaneous space at the nape of the neck along with the vascular catheters. For RSNA recordings, a 1 to 2 mm segment of a sympathetic fiber bundle emanating from the aorticorenal ganglion was isolated and placed on a stainless steel, Teflon-coated (bare di =.005 in., A-M Systems Inc., Everett, WA) bipolar electrode implanted through a left flank incision. Viability of the nerve preparation was determined by auditory assessment of the bursting activity, after which the preparation was embedded in a quick drying, lightweight silicon (Kwik sil, World Precision Instruments). The flank muscle incision was closed around the electrode lead wires. Subsequently, the abdominal side of the diaphragm was exposed through a small laparotomy just below the most caudal left rib. Stainless-steel Teflon-coated lead wires, like those described above, were fashioned to extend from the same microconnector and tied to the diaphragm using 6-0 nylon. The lead wires were coiled in the subcutaneous space and the incisions closed in layers. Animals were allowed to recover overnight prior to the experiment.

Data Acquisition

Arterial pressure, HR, RSNA and dEMG were recorded on a Macintosh G4 Powerbook computer using PowerLab data acquisition software (Chart v. 5.2.1, ADinstruments, Colorado Springs, CO). Arterial pressure was measured with a disposable pressure transducer (Transpac® IV, Abbott Labs, North Chicago, IL) and a PowerLab bridge amplifier (ADinstruments, CO). Heart rate was calculated using peak-to-peak detection of the pulse pressure wave. Sympathetic activity and dEMG were sampled (4,000 Hz) and amplified (10-20,000x) with PowerLab Bioamplifiers (ADinstruments, CO). The recorded neurograms were filtered (1-1000 Hz), rectified and integrated over a 20-ms time constant. Background noise in the RSNA recordings was determined at the end of each experiment by measuring the remaining signal following ganglionic blockade (hexamethonium chloride, 30 mg/kg, i.v.). Background noise was subtracted from nerve activity values to provide a measurement of RSNA. Background noise in the dEMG electrode recording was determined during expiration, when phrenic motor nerve activity was absent. Measurements of RSNA and dEMG obtained during the experiment were normalized to baseline determined over a 10 min period directly prior to the start of interventions. Only RSNA and dEMG data from animals with greater than a 2:1 signal to noise ratio in the respective neurograms were included in the data analysis. Respiratory rate (RR) was determined by peak to peak detection of the integrated dEMG signal.

Spontaneous BRS was determined from 5-min segments of BP and HR collected prior to hemorrhage. Data were analyzed with Nevrokard SA-BRS software v.3.2.4 to determine BRS by the sequence method (Padley et al., 2005). Gain was determined as the average slope of linear regressions obtained from a minimum of 3 sequences that satisfied the following constraints: 3 or more consecutive interbeat intervals (IBI) with variation in the same direction, >0.5 ms that correlated (r^2 >0.85) with systolic, diastolic or mean arterial BP variations of >0.5 mmHg with a 3 beat delay. These parameters were chosen based on prior analyses demonstrating that they retrieved the most sequences with the highest gain in intact male Sprague-Dawley rats of a similar age (Henze et al., 2008). Cross-spectral analyses were performed on IBI and BP data using a 128-point fast Fourier transformation with a smoothed Hamming window. Coherence between IBI and BP variability was determined as the square root of the ratio of the IBI and BP power spectra with 50% overlap and zero padding of 8. Values are reported as the alpha index in the low frequency (alpha LF) (0.06-0.6 Hz) and high frequency (alpha HF) (0.6-3.0) domains. In addition, BP variability was determined in the low frequency domain (LF power) and in the time domain, the latter of which was determined as the standard deviation of BP between normal beats (BP SDNN).

Alveolar - arterial O_2 differences were calculated to estimate the degree of ventilation perfusion mismatch in blood samples taken during hemorrhage. Alveolar O_2 was estimated using the equation PaO_2= FIO_2 * (Pb-Pwv)-$PaCO_2$/R,

where the fraction of inspired oxygen (FIO_2) was estimated as 0.21, barometric pressure (Pb) as 760 mm Hg, water vapor pressure (Pwv) as 47 mm Hg and the respiratory quotient (R) as 0.8. Arterial O_2 and CO_2 were determined from arterial blood gas measurements obtained before and during hemorrhage (Strittmatter and Schadt, 2007). Arterial blood gases were determined using an I-STAT 1 blood gas analyzer (ISTAT, East Windsor, NJ).

Experimental Protocols:

Central chemoreflex and hemorrhage experiments

At least 2 hrs prior to hemorrhage, rats subjected to sham- or hindbrain serotonin lesion were exposed to hyperoxic hypercapnia to determine their central chemoreflex sensitivity. The rats were placed unrestrained in a plastic box (4.5 inches deep, 11 inches long and 5 and 7/8 inches wide) flushed with 100% O_2. Blood pressure, HR, RSNA and dEMG were determined throughout the experiment. After at least 1 hr habituation, rats were exposed to 5% CO_2 added to the O_2 for 5 min after which a 100 µl arterial blood sample was taken for measurement of blood gases. The CO_2 level was raised to 8% for an additional 5 min, after which a second arterial sample was taken. Ambient CO_2 levels in the box were recorded using a capnometer (Vacu·Med, Ventura, CA.). Immediately following the hypercapnia experiment the rats were moved back to their home cage.

After at least 2 hrs of recovery from exposure to hypercapnia the rats were connected to a withdrawal pump and an arterial pressure transducer through an overhead swivel system. Rats were habituated after instrumentation for at least 1 hr while they rested unrestrained in their home cage. After habituation, arterial blood was withdrawn using an automated withdrawal pump set at a rate of 3.2 ml/min/kg for 6 min and adjusted to a slower withdrawal rate of 0.52 ml/min for 4 additional minutes. This procedure produces a consistent hypotensive response after approximately 3.5 min and maintains pressure at 40-50 mmHg for the remainder of active blood withdrawal. Data acquisition was begun 15 min prior to the experiment and continued throughout the hemorrhage and for an additional 50 min following termination of hemorrhage. Arterial and venous blood samples (150 µl) were taken at least 30 min before hemorrhage, at the end of hemorrhage, and 60 min after the start of hemorrhage for determination of blood gases, hematocrit and plasma protein. At the end of the experiment rats were given hexamethonium chloride (30 mg/kg, i.v.) for determination of background noise in the sympathetic recording. Animals were then rapidly anesthetized with sodium pentobarbital (65 mg/kg, i.v.) and quickly perfused transcardially with 90 ml of sodium nitrite (0.1 M) in 6.7 mM phosphate buffer followed by 90 ml 4% paraformaldehyde in 0.1 M PBS. The brains were removed and post-fixed for 1hr. The brainstem was blocked and post-fixed for an additional hour and subsequently dehydrated in 30% sucrose. Brains were cut in 40 µm sections and collected serially into 6 wells. Sections were saved in cryoprotectant (30%

sucrose and 30% ethylene glycol in phosphate buffered saline) and stored at -20ºC.

Immunohistochemistry: Tryptophan hydroxylase (TPH), Tyrosine hydroxylase (TH), serotonin (5HT)

Brain sections from rats were processed to expose tryptophan hydroxylase immunoreactivity (TPH-ir) in order to verify the extent of lesion. One of every six sections was incubated in 0.2% Triton X (40 min), 3% H_2O_2 (10 min), 6% goat serum and sheep anti-TPH primary antibody (1:1000, Chemicon) for 48 hrs at 4ºC. Sections were then incubated in biotinylated goat anti-rabbit IgG (1:1000, Vector) for 1 hr at room temperature followed by incubation with avidin-biotin complex (Vector) for 50 min. Immunoreactivity was exposed with nickel sulfate-intensified 3, 3'–diaminobenzadine tetrahydrochloride (DAB) chromagen to produce a black nuclear label. To verify that the neurotoxin did not affect noradrenergic neurons, an additional set of sections was incubated in the same solution as describe above, except that 6% horse serum and mouse-anti-TH (1:1000, Chemicon) antibody were substituted for goat serum and anti-TPH antibody. Sections were washed and incubated in the appropriate biotinylated IgG made in horse for 1 hr and incubated with avidin-biotin complex as described above. Sections were rinsed in PBS, mounted on gel-coated slides, dried with xylene and coverslipped with DPX mountanting media. The specificity of the primary antibodies was verified by characteristic labeling of known serotonergic

and adrenergic cell groups of the brainstem. Omission of the primary antibodies completely prevented cell labeling.

Serotonin nerve terminal density was determined in rats subjected to hindbrain lesion. Rabbit anti-serotonin antibody (1:200,000, Immunostar) was pre-incubated with 6 mM reduced L-glutathione (Sigma) in 1mM tris-EDTA buffer (pH 8) for 1hr at room temperature prior to incubation with the tissue (Rogers et al., 2006). One in six sections from lesioned- and sham-lesioned rats was incubated in 0.2% Triton X and the primary antibody for at least 48 hr at 4ºC. Sections were then washed and incubated in 6% donkey serum, 0.2%Triton X and donkey anti-rabbit Dylight 649 (1:200, Jackson ImmunoResearch) for 2 hr. Sections were rinsed in PBS, mounted on gel-coated slides and immediately coverslipped with fluoromount (Sigma). Sections were stored at 4ºC for 14 days prior to microscopy. Some sections containing the RVLM were double-labeled for serotonin and PNMT to enable examination of serotonin fiber density in the C1 region. In this case the above protocol was followed except that mouse anti-PNMT antibody (1:4000, Abnova) was added to the primary incubation step and donkey anti-mouse Cy3 (1:200, Jackson ImmunoResearch) was added to the second incubation.

Microscopy

Tryptophan hydroxylase and serotonin immunoreactivity in lesion studies

Given our experience that cell bodies of serotonergic neurons are better visualized with a TPH label, cell bodies showing TPH-ir were counted throughout the same raphe regions as described above. Every 6th section throughout the anatomical extent of each serotonin-rich nucleus or region was counted. These regions included the DR and MR nuclei, the vlPAG region, the RM and PPY, the RO, the SUB region and RP (Steinbusch, 1981).

Given that serotonin nerve terminals are better visualized with a serotonin label, 5-HT-ir was also assessed in terminal projections to brainstem areas known to regulate autonomic function, including the RVLM and the NTS. Serotonin immunoreactive fiber density in the NTS was determined unilaterally at the level of the medial and comNTS subnuclei approximately 13.4 and 14.1 mm caudal to Bregma, respectively. Serotonin fiber density was also determined in the RVLM at 3 levels; 11.8, 12.2 and 12.8 mm caudal to bregma. Fiber density was determined by thresholding a composite image made from thirty 1 μm deconvolved optical sections taken from each tissue section. Images were taken with an Olympus inverted IX81 epifluorescence microscope with a motor driven stage and a 10x objective. Background levels were determined from unlabeled neuropil measured at the same rostro-caudal level averaged from 3-5 tissue sections obtained from different sham-lesioned animals. All images obtained from the same region were subjected to the same degree of background

subtraction prior to thresholding. Tissues from equal numbers of lesioned and sham-lesioned animals were processed in parallel in two separate cohorts. All images were acquired at the same exposure length, on the same day, 14 days after immunohistochemical processing. Deconvolution was performed within each optical section using Vaytek Microtome software and the rapid nearest neighbor method. Deconvolved optical sections were merged into a single composite image using Image Pro analysis software (version 6.3). Measurements of serotonin nerve terminal content were made from images in which the sections were carefully oriented to keep the mid-line of the section aligned in a vertical plane with the camera. An area of interest (AOI) was placed over the 8-bit image and the percent area of the thresholded image that was occupied by thresholded signal was determined using NIH Image J software. For measurements of the comNTS an AOI box 825 pixel wide and 518 pixel high was placed such that the lower left corner of the AOI touched the most dorsomedial point of the central canal. For measurement of the medial NTS an AOI oval, with a maximal pixel width of 900 and maximal pixel height of 600 was centered such that the leading left edge of the AOI was centered over the right lateral border of the 4th ventricle where it met the right NTS. For measurements in the RVLM, an AOI 900 pixels in width and 800 pixels in height was placed 450 pixels from the mid-line such that the right lower corner touched the right ventrolateral subependymal surface of the section. Using this method, AOIs were consistently centered over the pressor region of the RVLM as determined by the density and

orientation of PNMT-positive cells which make up the C1 bulbospinal neurons that project to pre-ganglionic sympathetic cells of the spinal cord.

Data Analysis

The effect of lesion on BP, HR, RSNA, integrated dEMG (as an index of central respiratory drive), RR and 5-HT-ir nerve terminal fiber density and TPH-ir cell number was determined by two-way ANOVA with repeated measures. Significant interactions and main effects were followed up with Newman-Keuls post-hoc tests.

Results

Lesion did not significantly affect body weight or hemodilution during the course of hemorrhage (Table 1). Blood pressure, HR and RSNA of sham-lesioned showed typical biphasic responses during acute hemorrhage characterized by a short normotensive phase during which sympathetic activity increased, followed by a rapid fall in all three variables (Figure 9). After reaching their nadir between 6 and 8 minutes after the start of blood withdrawal, the three variables began to recover and reached a steady state within 20 minutes of hemorrhage termination. The respiratory response was characterized by tachypnea that developed at the start of hemorrhage during the sympatholytic phase, which began to normalize prior to the end of hemorrhage. Respiratory rate continued to decline slightly below baseline where it remained for the rest of

the recording period. The integrated dEMG response was somewhat variable. In general, it rose initially during the primary compensatory phase of hemorrhage but declined back to baseline during the sympatholytic phase and fluctuated thereafter throughout the second compensatory phase. In general, dEMG was elevated above baseline, but an overall ANOVA failed to show a significant effect of time in sham-lesioned animals.

Hindbrain neurotoxic lesion did not significantly affect the BP or HR responses to acute hemorrhage or during second compensatory phase (Figure 9). Qualitatively, baseline sympathetic burst frequency or amplitude did not appear different between groups (data not shown). The maximal rise in sympathetic activity during blood withdrawal did not differ between groups (106.6 ± 19.0 vs. 69.6 ± 23% of baseline for control and lesioned groups respectively). The sympatholytic response developed more quickly in the lesioned animals, but the nadirs of the two groups were similar. Sympathetic activity in lesioned rats recovered to a lower steady state overall ($P<0.01$). Respiratory rate in lesioned animals paralleled that of sham-lesioned animals during active blood loss but then declined to an overall lower level once blood loss was terminated ($P<0.05$). Integrated dEMG declined from the primary compensatory phase of hemorrhage and remained below baseline and below that of sham-lesioned rats throughout the second compensatory phase of hemorrhage ($P<0.01$).

Acid base balance did not differ between groups prior to hemorrhage. In sham-lesioned rats, a significant decrease in pH was only observed in the blood

sample taken 60 min after start of blood withdrawal (Table 2). Lactate accumulation and loss of base excess (BE) developed within the first 10 minutes of blood loss ($P<0.01$). In sham-lesioned animals, lactate and BE began to return to baseline by the end of the recording period. Loss of BE and lactate accumulation were exaggerated in lesioned animals and remained so through the end of the experiment ($P<0.01$). In accord, arterial pH of lesioned rats was significantly reduced compared to sham-lesioned rats at 10 and 60 minutes after the start of hemorrhage ($P<0.05$ and $P<0.01$ respectively).

Arterial PO_2 increased during the first 10 minutes of hemorrhage and remained elevated throughout the second compensatory phase of hemorrhage in sham-lesioned rats ($P<0.01$). Lesioned rats showed a similar increase in arterial PO_2 initially, that further increased and exceeded that of sham-lesioned animals during the second compensatory phase ($P<0.01$). Arterial PCO_2 declined initially during blood withdrawal ($P<0.01$) and recovered in the second compensatory phase similarly in both groups.

Exposure to hyperoxic hypercapnia increased sympathetic activity and ventilation but reduced HR in sham-lesioned rats (Figures 10 and 11). Increased ventilation was characterized by both increased rate and amplitude of phrenic nerve bursts with increasing CO_2. Lesion attenuated the ventilatory ($P<0.05$) and sympathetic ($P<0.01$) responses to 8% CO_2. However, the lesion did not affect bradycardia or tachypnic responses to increasing CO_2. Arterial pH and PCO_2 did

not differ between groups over the course of the chemoreflex experiment (Table 3).

Average spontaneous baroreflex gain of the HR reflex was increased in lesioned rats when assessed with the sequence method ($P<0.05$) when the IBI was related to systolic, mean or diastolic pressure (Table 4). There was a tendency for an increased baroreflex gain in lesioned groups when assessed by the spectral method ($P<0.06$). Similarly, the power of BP variability in the low frequency domain tended to be lower in lesioned animals, but the difference was not significant ($P<0.07$). However, BP variability in the time domain was significantly reduced in lesioned rats when either systolic, mean or diastolic pressures were assessed ($P<0.05$). The ratio of low frequency to high frequency HR variability (LF/HF) did not differ between groups.

Immunohistochemistry: TPH / TH / 5HT

Hindbrain neurotoxin injection resulted in a large reduction in the numbers of TPH-ir cells throughout the caudal serotonin-rich region of the brainstem (Figure 12). The degree of depletion following neurotoxin was most extensive between 13.5 and 11 mm caudal from Bregma. The hindbrain lesion did not affect TPH-ir positive cell numbers in midbrain nuclei (Figure 13).

Tyrosine hydroxylase immunoreactive cells in the locus coeruleus and A1 region showed no apparent difference in morphology following treatment with the neurotoxin (Figure 14A-D). Tyrosine hydroxylase immunoreactive cell number in

the A2 and A5 regions was not affected by neurotoxin injection (Figure 14E). Cell counts in the locus coeruleus were not determined due to the intense staining and inability to differentiate individual cells. The number of TH-ir cells in the A1 region was not determined since it was not possible to differentiate between noradrenergic cells of the A1 region and adrenergic cells of the C1 region within the same section using DAB labeling techniques. However, the apparent density of staining did not differ in either region (Figure 14A-D).

Serotonin fiber density was reduced by more than 80% at three rostral-caudal levels within the C1 region of the RVLM (Figure 15E-F and Table 5). Serotonin nerve terminal immunoreactivity in the NTS at the level of the commissural and medial subnuclei was diminished by 50-60% following targeted caudal hindbrain neurotoxin administration (Figure 15A-D and Table 5).

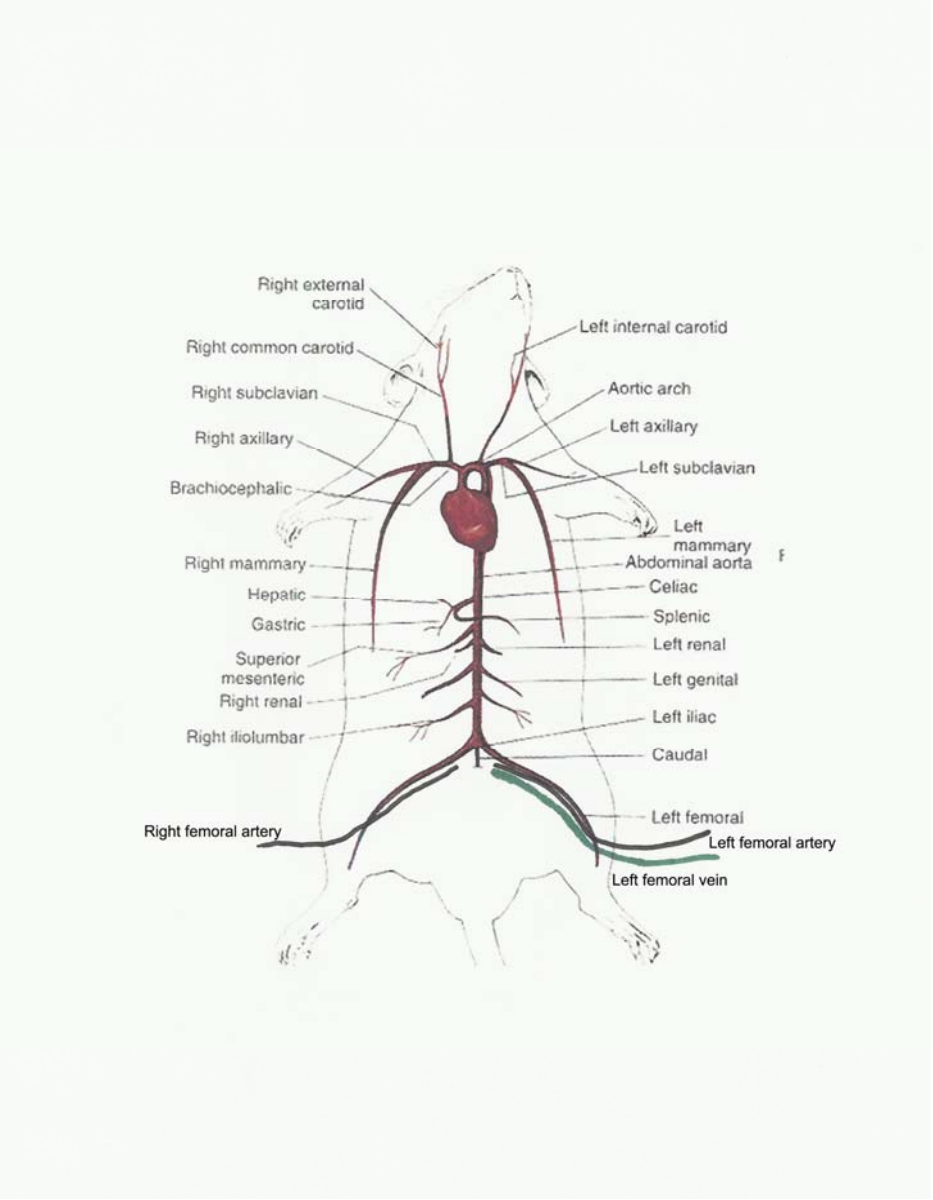

Figure 7: Illustration of catheter placement in a rat. Two catheters were placed bilaterally in the femoral arteries and the third catheter was placed unilaterally in a femoral vein. Catheters were occluded by a 23 ga wire and externalized at the nape of the neck and secured with sutures (not shown). Figure modified from http://www.biologycorner.com/bio3/anatomy/rat_circulatory.html

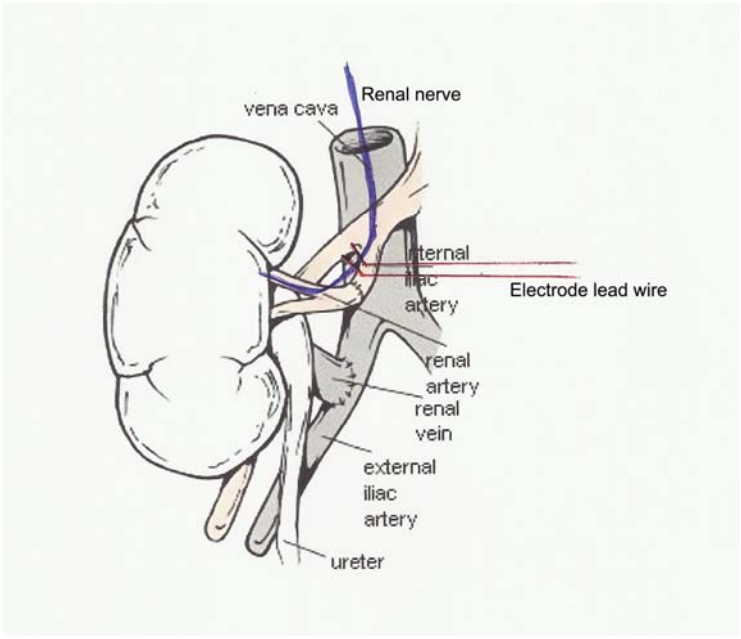

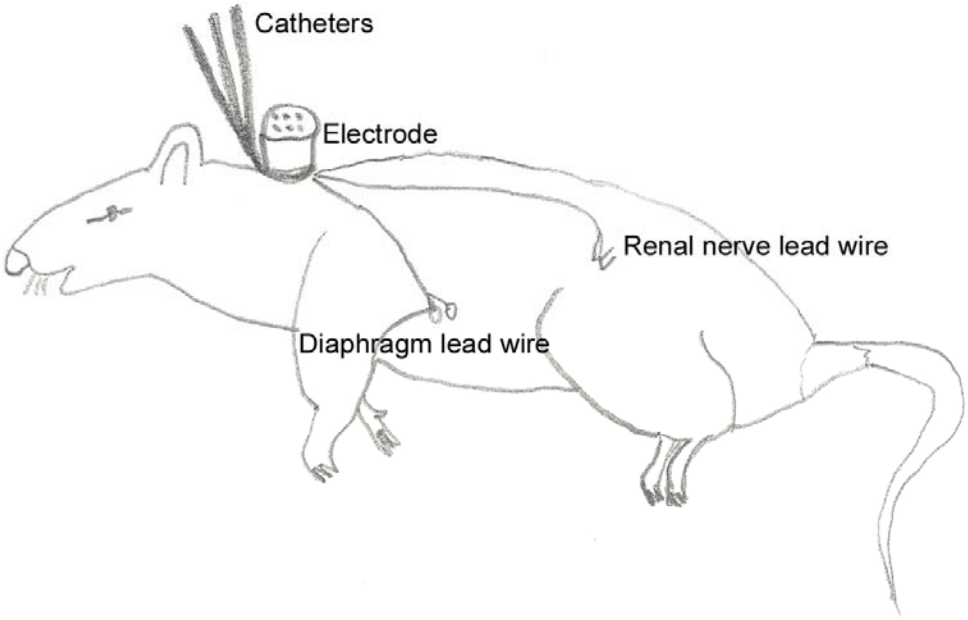

Figure 8: Simplified illustration of the placement of dual recording electrode and external catheters. Dual recording electrode leads were placed around a renal sympathetic nerve fiber bundle (see above) and against the abdominal side of

the diaphragm to enable recording of RSNA and dEMG, respectively. The electrode connector was externalized through the subcutaneous space at the nape of the neck along with the three vascular catheters. Electrode and catheters were sewed and stabilized on the skin. Top figure is modified from http://focosi.altervista.org/grafts.html

Table 1. Body weight at start of experiment and hematocrit and plasma protein concentration before and after hemorrhage

Group	BW	Hematocrit (%)		Plasma Protein (g/dL)	
		BL	60 min	BL	60 min
Control (15)	377.2 ± 4.7	39.7 ± 0.6	30.6 ± 0.7**	5.6 ± 0.07	4.6 ± 0.07**
Lesion (10)	389.7 ± 6.9	39.8 ± 1.7	29.5 ± 1.0**	5.8 ± 0.14	4.6 ± 0.08**

Values are group means ± SEM before baseline and 60 min after the start of hemorrhage. Group n are shown in parentheses.

Data were analyzed by 2-way ANOVA with repeated measures using Lesion and Time as factors. Main effects and significant interactions were followed up with between- and within-group comparisons using Newman-Keul post-hoc test. **P<0.01 vs. baseline within group.

An overall 2-way ANOVA with repeated measures examining the effect of Lesion and Time on hematocrit (%) showed significant main effect of Time [$F(1,23) = 524.59$, P<0.01] due to a decline of hematocrit with hemorrhage in both groups.

An overall 2-way ANOVA with repeated measures examining the effect of Lesion and Time on plasma protein showed a main effect of Time [$F(1,23) = 222.51$,

P<0.01] due to a decline in plasma protein concentration during hemorrhage in both groups.

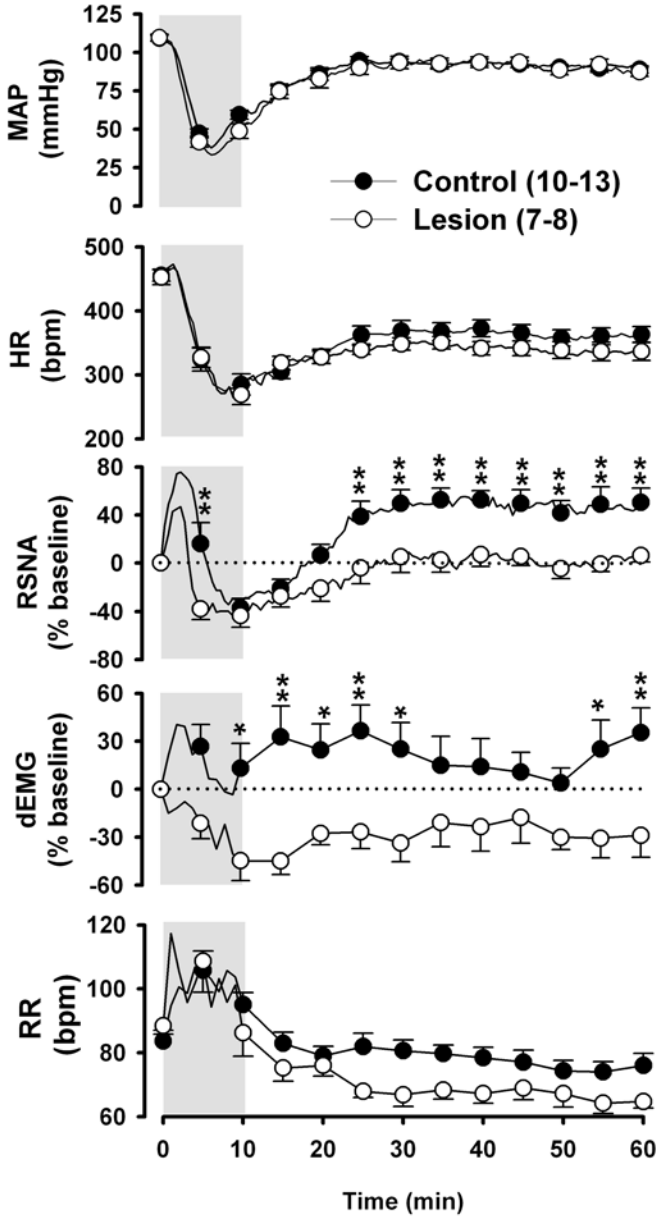

Figure 9. Mean arterial pressure (MAP), heart rate (HR), renal sympathetic nerve activity (RSNA), integrated diaphragmatic EMG (dEMG) and respiratory rate (RR) during hemorrhage (gray shaded region) and subsequent recovery in rats treated with vehicle (Control) and neurotoxin (Lesion) targeted to the caudal

raphe nuclei. Data are group mean ± S.E.M. Number of subjects in control group is 13 for MAP, HR and RR, 10 for RSNA and 11 for dEMG. Number of subjects in lesion group is 8 for all parameters except RSNA which includes 7 subjects.

Data were analyzed by 2-way ANOVA with repeated measures using Lesion and Time as factors. Main effects and significant interactions were followed up with between-group comparisons using Newman-Keul post-hoc test. *, ** $P<0.05$, <0.01 sham-lesioned vs. lesioned animals, respectively.

Overall 2-way ANOVA with repeated measures examining the effect of Lesion and Time on MAP showed a main effect of Time [$F(1,228) = 104.64$, $P<0.01$] due to the decline and recovery of MAP over the course of hemorrhage and second compensatory phase.

Overall 2-way ANOVA with repeated measures examining the effect of Lesion and Time on HR showed a main effect of Time only [$F(1,228) = 33.04$, $P<0.01$] due to the decline and recovery of HR over the course of hemorrhage and the second compensatory phase.

An overall 2-way ANOVA with repeated measures examining the effects of Lesion and Time on RSNA showed a Lesion x Time interaction [$F(1,180) = 2.41$,

P<0.01] due to the lack of recovery over time in lesioned rats. Significant main effects of Lesion [F (1,180) = 13.85, *P*<0.01] and Time [F(1,180) = 14.37, *P*<0.01] was also found. A main effect of Lesion was due to the overall lower RSNA in lesioned animals, while the main effect of Time was due to the decline and recovery in RSNA over the course of hemorrhage and the second compensatory phase.

An overall 2-way ANOVA with repeated measures examining the effects of Lesion and Time on dEMG activity showed a main effect of Lesion [F (1,204) = 10.61, *P*<0.05] due to the significant attenuation of dEMG in lesioned rats.

An overall 2-way ANOVA with repeated measures examining the effects of Lesion and Time on RR showed a main effect of Lesion [F (1,228) = 4.93, *P*<0.05] and Time [F (1,228) = 17.88, *P*<0.05]. A main effect of Lesion was due to the slight, but significantly lower RR in lesioned animals, while the main effect of Time was due to the increase and subsequent decline of RR over the course of hemorrhage and the second compensatory phase compared to baseline.

Table 2. Effects of the hemorrhage on blood gases and acid-base status in hindbrain lesion and sham-lesioned rats

GROUP	Time (min)	pH	PaO_2 (mmHg)	A-a diff (mmHg)	$PaCO_2$ (mmHg)	BE (mmol/L)	Lactate (mmol/L)
Control (8)	0	7.53 ± 0.01	70.6 ± 1.3	31.2±1.6	38.2 ± 0.5	9.25 ± 1.0	0.96 ± 0.04
	10	7.54 ± 0.02	87.1 ± 0.8$^{\#\#}$	24.8±1.3$^{\#}$	30.2 ± 0.7$^{\#\#}$	3.75 ± 1.1$^{\#\#}$	5.05 ± 0.25$^{\#\#}$
	60	7.49 ± 0.02$^{\#\#}$	86.8 ± 0.7$^{\#\#}$	14.9±1.4$^{\#\#}$	38.3 ± 1.0	5.87 ± 1.0	3.32 ± 0.32$^{\#\#}$
Lesion (5)	0	7.51 ± 0.01	71.4 ± 0.2	31.5±1.6	37.4 ± 1.1	7.4 ± 1.0	1.14 ± 0.1
	10	7.51 ± 0.01*	88.8 ± 1.6$^{\#\#}$	25.9±2.2	27.9 ± 2.4$^{\#\#}$	-0.6 ± 2.16**$^{\#\#}$	7.56 ± 0.8**$^{\#\#}$
	60	7.45 ± 0.01**$^{\#\#}$	98.0 ± 3.6**$^{\#\#}$	9.8±2.9*$^{\#\#}$	33.5 ± 3.8	-1.0 ± 2.8**$^{\#\#}$	6.19 ± 0.92**$^{\#\#}$

Values are group means ± SEM 0, 10 and 60 min after start of hemorrhage. A-a diff, difference in alveolar and arterial O_2 pressure; PaO2, arterial blood O_2 pressure; BE, base excess. Values are group means ± SEM. Group n are shown in parentheses. Data were analyzed by 2-way ANOVA with repeated measures using Lesion and Time as factors. Between- and within-group differences were compared using Newman-Keuls post hoc tests. *, ** P<0.05, 0.01 lesion vs. control at same sampling time. $^{\#, \#\#}$ P<0.05, 0.01 vs. baseline (time 0) within group.

An overall 2-way ANOVA with repeated measures examining the effect of Lesion and Time on arterial pH showed a main effect of Time [F (1,22) = 40.88, $P<0.01$] due to an overall decrease in pH over time in both groups.

An overall 2-way ANOVA with repeated measures examining the effect of Lesion and Time on PaO_2 over the course of hemorrhage showed a Lesion x Time interaction [F (1,22) = 9.35, $P<0.01$] due to the greater increase in PaO_2 of lesioned rats over the course of hemorrhage. A main effect of Lesion [F (1,22) = 8.11, $P<0.01$] was due to a greater overall increase in PaO_2 in lesioned rats. A main effect of Time [F (1,22) = 145.74, $P<0.01$] was due to an overall increase in PaO_2 in both groups.

An overall 2-way ANOVA with repeated measures examining the effect of Lesion and Time on arterial A-a difference over the course of hemorrhage showed a main effect of Time [F (1,22) = 71.23, $P<0.01$] due to an overall decrease of A-a difference over time in both groups.

An overall 2-way ANOVA with repeated measures examining the effect of Lesion and Time on $PaCO_2$ over the course of hemorrhage showed a main effect of Time [F (1,22) = 20.40, $P<0.01$] due to the fall in $PaCO_2$ observed during the primary compensatory phase of hemorrhage in both groups.

An overall 2-way ANOVA with repeated measures examining the effect of Lesion and Time on BE over the course of hemorrhage showed a main effect of Lesion [F (1,22) = 6.41, $P<0.01$] due to a greater overall decrease of BE in lesioned rats. A main effect of Time [F (1,22) = 22.67, $P<0.01$] was due to an overall decrease of BE in both groups over time.

An overall 2-way ANOVA with repeated measures examining the effect of Lesion and Time on lactate over the course of hemorrhage showed a Lesion x Time interaction [F (1,22) = 5.78, $P<0.01$] due to the continued elevation in lactate level in lesion rats that persisted up to 60 min after initiation of hemorrhage, while lactate levels in control animals began to decline back to baseline in hemorrhaged rats. A main effect of Lesion [F (1,22) = 6.92, $P<0.01$] was due to the overall greater elevation of lactate level in lesioned rats. A main effect of Time [F (1,22) = 61.81, $P<0.01$] was due to increased lactate levels over time in both groups.

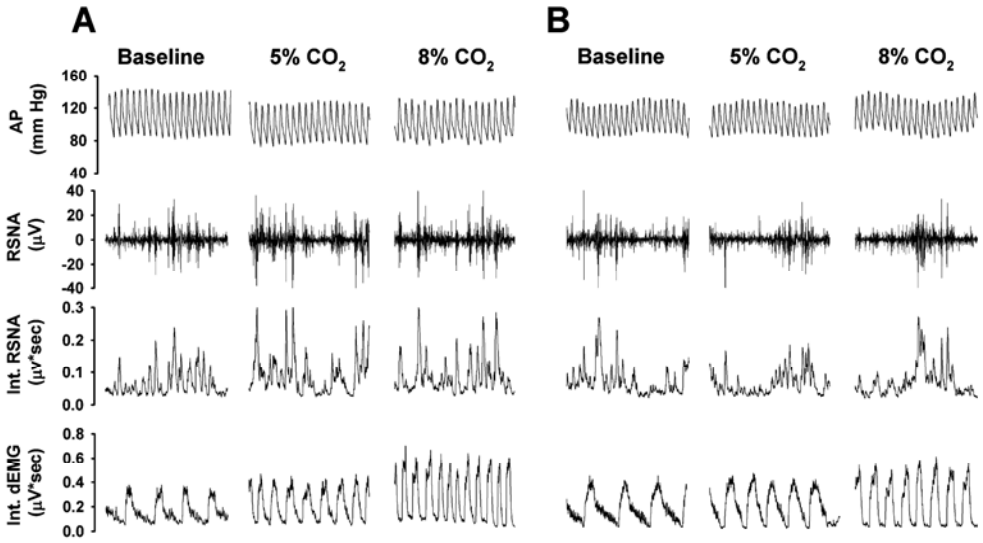

Figure 10. Three second segments of arterial pressure, raw renal sympathetic nerve activity (RSNA), integrated renal sympathetic activity (int. RSNA) and integrated diaphragmatic EMG (int. dEMG) during exposure to 100% O_2 (baseline), 5% CO_2 + 95% O_2 (5%) and 8%CO_2 + 92% O_2 (8%) in rats treated with vehicle (A) or 5,7-dihydroxytryptamine in the hindbrain (B).

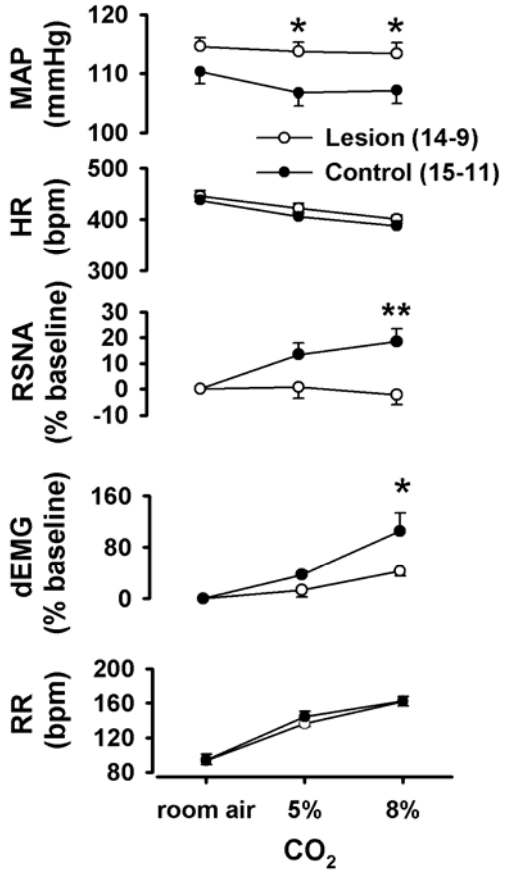

Figure 11. Summary data of mean arterial pressure (MAP), heart rate (HR), renal sympathetic nerve activity (RSNA), integrated diaphragmatic EMG (dEMG) and respiratory rate (RR) during exposure to increasing concentrations of ambient CO_2 in rats treated with vehicle (Control) and 5,7-dihydroxytryptamine (Lesion) targeted to the caudal raphe. Data are group mean ± S.E.M. Number of subjects in control group is 15 for MAP and HR, 10 for RSNA, 8 for dEMG and 11 for RR. Number of subjects in lesion group is 14 for MAP and HR, 9 for RSNA, 8 for dEMG and 13 for RR.

Data were analyzed by 2-way ANOVA with repeated measures using Lesion and CO_2 level as factors. Main effects and significant interactions were followed up with between-group comparisons using Newman-Keul post-hoc test. *, ** $P<0.05$, <0.01 sham-lesioned vs. lesioned animals, respectively.

An overall 2-way ANOVA with repeated measures examining the effect of Lesion and CO_2 level on MAP showed a main effect of Lesion [$F(1,54) = 5.23$, $P<0.05$] due to the overall higher MAP in lesioned animals. A main effect of CO_2 level [$F(1,54) = 7.38$, $P<0.01$] was due to a reduction of MAP with increasing CO_2.

An overall 2-way ANOVA with repeated measures examining the effect of Lesion and CO_2 level on HR showed a main effect of CO_2 level [$F(1,54) = 62.59$, $P<0.01$] due to an overall bradycardic effect of increasing CO_2.

An overall 2-way ANOVA with repeated measures examining the effect of Lesion and CO_2 levels on RSNA showed an interaction between Lesion and CO_2 level [$F(1,34) = 5.86$, $P<0.01$] due to an attenuation of the sympathoexcitatory effect of CO_2 in lesioned rats. A main effect of Lesion [$F(1,34) = 8.08$, $P<0.01$] was due to the overall lower level of RSNA in lesioned animals. A main effect of CO_2 level [$F(1,34) = 4.18$, $P<0.01$] was due to the overall increase in RSNA over the course of the central chemoreflex challenge.

An overall 2-way ANOVA with repeated measures examining the effect of Lesion and CO_2 level on dEMG activity showed a Lesion and CO_2 level interaction [$F(1,28) = 3.65$, $P<0.05$] due to the greater increase of dEMG during increasing CO_2 in sham-lesioned rats. Main effects of Lesion [$F(1,28) = 5.56$, $P<0.01$] and CO_2 level [$F(1,28) = 20.50$, $P<0.01$] were also observed. The main effect of Lesion was due to an overall higher dEMG in sham-lesioned rats, while the main effect of CO_2 level was due to increased dEMG with increasing CO_2.

An overall 2-way ANOVA with repeated measures examining the effect of Lesion and CO_2 level on RR activity showed a main effect of CO_2 level [$F(1,44) = 137.08$, $P<0.01$] due to increasing RR activity in both groups during increasing CO_2.

Table 3. Arterial blood pH and $PaCO_2$ at the end of 5 min exposure to hyperoxic, hypercapnia

	pH			$PaCO_2$		
	Baseline	5%	8%	Baseline	5%	8%
Control (7)	7.50±0.01	7.46±0.01	7.36±0.01	43.0±0.8	50.8±0.6	64.3±0.6
Lesion (6)	7.50±0.01	7.46±0.01	7.37±0.01	42.8±0.6	50.7±1.2	64.4±1.2

Values are group means ± SEM in rats subjected to sham-lesioned (Control) or neurotoxin lesioned (Lesion) 2 weeks prior to exposure to hyperoxic hypercapnia. Group n are indicated in parentheses. Two-way ANOVA with repeated measures were used to determine effects of Lesion and Ambient CO_2 on pH and $PaCO_2$. There were no significant differences found between groups.

Table 4. Indices of baroreflex gain, heart rate and blood pressure variability in lesioned and control rats

		Up Sequences (ms/mmHg)	Down Sequences (ms/mmHg)	All Sequences (ms/mmHg)	Alpha (LF)	Alpha (HF)	LF power ($mmHg^2$)	BP SDNN	LF/HF
Control (15)	SBP	0.98 ± 0.11	0.84 ± 0.06	0.94 ± 0.09	0.37 ± 0.04	0.75 ± 0.13	53.6 ± 11.8	7.62 ± 0.74	
	MBP	1.18 ± 0.13	1.23 ± 0.09	1.21 ± 0.10	0.39 ± 0.05	0.98 ± 0.20	42.5 ± 9.1	6.56 ± 0.59	1.25 ± 0.23
	DBP	1.27 ± 0.15	1.18 ± 0.09	1.24 ± 0.11	0.42 ± 0.05	1.01 ± 0.20	38.9 ± 8.5	6.25 ± 0.55	
Lesion (9)	SBP	1.40 ± 0.18*	1.13 ± 0.14*	1.30 ± 0.16*	0.48 ± 0.10	1.09 ± 0.23	33.3 ± 18.8	4.87± 0.88*	
	MBP	1.87 ± 0.27*	1.65 ± 0.18*	1.77 ± 0.22*	0.53 ± 0.11	1.51 ± 0.39	25.2 ± 14.1	4.06 ± 0.75*	0.71 ± 0.16
	DBP	1.85 ± 0.26*	1.60 ± 0.15*	1.74 ± 0.20*	0.55 ± 0.12	1.53 ± 0.34	22.5 ± 12.6	3.89 ± 0.70*	

Spontaneous baroreflex gain was determined by the sequence method using ascending (up) only, descending only (down) or all sequences that met criteria outlined in the text. Values are group means ± SEM. Group n are indicated in parentheses. * $P<0.05$, lesioned vs. sham-lesioned animals. Gain was determined by the sequence method using systolic blood pressure (SBP), mean blood pressure (MBP), diastolic blood pressure (DBP). Spectral coherence between IBI and BP variability are reported as coherence in the low frequency domain (alpha LF) or high

frequency domain (alpha HF). Power of BP variability in the low frequency domain (LF power) and in the time domain (BP SDNN) and the ratio of low frequency to high frequency heart rate variability (LF/HF) are also included in the analysis.

Gain using SBP on up sequences [df = 22, t = 2.18, $P<0.05$], down sequences [df = 22, t = 2.16, $P<0.05$] and all sequences [df = 22, t = 2.24, $P<0.05$] was higher in lesioned animals. Gain using MBP on up sequences [df = 22, t = 2.64, $P<0.05$], down sequences [df = 22, t = 2.53, $P<0.05$] and all sequences [df = 22, t = 2.70, $P<0.05$] was higher in lesioned rats. Gain using DBP on up sequences [df = 22, t = 2.23, $P<0.05$], down sequences [df = 22, t = 2.48, $P<0.05$] and all sequences [df = 22, t = 2.40, $P<0.05$] were higher in lesioned rats.

Coherence of variability in IBI and BP did not differ regardless of whether SBP, MBP or DBP was used.

No significant differences were found in the power of BP variability of the LF domain or in the HR variability LF/HF ratio between groups. However, systolic BP SDNN [df = 22, t = 2.3474, $P<0.05$], DBP [df = 22, t = 2.6443, $P<0.05$] and MBP [df = 22, t = -2.6010, $P<0.05$] were significantly lower in lesioned rats.

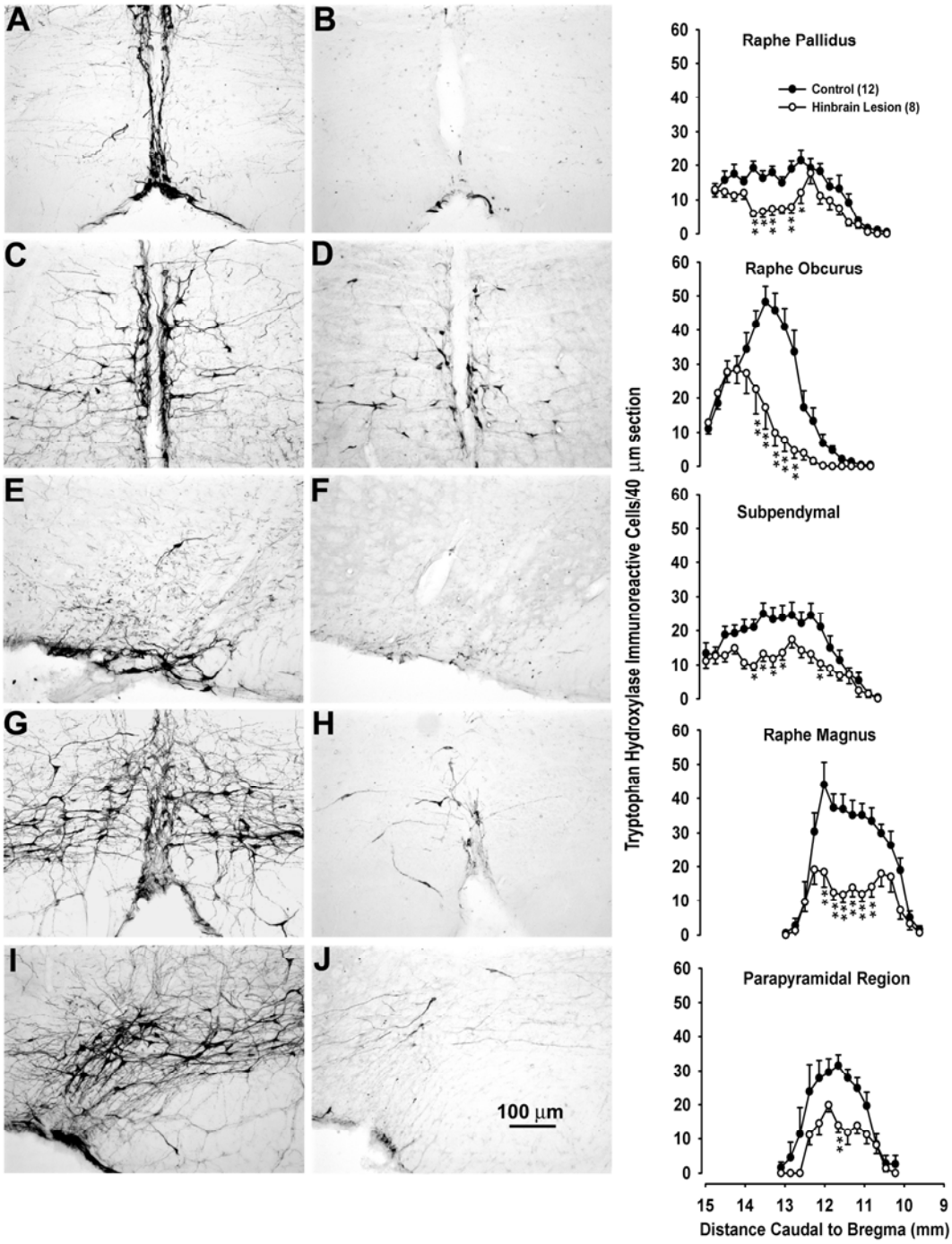

Figure 12. Typical tryptophan hydroxylase immunoreactivity (TPH-ir) is shown in the raphe pallidus (A,B), the raphe obscurus (C,D), the subependymal cells of

the parapyramidal region (E,F), the raphe magnus (G,H) and the parapyramidal cells (I,J) from 40 μM sections obtained from rats subjected to hindbrain injection of vehicle (A,C,E,G,I) or 5,7-dihydroxytryptamine (B,D,F,H,J). Cell profiles of TPH-ir positive cells are shown for each serotonin-rich nucleus throughout the extent of the nucleus. Data are group means ± SEM. Group n are indicated in parentheses.

Data were analyzed by 2-way ANOVA with repeated measures using Lesion and Distance from Bregma as factors. Main effects and significant interactions were followed up with between-group comparisons using Newman-Keul post-hoc test. *, ** $P<0.05$, <0.01 sham-lesioned vs. lesioned animals, respectively.

An overall 2-way ANOVA with repeated measures examining the effect of Lesion and Distance from Bregma on TPH-ir positive cell numbers in RP showed a Lesion x Distance from Bregma interaction [$F(1,324) = 2.60$, $P<0.01$] due to lower numbers of TPH-ir positive cells in the region around the obex, but not at the caudal and rostral portion of the nucleus of lesioned rats compare to sham-lesioned rats. A main effect of Lesion [$F(1,324) = 8.66$, $P<0.01$] was due to an overall decrease in cell number in lesioned rats. A main effect of Distance from Bregma [$F(1,324) = 18.38$, $P<0.01$] was due to the change in TPH-ir positive cell number along the nucleus.

An overall 2-way ANOVA with repeated measures examining the effects of Lesion and Distance from Bregma in the RO showed a Lesion x Distance from Bregma interaction [F (1,306) = 9.07, $P<0.01$] due to the significant effect of Lesion in the center of the nucleus with only a limited effect at the caudal end of the nucleus. A main effect of Lesion [F (1,306) = 11.45, $P<0.01$] was due to the overall decreased number of TPH-ir positive cells in the nucleus of the lesioned rats. A main effect of Distance from Bregma [F (1,306) = 32.85, $P<0.01$] was due to the change in number of TPH-ir positive cell throughout the extent of the normal nucleus.

An overall 2-way ANOVA with repeated measures examining the effect of Lesion and Distance from Bregma in the SUB region showed a Lesion x Distance from Bregma interaction [F (1,324) = 2.07, $P<0.01$] due to a decrease in TPH-ir positive cell number throughout the center of the nucleus, but not the most rostral and caudal ends of the nucleus. Main effects of Lesion [F (1,324) = 5.58, $P<0.01$] and Distance from Bregma [F (1,324) = 17.01, $P<0.01$] were due to the decrease TPH-ir positive cell numbers in lesioned rats and differences in TPH-ir positive cell number over the length of the whole nucleus.

An overall 2-way ANOVA with repeated measures examining the effect of Lesion and Distance from Bregma on TPH-ir cell number in the RM showed a Lesion x Distance from Bregma interaction [F (1,252) = 4.38, $P<0.01$] due to the decrease

of TPH-ir positive cell numbers in the center of the nucleus in lesioned rats. A main effect of Lesion [F (1,252) = 19.84, $P<0.01$] was due to the overall decrease in TPH-ir positive cell numbers in lesioned rats. An effect of Distance from Bregma [F (1,252) = 19.78, $P<0.01$] was due to the change in TPH-ir positive cell number along the extent of the nucleus.

An overall 2-way ANOVA with repeated measures examining the effect of Lesion and Distance from Bregma on TPH-ir cell numbers in the PPY region showed a main effect of Lesion [F (1,216) = 12.58, $P<0.01$] due to an overall decrease in TPH-ir positive cell numbers in lesioned rats. A main effect of Distance from Bregma [F (1,216) = 11.19, $P<0.01$] was due to the change in TPH-ir positive cell numbers along the extent of the whole nucleus.

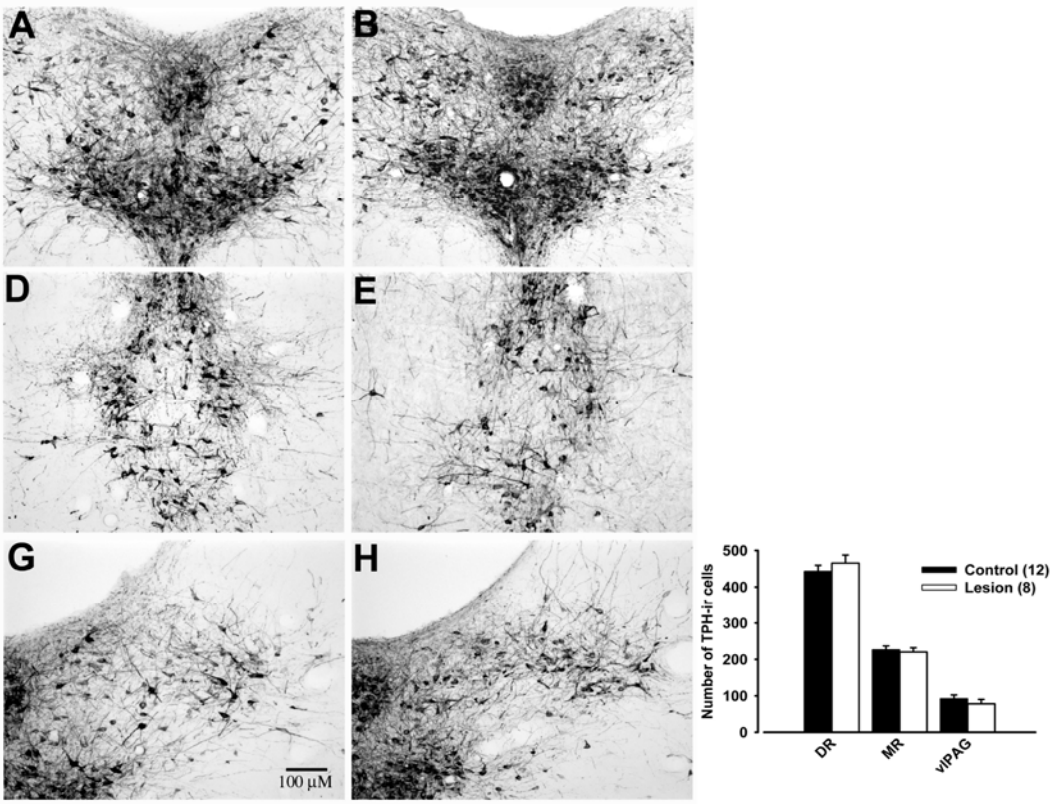

Figure 13. Representative images of the midbrain serotonergic nuclei demonstrating tryptophan hydroxylase immunoreactivity (TPH-ir) in the dorsal raphe (DR) (A,B), the median raphe (MR) (D,E) and the ventrolateral periaqueductal gray (G,H) in rats treated with vehicle (A,D,G, control) or 5,7-dihydroxytryptamine (B,E,H, lesion) in the hindbrain raphe regions. Also shown are total TPH-ir cells counted from sections throughout the two major midbrain nuclei, the DR and MR as well as the vlPAG averaged across groups. Student's t tests were performed. There were no significant group differences found in TPH-ir positive cell number. Group n are indicated in parentheses.

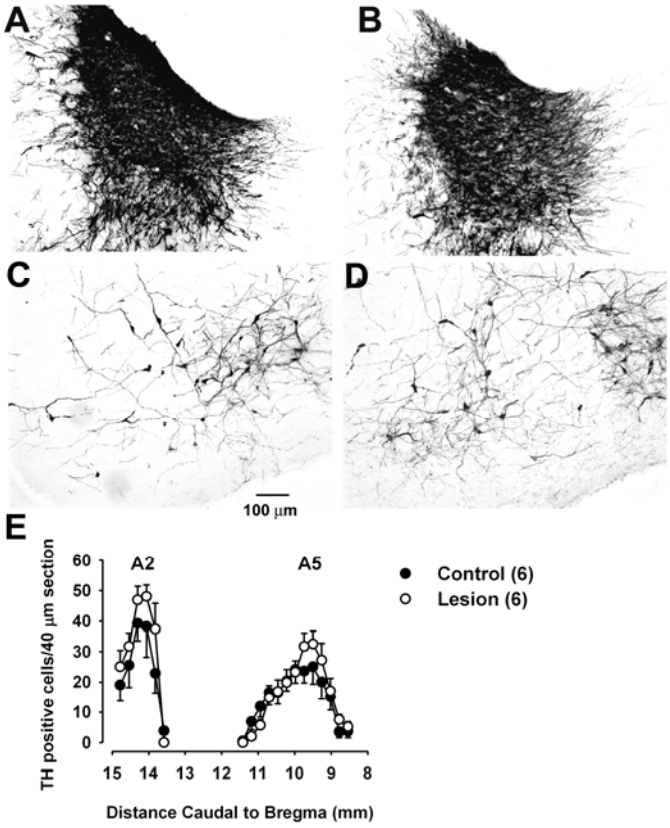

Figure 14. Images of representative sections showing tyrosine hydroxylase immunoreactivity (TH-ir) in the locus coeruleus (A, B), and the ventrolateral medulla (C, D) in vehicle-treated (A, C) and 5,7- dihydroxytryptamine treated rats (B, D). Cell profiles of TH-ir positive cells are shown for the A2 and A5 cell groups in control and lesioned rats (E). Data are group means ± SEM. Group n are indicated in parentheses. Overall 2-way ANOVA with repeated measures were preformed to examine the effect of Lesion and Distance from Bregma on TH-ir positive numbers of each region (A2 and A5). There was no significant difference found between groups.

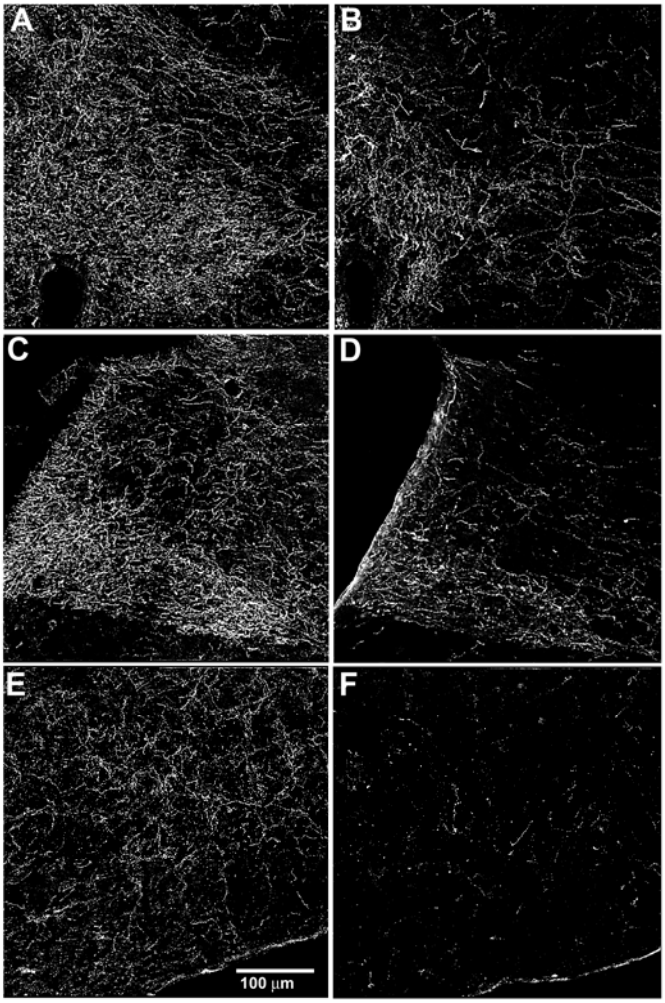

Figure 15. Typical serotonin immunoreactivity in the terminal fields of the dorsomedial medulla at the level of the comNTS (A, B), the medial subnucleus of the NTS (C, D) and the C1 region of the RVLM (~11.8 mm caudal from Bregma; E-F) in sham-lesioned (A,C,E) and lesioned rats (B,D,F).

Table 5 Serotonin immunoreactivity in medullary terminal fields

	comNTS	mNTS	RVLM (-11.8)	RVLM (-12.1)	RVLM (-12.8)
Control (12)	19.9 ± 6.2	16.6 ± 5.4	22.4 ± 9.1	17.4 ± 5.0^{-8}	14.4 ± 3.4
Lesion (10)	9.9 ± 3.9 **	7.3 ± 5.5 **	3.4 ± 2.5 **	3.4 ± 2.6 **	2.0 ± 1.1 **
% decrease	50.3%	56.0%	84.8%	80.5%	86.1%

Data are expressed as percent of thresholded area occupied by thresholded signal. Fiber density is reported for the commissural subnucleus of the NTS (comNTS), the medial subnucleus of the NTS (mNTS), and in 3 rostro-caudal planes of the RVLM at the indicated distance in mm caudal to Bregma.

Serotonin fiber density was compared between groups by Student's t-test. Values are group means ± SD. Group n are indicated in parentheses. * $P<0.05$, lesioned vs. sham-lesioned animals.

Fiber density in the comNTS [df = 20, t = 4.55, $P<0.01$] and mNTS [df = 20, t = 3.87, $P<0.01$] were significantly lower in lesioned rats. Fiber content in the RVLM was reduced in lesioned rats at all levels tested (-11.8 mm) [df = 20, t = 6.41, $P<0.01$], (-12.12 mm) [df = 20, t = 7.95, $P<0.01$] and (-12.80 mm) [df = 20, t = 11.07, $P<0.01$].

Discussion

Previously our lab found that serotonin cells of 5 serotonin-rich regions were selectively activated by hypotensive hemorrhage in unanaesthetized rats (Glasgow et al., 2009; Ruszaj et al., 2006). These regions include 4 caudal medullary regions: RO, RM, SUB and the PPY. In addition, more rostral serotonin cells in the vlPAG region were also selectively activated by acute hypotensive hemorrhage. In the current study, selective destruction of serotonin cells in the same caudal raphe nuclei produced substantial loss of serotonin innervation of the RVLM (>80%) and NTS (>50%). Lesion also slightly accelerated the sympatholytic response to blood loss and attenuated recovery of sympathetic activity and ventilation during the second compensatory phase of hemorrhage compared to sham-lesioned rats.

These findings contradict several lines of evidence that propose that serotonin release contributes to the sympatholytic response to severe blood loss. In prior studies, systemic administration of the tryptophan hydroxylase inhibitor, p-CPA, was found to attenuate the hypotensive and bradycardic responses to severe hemorrhage in the pentobarbital-anesthetized cat (Elam et al., 1985). Systemic p-CPA treatment also prevented the sympatholytic response to severe blood loss in chloralose-anesthetized rats (Morgan et al., 1988). A more recent study found that unilateral injection of a selective serotonin 5-HT_{1A}-receptor antagonist in the pressor region of the RVLM prevented the sympatholytic response and delayed the depressor response to blood loss in rats hemorrhaged

under sodium pentobarbital anesthesia (Dean and Woyach, 2004). Together, these studies have led to the view that blood loss stimulates serotonin release which acts on 5-HT_{1A}-receptors expressed by bulbospinal pre-sympathetic neurons to cause membrane hyperpolarization and loss of tonic excitatory drive to sympathetic neurons.

Similar to us, Evans et al. also failed to demonstrate any effect of serotonin depletion on the depressor response to simulated hemorrhage in unanaesthetized rabbits. In their studies a similar regimen of p-CPA treatment that caused a 70% reduction in medullary serotonin content had no effect on the depressor response to caval vein occlusion (Evans et al., 1992). It could be argued that a more substantial depletion of serotonin must be achieved to affect the depressor response to hemorrhage, particularly in the absence of anesthesia when serotonin cell activity is typically greater (Trulson, 1985). However, even a very discrete (14 pmol), unilateral injection of 5-HT_{1A}-receptor antagonist in the RVLM attenuated the sympatholytic response to blood loss in anesthetized rats (Dean and Bago, 2002). Thus, if a similar mechanism mediates the onset of hypotension in the unanaesthetized animal, then even partial depletion of serotonin should be sufficient to observe some attenuation of the response. In the present study, loss of more than 80% of serotonin nerve terminal immunoreactivity in the C1 region of the RVLM had no effect on the depressor response to blood loss. Moreover, there was no correlation between the extent of serotonin depletion in the RVLM and the volume of blood loss that produced a

40 mmHg drop in BP (data not shown). Instead, serotonin lesion shortened the primary compensatory response to blood loss, suggesting that serotonin neurons facilitate responses that counteract sympathoinhibition in conscious rats.

Prior work has shown that inactivation of cells in the ventromedial medullary raphe region interferes with normal recovery of BP and HR following blood loss (Henderson et al., 2000a). Chemical inactivation of the ventromedial raphe region that lies caudal to the obex exaggerates hypotension and slows the secondary compensatory recovery of BP and HR, while inactivation of regions rostral to obex delays the sympatholytic phase of hemorrhage in urethane-anesthetized rats (Heslop et al., 2002). In the present study, hindbrain neurotoxin injections were effective in depleting serotonin cells rostral to obex, but had little effect on more caudal cells. Taken together, the evidence is consistent with the view that neurons in the ventromedial medulla that mediate the depressor response during sympatholytic phase of hemorrhage are either not serotonergic, or contribute to a redundant serotonin-dependent pathway that mediates sympatholysis under anesthesia, while an alternative non-serotonergic pathway is activated in the unanaesthetized rats. Alternatively, it is plausible that a non-serotonergic pathway that remains inactive under anesthesia compensates for serotonergic-mediated sympatholytic effects after lesion in unanaesthetized animals.

It is not likely that loss of serotonin neurons inhibited sympathetic recovery during the secondary compensatory phase of hemorrhage by disrupting the

baroreflex. Instead, our data indicate that medullary serotonin cells may actually reduce BRS. Lesion of serotonin cells enhanced spontaneous baroreflex control of HR (Table 4). Spontaneous baroreflex assessment by this method tends to be biased towards the vagal component of the reflex, given the more rapid cadiovagal reflex response to changes in BP. Thus, the sequence method may not adequately reflect alterations in sympathetic baroreflex function. While we did not directly test baroreflex control of sympathetic function, we did note a reduction in the SDNN of BP in lesioned animals. Baroreflex-mediated oscillations in sympathetic vasomotor control provide an important buffer that limits BP variability (Julien et al., 1995). Reduced fluctuations in BP suggest that sympathetic baroreflex control of vasomotor tone was enhanced in lesioned animals. Indices of baroreflex gain and sensitivity using frequency analysis methods failed to demonstrate a significant effect of lesion, but this may have been due to the higher variability associated with spectral methods. Interestingly, the gain of HR and renal sympathetic baroreflex responses to nitroprusside is increased following more discrete lesions of serotonin nerve terminals in the NTS with 5,7-DHT (Itoh et al., 1992). In our study, we also observed significant loss of serotonin nerve terminals within the medial subnucleus of the NTS where the majority of baroreceptor afferents terminate.

The attenuated recovery of sympathetic activity during the secondary compensatory phase of hemorrhage could have been due to enhanced baroreflex suppression of sympathetic activity during recovery of BP. However,

this seems unlikely given that HR responses were similar in lesioned and sham-lesioned animals. Moreover, ventilation normally increases with decreasing pressure due to baroreceptor unloading, yet ventilation slowed with the onset of blood withdrawal in lesioned animals (Brunner et al., 1982). Deficits in ventilation and sympathoexcitation seemed to parallel one another, suggesting that altered sympathetic function may have been a consequence of suppressed central respiratory drive.

In accord, serotonin lesion may have disrupted peripheral chemoreflex function and thus ventilatory and sympathetic responses to hemorrhage. Hypoxia is a potent stimulus for c-Fos expression in serotonin neurons and produces patterns of activation similar to those observed with our hemorrhage protocol (Erickson and Millhorn, 1994; Glasgow et al., 2009; Ruszaj et al., 2006). Though we did not observe direct evidence of arterial blood hypoxia during the course of the study, arterial blood pH was reduced, suggesting that peripheral chemoreceptors could have been activated, particularly during recovery (Table 3). However, the role of serotonin neurons in modulating the sensitivity of the peripheral chemoreflex has not been well studied and remains controversial. In humans, dietary tryptophan depletion does not affect chemoreflex activation or sensitivity (Struzik et al., 2002). However, electrical or chemical stimulation of the medullary raphe decreased activation of chemoresponsive cells in the NTS during exposure to cyanide in rats (Perez and Ruiz, 1995). Nucci and colleagues showed that blockade of 5-HT_{1A} receptors in the RM increased

hypoxic ventilatory response in conscious rats, suggesting that serotonin neuronal activity in the caudal raphe suppresses hypoxic responses to chemoreceptor activation (Nucci et al., 2008). These findings would seem to contradict the possibility that serotonin lesion decreased ventilatory and sympathetic activity during the 2^{nd} compensatory phase of hemorrhage by suppressing chemoreflex activity.

More compelling data suggest that caudal serotonin cells are important in central chemoreception, particularly in the absence of anesthesia. Recently it was found that the integrity of RM serotonin cells is necessary for normal ventilatory responses to hypercapnia in conscious rats (Dias et al., 2007). We extended these findings by demonstrating that serotonin cells of the caudal raphe are necessary for both normal ventilatory and sympathetic responses to selective activation of the central chemoreceptors with hyperoxic hypercapnia. Moreover, hypercapnia produces a similar pattern of serotonin c-Fos expression as that observed after our hemorrhage protocol (Miura et al., 1998). In our hemorrhage study, we did not observe overt signs of respiratory acidosis. In fact, $PaCO_2$ fell during active blood loss, likely in response to the increased ventilation that developed during the initial stage of blood loss. However, $PaCO_2$ subsequently rose almost 30% during the post-hemorrhage recording period despite slightly higher ventilation and increased PaO_2. Thus, the rise in $PaCO_2$ likely resulted from the buffering of metabolic acidosis. Lesioned rats showed attenuated ventilatory and sympathetic responses during a similar rise in $PaCO_2$, consistent

with the possibility that central chemoreceptor activation contributes to normal ventilatory and sympathetic responses to blood loss.

Lesioned animals developed higher PaO_2 by the end of hemorrhage despite evidence of reduced ventilation throughout recovery. This may have resulted from reduced ventilation/perfusion mismatch, since lesioned animals also demonstrated a reduced estimated alveolar arterial oxygen pressure difference by the end of the recording period. Lesioned animals also experienced more severe tissue hypoxia as evidenced by an exaggerated accumulation of lactate and lower pH following recovery from hemorrhage. These data suggest that lesioned animals had higher lung perfusion and/or reduced ventilatory mismatch than controls. It is not readily apparent how lesioned animals were able to maintain PaO_2 despite lower ventilation. It is possible that a lower extracellular pH in pulmonary tissue of serotonin lesioned animals may have reduced the stimulus for bronchiole constriction and facilitated correction of the ventilation/perfusion mismatch. The cumulative evidence suggests that lesioned animals experienced more severe tissue hypoxia due, in part, to reduced delivery of blood to peripheral tissue. Reduced blood delivery developed in lesioned rats despite normal BP recovery. These data further suggest that lesioned animals maintained BP through a potentially detrimental increase in arterial resistance. Though this idea remains to be confirmed with direct measures of cardiac output, the data do suggest that caudal hindbrain

serotonin neurons may help to preserve cardiac output following hemorrhage, possibly by facilitating sympathetic-dependent increases in venous return.

It remains to be determined how arterial vascular resistance was elevated when sympathetic activity was attenuated. We used renal sympathetic activity as an index of sympathetic vasomotor tone, despite its better characterized role in volume regulation. It is clear that changes in renal sympathetic nerve activity often times do not track with changes in sympathetic drive to other vascular beds that are important in maintaining peripheral resistance. In fact, renal sympathetic nerves provide little contribution to overall vasomotor tone and instead contribute more to volume regulation (Osborn and Fink, 2009). Nevertheless, we have found that changes in renal sympathetic activity parallel those of splanchnic nerve activity during progressive blood loss and subsequent hemorrhagic shock (Tiniakov and Scrogin, 2009). Thus, the uncoupling of BP recovery from RSNA recovery was surprising. This would suggest that vasoactive hormones may have maintained BP in the absence of sympathetic-mediated vasoconstriction in lesioned rats.

Both rostral and caudal raphe neurons of the ventromedial medulla provide major direct projections to pre-ganglionic sympathetic cells, including those that contribute to activation of brown adipose tissue and thermogenesis (Nakamura et al., 2004). Though body temperature was not measured in our studies, a report in awake rabbits indicated that blood loss of a similar magnitude to that used in our studies resulted in a rapid decrease in core body temperature,

metabolism, and oxygen consumption (Henderson et al., 2000b). Ambient cooling sufficient to reduce core temperature also reduces renal sympathetic activity in anesthetized rats (Kenney et al., 1999; Sabharwal et al., 2004). Thus, a loss of raphe-mediated thermogenesis could have contributed to an exaggerated fall in core temperature and sustained inhibition of renal sympathetic activity following hemorrhage. However, studies in hemorrhaged rabbits indicate that decreases in body temperature preceded decreased metabolism, suggesting instead that thermogenesis is suppressed during hypovolemia. In accord, transient hypotensive hemorrhage reduces the threshold for shivering in barbiturate-anesthetized cats, as does hypoxia in conscious cats (Gautier et al., 1987; Little et al., 1980). Anatomical data indicate that the majority of ventromedial raphe cells that express c-Fos following exposure to thermogenic stimuli are glutamatergic rather than serotonergic (Nakamura et al., 2004). Thus, it seems unlikely that serotonin cell lesion attenuated recovery of renal sympathetic activity by preventing thermogenic responses to blood loss.

It should be noted that 5,7-DHT destroys the entire cell and in so doing depletes not only serotonin, but also important co-transmitters that have been implicated in the control of ventilation, including thyrotropin releasing hormone and substance P (Gray et al., 1999; Greer et al., 1996). It remains to be determined whether loss of serotonin *per se* contributes to the observed effects. Moreover, 5,7-DHT is not entirely selective for serotonin neurons. The

neurotoxin has a high affinity for the serotonin reuptake transporter through which the toxin is thought to gain access to the cell to promote oxidative stress and retrograde degeneration (Tabatabaie et al., 1993). The neurotoxin 5,7-DHT also has affinity for NE and dopamine transporter proteins (Horn et al., 1973). Noradrenergic neurons of the A1, A2 and A5 cell groups express NE reuptake transporter protein and also regulate sympathetic function (Lorang et al., 1994). However, in our study prior administration of nomifensine appeared to be effective in preventing cell death or morphologic changes of TH-ir cells. Thus, it is unlikely that diminished sympathetic recovery was due to toxic effects on noradrenergic cells.

In summary, the current study provides further evidence that serotonin does not contribute to the sympatholytic response to blood loss in unanaesthetized animals. In addition, the data provide compelling evidence that caudal medullary serotonergic neurons contribute to normal ventilatory and sympathetic reflex responses to acidosis during the secondary compensatory phase of hypotensive hemorrhage, which may, in turn, facilitate beneficial hemodynamic responses to support microcirculation during hemorrhagic shock.

CHAPTER IV

5-HT_{1A}-receptor agonists act on non-serotonergic cells to accelerate sympathetic recovery following hypotensive hemorrhage in conscious rats

Abstract

Substantial evidence suggests that serotonin contributes to the sympatholytic response to blood loss. Yet, the 5-HT_{1A}-receptor agonist, 8-OH-DPAT, accelerates recovery of BP in animals subjected to hypotensive hemorrhage. Here, we tested whether 8-OH-DPAT mediates its effects through activation of inhibitory 5-HT_{1A} autoreceptors expressed on serotonergic neurons. Blood pressure, HR, and renal sympathetic responses to hypotensive hemorrhage and subsequent injection of 8-OH-DPAT (30 nmol/kg, i.v.) were measured in conscious rats subjected to global serotonergic lesion. Cerebroventricular injection of the serotonin neurotoxin, 5,7-DHT, reduced serotonin cell numbers (30-60%) in all serotonergic nuclei. Global lesion did not affect the sympatholytic response to blood loss or the sympathoexcitatory response to 8-OH-DPAT following hypotensive hemorrhage. Instead, sympathetic activity was attenuated after termination of hemorrhage in rats

subjected to global lesion (40.5 ± 24.6 vs. -11.0 ± 10.1 %baseline 25 min after start of hemorrhage, $p<0.05$). These data indicate that serotonin neurons are not critical for the sympatholytic response to hemorrhage in conscious rats, and that the sympathoexcitatory effect of 8-OH-DPAT is likely not mediated by inhibition of serotonergic neurons. Instead, the data confirm our prior findings that serotonin neurons contribute to the secondary compensation that follows hypotensive hemorrhage and that 8-OH-DPAT mediates the sympathoexcitatory effect following hypotensive hemorrhage by acting on non-serotonergic cells.

Introduction

Progressive hemorrhage leads to a complex, multiphasic autonomic response. The primary compensatory phase of blood loss is mediated by arterial baroreceptor unloading, which activates sympathetic drive and increases HR. This process is also augmented by cardiopulmonary reflex activation (Osei-Owusu and Scrogin, 2006; Quail et al., 1987; Schreihofer et al., 1994). After significant blood loss, these compensatory responses suddenly cease, resulting in a sympatholytic phase characterized by rapid sympathetic withdrawal and cardiac vagal activation (Barcroft and Edholm, 1945; Osei-Owusu and Scrogin, 2006; Schadt and Ludbrook, 1991). This phase is similar to fainting and is therefore often referred to as the syncopal response. If blood loss continues, circulatory shock develops. During this secondary compensatory phase autonomic compensation is slowly re-established, resulting in tachycardia and

sympathoexcitation (Tiniakov and Scrogin, 2006). However, if blood loss persists, a decompensation phase develops. During this phase, the vasculature becomes unresponsive to catecholamines, leading to a vascular decompensation that is difficult to treat (Liu et al., 2003).

The sympatholytic syncopal response to blood loss is attenuated in anesthetized animals subjected to global serotonin depletion (Blum and Spath, 1986; Elam et al., 1985; Morgan et al., 1988). Similarly, systemic administration of the broad-spectrum serotonin receptor antagonist, methysergide, rapidly reverses the sympatholytic response to blood loss and improves survival of anesthetized cats subjected to severe hemorrhage (Elam et al., 1985). However, subsequent studies have repeatedly failed to identify specific serotonin receptor antagonists that can prevent the sympatholytic response to blood loss in conscious animals (Evans et al., 1992; Scrogin et al., 2000). Instead, the serotonin 5-HT_{1A}-receptor agonist, 8-OH-DPAT, was found to mimic methysergide's ability to delay the onset of the sympatholytic response in conscious rabbits and rats, as well as to reverse the response to acute hemorrhage in rats (Evans et al., 1992; Scrogin, 2003; Scrogin et al., 2000). The cardiovascular effects of both 8-OH-DPAT and methysergide observed in hypovolemic rats are prevented by prior treatment with the selective 5-HT_{1A}-receptor antagonist, WAY-100635 (Scrogin et al., 2000).

Subsequent studies have shown that injection of 8-OH-DPAT in the cisterna magna in the vicinity of dorsomedial brainstem rapidly reverses the

hypotensive response to hypovolemia (Scrogin, 2003). In marked contrast, injection of the 5-HT_{1A}-receptor antagonist, WAY-100635, directly into the pressor region of the RVLM attenuates the sympatholytic response to blood loss in anesthetized rats suggesting that 5-HT_{1A} receptors in the RVLM mediates sympathoinhibition during hemorrhage (Dean and Bago, 2002). Together, the data suggest that a so far unidentified population of hindbrain 5-HT_{1A} receptors, distinct from those that promote sympathoinhibition in the RVLM, stimulate a paradoxical sympathoexcitatory response in hypovolemic animals.

5-HT_{1A} receptors are expressed by non-serotonergic targets of serotonin cells as well as by serotonergic cells themselves (Kheck et al., 1995; Riad et al., 2000). Agonist binding of somatodendritic 5-HT_{1A} autoreceptors expressed in serotonergic neurons of the raphe nuclei inhibits the frequency of serotonergic neuron firing and reduces nerve terminal serotonin release (Sprouse and Aghajanian, 1987; Trulson, 1985). Therefore, the possibility remains that 5-HT_{1A}-receptor agonists reverse the sympatholytic response to blood loss by inhibiting serotonin cell firing and thus reducing serotonin release from nerve terminals that mediate a sympatholytic effect during hemorrhage. To test this hypothesis, cardiovascular responses to hemorrhage were measured in animals subjected to global serotonin cell lesion in order to remove inhibitory 5-HT_{1A} autoreceptors. It was reasoned that if serotonin cells mediate the sympatholytic response, their destruction would delay the response. At the same time, removal of the autoinhibitory 5-HT_{1A} receptor population would prevent or attenuate the

sympathoexcitatory effect of 8-OH-DPAT during hemorrhage if the agonist acts on autoreceptors to reverse downstream sympathoinhibitory effects of endogenous serotonin release. In our previous study, neurotoxic lesion of serotonin cells limited to the caudal hindbrain did not delay the sympatholytic response, leaving the possibility open that more rostral serotonin cells contribute to this phase. Therefore, in this study we attempted to lesion all serotonin neurons to investigate this hypothesis.

Methods

Animals

Male Sprague-Dawley rats (300 - 350 g, Harlan, Indianapolis, IN) were given *ad libitum* access to food and water while being acclimated to the housing facility at least 1 wk prior to surgery. The facility was maintained at a constant temperature of 22 ± 2 °C with a light/dark cycle of 12:12 hrs. All experiments were approved by the Institutional Animal Care and Use committee and were conducted in accordance with the Guide for the Care and Use of Laboratory Animals as adopted and promulgated by the US National Institutes of Health.

Surgery

Neurotoxin studies: Rats were pre-treated with the dopamine and norepinephrine re-uptake blocker nomifensine (15 mg/kg). Rats were then anesthetized with sodium pentobarbital (65 mg/kg, i.p.) and placed in a

stereotaxic apparatus, after which 5-µl injections of either vehicle (0.1% ascorbic acid) or 5,7-DHT (5 mM in 0.1% of ascorbic acid) were made in both the lateral ventricle (randomly determined left or right hemisphere) and the cisterna magna. For lateral ventricle injections, rats were positioned in the stereotaxic apparatus with the head leveled between Bregma and Lamda. Injections were made through a burr hole positioned 1.6 mm lateral-, and 1.0 mm caudal to Bregma. The injector (25 ga. hypodermic needle) was lowered 3.8 mm ventral to the skull surface. Neurotoxin or vehicle was injected into the lateral ventricle over 5 min. The needle was left in place for an additional 5 min. For cisterna magna injection, the rat's nose was lowered to enable exposure of the occipital membrane. The neck muscles were separated from the nuchal crest exposing the occipital bone. The occipital membrane was pierced just caudal to the edge of the occipital bone and the needle was positioned approximately 1 mm below the membrane taking care not to pierce the underlying tissue. Either 5,7-DHT (5 mM in 0.1% ascorbic acid) or vehicle (0.1% ascorbic acid) was infused into the 4^{th} ventricle over 5 min, after which the injector was left in place for an additional 5 min. The injector was then removed slowly and the incision was sutured using non-absorbable 3-0 silk suture.

Two weeks later rats injected with neurotoxin or vehicle were re-anesthetized with sodium pentobarbital (65 mg/kg, i.p.) and implanted with vascular catheters (PE-50 heat-welded to a length of PE-10) one day prior to the experiment. Catheters were placed bilaterally in the femoral arteries to enable

direct measurement of arterial pressure and simultaneous arterial blood withdrawal. A third catheter was placed unilaterally in the femoral vein for drug injections. Catheters were occluded with 25 ga wire and were externalized at the nape of the neck and secured with sutures. During the same surgery, a renal sympathetic recording electrode was implanted as previously described (Scrogin, 2003). Briefly, a 1-2 mm segment of a sympathetic fiber bundle emanating from the aorticorenal ganglion was isolated and placed on a stainless steel, Teflon-coated (bare diameter =.005 in., A-M Systems Inc., Everett, WA) bipolar electrode implanted through a left flank incision. The electrode connector was externalized subcutaneously at the nape of the neck along with the three vascular catheters. Viability of the nerve preparation was determined by auditory assessment of the bursting activity, after which the preparation was embedded in a quick drying, lightweight silicon (Kwik-sil, World Precision Instruments). The flank incision was sutured closed in two layers with the electrode leads coiled within the subcutaneous space. Animals were allowed to recover overnight prior to experimentation.

Data Acquisition

Arterial pressure, HR, and RSNA were recorded on a Macintosh G4 Powerbook computer using PowerLab data acquisition software (Chart v. 5.2.1, ADinstruments, Colorado Springs, CO). Arterial pressure was measured with a disposable pressure transducer (Transpac® IV, Abbott Labs, North Chicago, IL)

and a PowerLab bridge amplifier (ADinstruments, CO). Heart rate was calculated using peak-to-peak detection of the pulse pressure wave. Sympathetic activity was sampled (4,000 Hz) and amplified (10-20,000x) with a PowerLab Bioamplifier (ADinstruments, CO). The recorded neurogram was filtered (1-1000 Hz), rectified and integrated over a 20-ms time constant. Background noise in the electrode recording was determined at the end of each experiment by measuring the remaining signal following ganglionic blockade (hexamethonium chloride, 30 mg/kg, i.v.). Background noise was subtracted from nerve activity values to provide a measurement of RSNA. All measurements of RSNA were normalized to basal nerve activity determined over a 10 min period recorded directly prior to the start of hemorrhage. Only RSNA data from animals with greater than a 2:1 signal to noise ratio were included in the data analysis.

Spontaneous BRS was determined from 5-min segments of simultaneously recorded BP and HR collected prior to hemorrhage. Data were analyzed with Nevrokard SA-BRS software v.3.2.4 to determine BRS by the sequence method (Padley et al., 2005). Gain was determined as the average slope of linear regressions obtained from a minimum of 3 cardiac cycle sequences that satisfied the following constraints: 3 or more consecutive IBI with variation in the same direction that was >0.5 ms and that correlated (r^2 >0.85) with systolic, diastolic or mean arterial BP variations of >0.5 mmHg, with a 3 beat delay. These parameters were chosen based on prior analyses demonstrating

that they retrieved the most sequences with the highest gain in intact rats (Henze et al., 2008). Cross-spectral analyses were performed on IBI and BP data using a 128-point fast Fourier transformation with a smoothed Hamming window. Coherence between IBI and BP variability was determined as the square root of the ratio of the IBI and BP power spectra with, 50% overlap, and zero padding of 8. Values are reported as the alpha index in the low frequency (0.06-0.6 Hz) and high frequency (0.6-3.0) domains. In addition, BP variability was determined in the low frequency domain and in the time domain, the latter of which was determined as the standard deviation of BP between normal beats (SDNN).

Protocols

Hemodynamic Studies

Rats subjected to prior global serotonin sham- or real lesions were connected to a withdrawal pump and an arterial pressure transducer through an overhead swivel system while resting in their home cage. Lead wires from the recording electrode were also connected through the overhead swivel system. Vehicle- and toxin-treated rats were randomly assigned to receive either drug or saline during the experiment. Each rat's venous catheter was connected to pre-filled tubing containing 8-OH-DPAT or saline via the overhead swivel system. After 1-2 hrs habituation following instrumentation, arterial blood was withdrawn using an automated withdrawal pump set at a rate of 3.2 ml/min/kg for 6 min followed by a slower withdrawal rate of 0.52 ml/min for 4 additional minutes. In

prior studies, this protocol was found to produce a consistent hypotensive response after approximately 3.5 min after which BP stabilized at 40-50 mmHg for the remaining period of blood withdrawal (Scrogin, 2003). Exactly 7 min after the start of blood withdrawal, 8-OH-DPAT (30 nmol/kg/35 µl, iv.) or saline was injected followed by a 150 µl saline flush. Data acquisition began 15 min prior to the experiment and continued during the 10 min of blood withdrawal and an additional 30 min following termination of hemorrhage. Rats were then given a bolus of hexamethonium chloride (30 mg/kg, iv.) to block ganglionic transmission for determination of electrode noise. After the experiment animals were anesthetized with sodium pentobarbital (65 mg/kg, iv.) and perfused transcardially with fixative to enable collection of brain tissue for immunohistochemical verification of serotonin lesion.

Immunohistochemistry

Following the hemorrhage protocol all rats were perfused transcardially with 90 ml sodium nitrite (0.1 M) in 6.7 mM phosphate buffered saline (PBS) followed by 90 ml 4% paraformaldehyde. The brains were removed and post-fixed for 1hr. The brainstem was then blocked and post-fixed in 4% paraformaldehyde for an additional hour and subsequently dehydrated in 30% sucrose. Brains sections were cut in 40 µm sections and collected serially into 6 wells filled with PBS. Sections were saved in cryoprotectant (30% sucrose + 30% ethylene glycol in phosphate buffered saline) and stored at -20ºC.

For processing, brain sections were rinsed in PBS and incubated in 0.2% Triton X (40 min), 3% H_20_2 (10 min) and sheep anti-TPH (1:1000, Chemicon). To verify that the neurotoxin did not affect catecholamine containing neurons, additional sections were incubated in mouse-anti-TH (1:1000, Chemicon). Sections were washed and incubated in biotinylated anti-sheep or mouse antibody (1:1000, Vector) for 1hr. Sections were then incubated with avidin-biotin complex (Vector) for 50 min. Immunoreactivity was exposed with nickel ammonium sulfate-intensified 3, 3'–diaminobenzadine tetrhydrochloride (DAB) chromagen. Specificity of the primary antibodies was verified by characteristic labeling of known serotonergic and adrenergic regions of the brainstem. Omission of the primary antibodies completely prevented cell labeling.

Microscopy

Tryptophan hydroxylase immunoreactive cell numbers were determined in every 6th section throughout the anatomical extent of each serotonin-rich nucleus or region. These included the three major regions of midbrain raphe, including the DR and MR nuclei and the vlPAG region. The TPH-ir cell count was also determined in the RM, RO, RP, PPY and SUB regions (Steinbusch HW 1981).
To determine if the neurotoxin affected noradrenergic neurons in the A2 and A5 region, TH-ir cell numbers was counted bilaterally in these two regions.

Results

Administration of 5,7-DHT into the cerebroventricles produced a diffuse decrease in TPH-ir throughout the entire midbrain and the medullary raphe as shown in Figures 16 and 17. Multiple 2-way repeated measure ANOVAs were used to examine TPH-ir cell numbers between saline- or 8-OH-DPAT-injected animals subjected to lesions in each region. There was no difference found between the two groups in any serotonin-rich region. Therefore, cell number data were pooled to better represent the overall lesion effect. Tryptophan hydroxylase immunoreactive positive cell numbers were significantly decreased in all raphe regions (Figure 17). The lesion produced a 30 to 60% overall reduction of TPH-ir neurons in all serotonin-rich nuclei, including the midbrain raphe regions (Table 6).

Tyrosine hydroxylase-ir cells in the A1 region showed no apparent difference in morphology following treatment with the neurotoxin. Tyrosine hydroxylase-ir cell numbers in the A2 and A5 regions were not affected by neurotoxin injection. Cell counts in the locus coeruleus region were not made due to the intense staining and inability to differentiate single cells (Figure 18). The number of TH-ir cells in the A1 region was not determined since it was not possible to differentiate between noradrenergic cells of the A1 region and adrenergic cells of the C1 region within the same section using DAB labeling techniques. However, the apparent density of staining did not differ (Figure 18).

Global neurotoxin lesion had no effect on either the initial compensatory- or syncopal response to blood withdrawal (Figure 19). As shown in Figure 19, baseline BP was slightly but not significantly lower in rats subjected to the more global lesion, but this was not a consistent finding since the two groups treated with 8-OH-DPAT showed no difference in baseline BP. Neither the latency to onset of the hypotensive response, nor the nadir in pressure during hemorrhage was affected by the global lesion. In rats treated with saline during hemorrhage, BP recovered to a slightly lower level in lesioned animals, which was similar to the slight reduction in BP seen in both groups given 8-OH-DPAT. A 3-way ANOVA showed a significant interaction of Lesion x Time on MAP. The source of the effect of Lesion and Time on MAP appeared to be that lesioned rats given saline showed a slight reduction of MAP in the plateau phase, which was very similar to the BP level observed in both groups given 8-OH-DPAT. Thus, the two lesioned groups had a slightly lower recovery of BP compared to the pooled control group. However, a follow up 2-way ANOVA assessing Lesion and Time in which groups were pooled across drug treatment failed to demonstrate a significant effect of Lesion.

Similarly, the lesion did not affect the latency of the HR bradycardic response following the start of hemorrhage. However, a spurious response in one lesioned rat led to a slight, but non-significant, attenuation in the extent of the bradycardic response.

The latency to onset of the sympatholytic RSNA response was also unaffected by lesion. However, the plateau reached by the end of hemorrhage was significantly lower and the secondary compensatory recovery of sympathetic activity significantly less in lesioned rats than sham-lesioned rats.

Systemic administration of 8-OH-DPAT following the onset of the sympatholytic response produced identical MAP pressor, HR and RSNA responses in lesioned and sham-lesioned animals that developed rapidly after administration. In each case the parameters plateaued at the levels similar to that seen in saline-treated animals (Figure 19B).

Average spontaneous baroreflex gain of the HR reflex was not different in lesioned rats when assessed either with the sequence method or by the spectral method (Table 7). However, BP variability in the time domain and in the low frequency domain were significantly reduced in lesioned rats when either mean or diastolic pressure was assessed ($P<0.05$). The LF/HF ratio of HR variability also did not differ between groups.

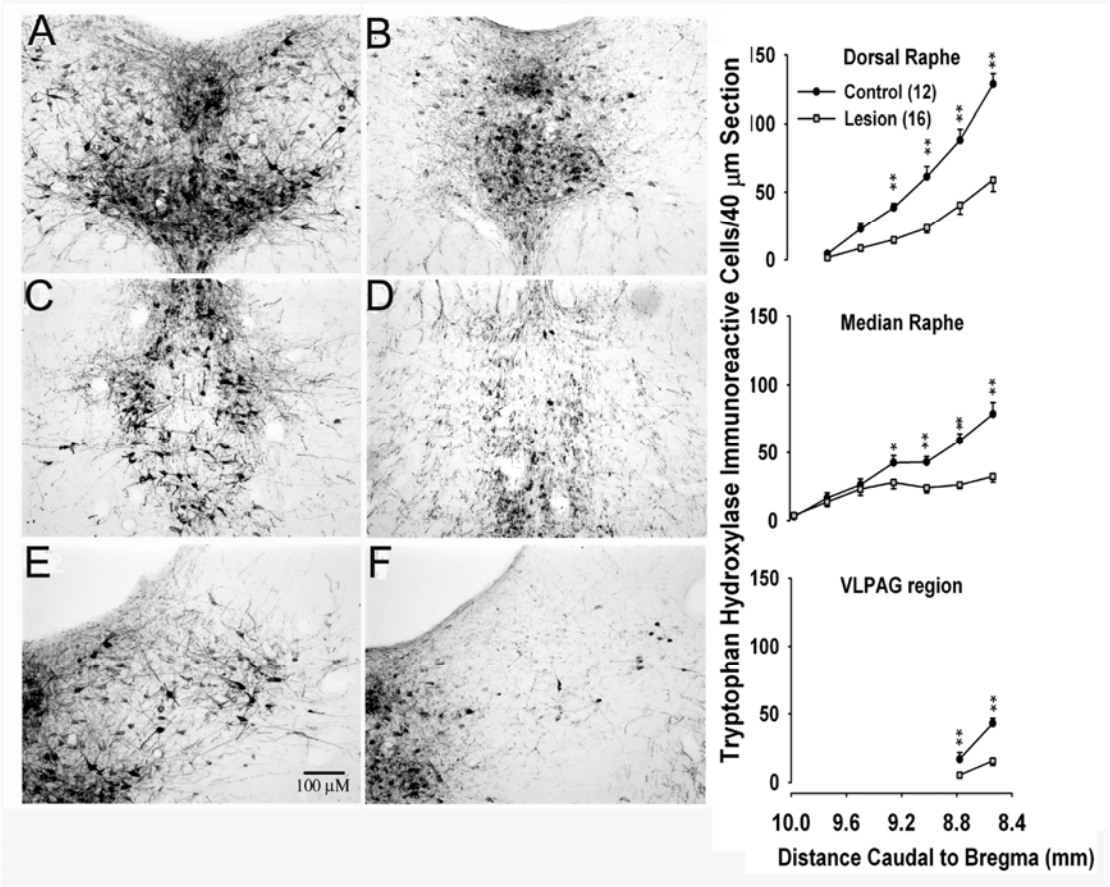

Figure 16. Representative photomicrographs of the midbrain raphe nuclei demonstrating TPH-ir in the DR (A, B), the MR (C, D) and the vlPAG (E, F) in rats treated with vehicle (A, C, E) or 5,7-dihydroxytryptamine (B, D, F). Also shown are cell profiles of TPH-ir neurons counted in one of every 6th 40 µm section throughout the extent of the midbrain raphe nucleus. Data are group means ± SEM. Group n are indicated in parentheses.

Data were analyzed by 2-way ANOVA with repeated measures using Lesion and Distance from Bregma as factors. Main effects and significant interactions were followed up with between-group comparisons using Newman-Keul post-hoc test. *, **P<0.05, <0.01 lesion vs. control.

An overall 2-way ANOVA with repeated measures examining the effect of Lesion and Distance from Bregma of TPH-ir cell number in the DR showed a Lesion x Distance from Bregma interaction [F (1,130) = 15.16, P<0.01] due to the greater extent of depletion of TPH-ir cells in more rostral regions where the normal TPH-ir cell density was greatest. A main effect of Lesion [F (1,130) = 40.67, P<0.01] was due to the overall reduction of TPH-ir cell number in lesioned rats. A main effect of Distance [F (1,130) = 116.51, P<0.01] was due to the change in number of TPH-ir cells over the extent of the nucleus.

An overall 2-way ANOVA with repeated measures examining the effect of Lesion and Distance from Bregma in the MR showed a Lesion x Distance interaction [F (1,156) = 12.46, P<0.01] due a more extensive lesion in the more rostral region of the nucleus where the normal TPH-ir cell density was greatest. A main effect of Lesion [F (1,156) = 17.19, P<0.01] was due to an overall decrease in TPH-ir cell number in lesioned rats. A main effect of Distance from Bregma [F (1,156) = 49.19, P<0.01] was due to the change in TPH-ir cell number over the whole nucleus.

An overall 2-way ANOVA with repeated measures examining the effect of Lesion and Distance from Bregma in the vlPAG showed a Lesion x Distance interaction [F (1,26) = 11.74, $P<0.01$] due to the greater extent of the lesion in the more rostral portion of the nucleus where the TPH-ir cell density was greatest. A main effect of Lesion [F (1,26) = 21.51, $P<0.01$] was due to the overall decrease of TPH-ir cell numbers in lesion rats. A main effect of Distance from Bregma [F (1,26) = 62.88, $P<0.01$] was due to the larger number of TPH-ir cell in the more rostral sections.

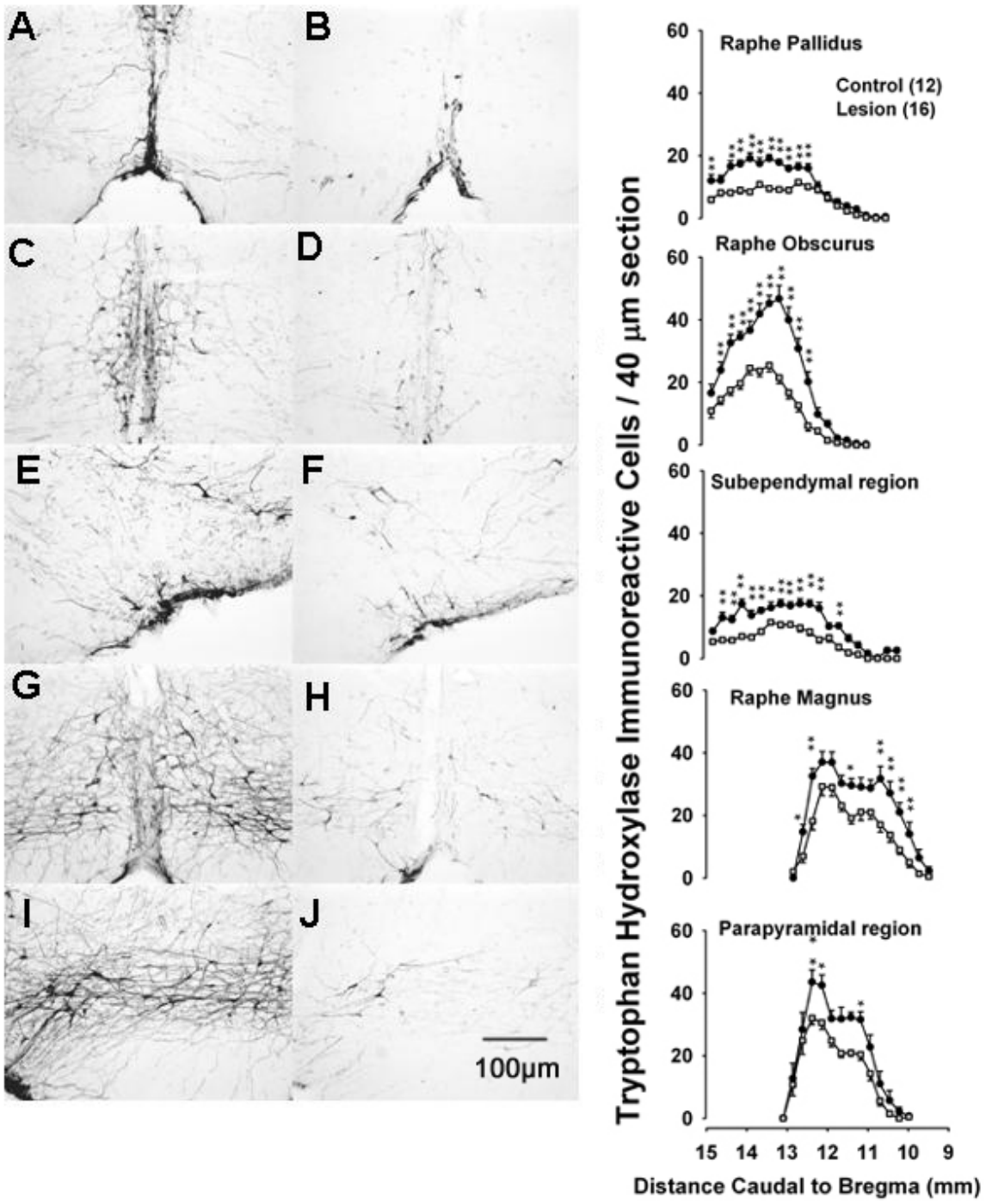

Figure 17. Representative images of the caudal hindbrain showing TPH-ir in the raphe pallidus (A, B), the raphe obscurus (C, D), the subependymal region (E,F),

the raphe magnus (G,H) and the parapyramidal region (I, J) in sham-lesioned (A,C,E,G,I) and lesioned rats (B,D,F,H,J). Cell profiles of TPH-ir positive cells are shown for each serotonin-rich caudal raphe nucleus throughout the extent of the nucleus in toxin- and vehicle-treated rats. Data are group means ± SEM. Group n are indicated in parentheses.

Data were analyzed by 2-way ANOVA with repeated measures using Lesion and Distance from Bregma as factors. Main effects and significant interactions were followed up with between-group comparisons using Newman-Keul post-hoc test. *, ** $P<0.05$, <0.01 lesion vs. control.

An overall 2-way ANOVA with repeated measures examining the effect of Lesion and Distance from Bregma in the SUB region showed a Lesion x Distance from Bregma interaction [$F(1,494) = 3.83$, $P<0.01$] due to a decrease in TPH-ir cell numbers in lesioned rats throughout most of the nucleus that dissipated toward the rostral end of the nucleus. A main effect of Lesion [$F(1,494) = 122.24$, $P<0.01$] was due to an overall lower TPH-ir cell number in lesioned rats. A main effect of Distance from Bregma [$F(1,494) = 47.87$, $P<0.01$] was due to the variation in positive cell numbers over the extent of the nucleus.

An overall 2-way ANOVA with repeated measures examining the effect of Lesion and Distance from Bregma in the RP showed a Lesion x Distance from Bregma

interaction [F (1,468) = 6.87, *P*<0.01] due to the greater extent of TPH-ir positive cell loss in the more caudal portion of the nucleus. A main effect of Lesion [F (1,468) = 47.84, *P*<0.01] was due to an overall decrease in TPH-ir cell number in lesioned rats. A main effect of Distance from Bregma [F (1,468) = 61.24, *P*<0.01] was due to the variation in TPH-ir positive cell number throughout the length of the nucleus.

An overall 2-way ANOVA with repeated measures examining the effect of Lesion and Distance from Bregma in the RO showed a Lesion x Distance from Bregma interaction [F (1,416) = 11.49, *P*<0.01] due to the greater extent of TPH-ir positive cell loss in the center of the nucleus where the highest density of TPH-ir cells was found. A main effect of Lesion [F (1,416) = 43.89, *P*<0.01] was due to an overall decrease in TPH-ir cell numbers in lesioned rats. A main effect of Distance from Bregma [F (1,416) = 116.92, *P*<0.01] was due to the variation in TPH-ir positive cell number throughout the length of the nucleus.

An overall 2-way ANOVA with repeated measures examining the effect of Lesion and Distance from Bregma in the RM showed a Lesion x Distance from Bregma interaction [F (1, 390) = 2.93, *P*<0.01] due an overall lower TPH-ir cell number in lesioned rats in the center of the nucleus, but not in the rostral and caudal ends of the nucleus. A main effect of Lesion [F (1,390) = 15.97, *P*<0.01] was due to an overall lower TPH-ir cell number in lesioned rats. A main effect of Distance

from Bregma [F (1,390) = 66.57, $P<0.01$] was due to the variation in cell number throughout the length of the nucleus.

An overall 2-way ANOVA with repeated measures examining the effect of Lesion and Distance from Bregma in the PPY region showed a main effect of Lesion [F (1,338) = 19.57, $P<0.01$] due to decreased TPH-ir cell numbers in lesioned rats. A main effect of Distance from Bregma [F (1,338) = 57.39, $P<0.01$] was due to the variation in TPH-ir cell numbers through the length of the nucleus.

Table 6 Tryptophan hydroxylase immunoreactive cell numbers in each serotonin-rich nucleus

	DR	MR	VLPAG	RM	PPY	RO	RP	SUB
Control (12)	343 ± 22	260 ± 16	59 ± 8	341 ± 26	308 ± 15	389 ± 27	209 ± 12	214 ± 7
Lesion (16)	148 ± 20 **	151 ± 19**	20 ± 3**	215 ± 18 **	208 ± 13 **	206 ± 15 **	125 ± 6 **	119 ± 7 **
% decrease	56.8%	41.9%	66.1%	36.9%	32.5%	47.0%	40.2%	44.4%

Data are expressed as group mean ± S.E.M. Positive cell numbers are reported for the dorsal raphe (DR), median raphe (MR), ventrolateral of periaqueductral gray region (vlPAG), raphe magnus (RM), parapyramidal region (PPY), raphe obscurus (RO), raphe pallidus (RP), and subependymal region (SUB). Values are group means ± SD. Group n are indicated in parentheses.

The total TPH-ir cell number of each region was compared between groups by Student's t-test. Significant decreases in TPH-ir cell numbers were found in all nuclei. ** $P<0.01$, lesioned vs. sham-lesioned animals.

Tryptophan hydroxylase immunoreactive cell number was lower in the DR [df = 26, t = 6.37, $P<0.01$], MR [df = 26, t = 4.06, $P<0.01$], vlPAG [df = 26, t = 4.59, $P<0.01$], RM [df = 26, t = 4.06, $P<0.01$], PPY [df = 26, t = 6.44, $P<0.01$], RO [df = 26, t = 6.32, $P<0.01$], RP [df = 26, t = 6.80, $P<0.01$] and SUB [df = 26, t = 9.55, $P<0.01$] of lesioned rats.

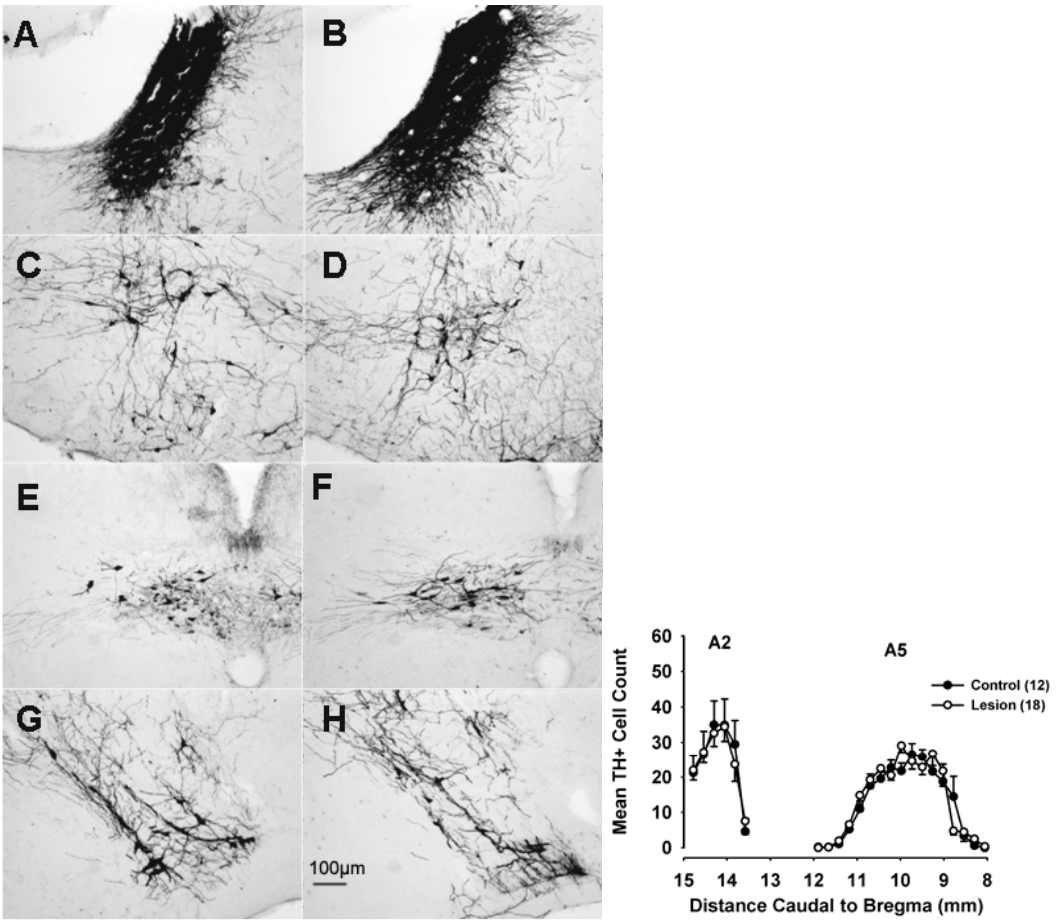

Figure 18. Representative brain sections labeled for TH-ir in the locus coeruleus (A,B), rostroventrolateral region of the medulla (C,D), as well as the A2 regions (E,F) and A5 region (G,H), in sham-lesioned (A, C, E, G) and lesioned animals (B, D, F, H). Tyrosine hydroxylase immunoreactive cell profiles are shown for sham-lesioned (control) and lesioned rats for the A2 and A5 adrenergic cell groups in the right graph. Group n are indicated in parentheses. Overall 2-way ANOVA with repeated measure were preformed to examine the effect of Lesion and Distance on TH-ir cell number of the A2 and A5 regions. There were no significant differences found between groups.

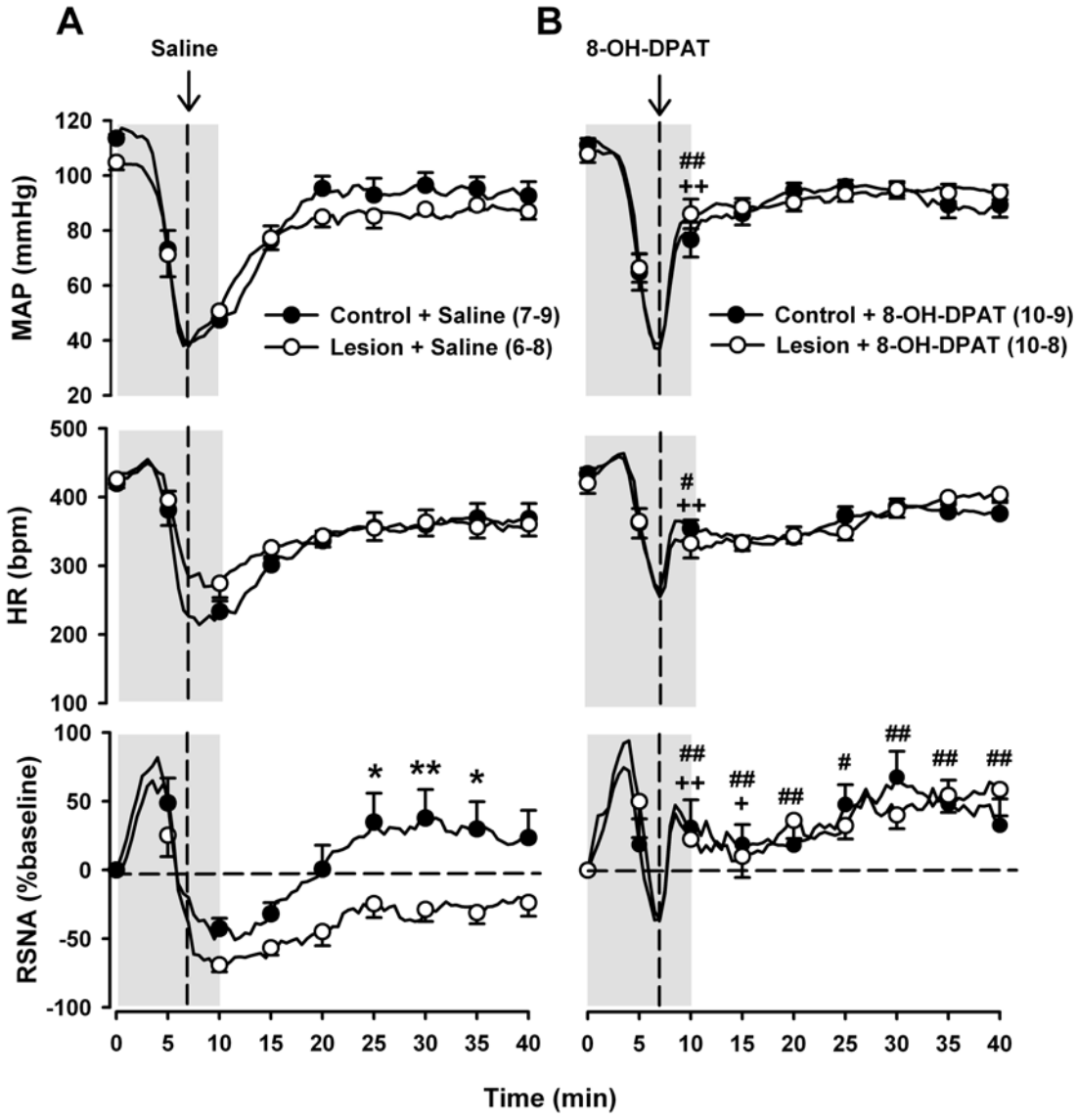

Figure 19. Mean arterial pressure (MAP), heart rate (HR), and renal sympathetic nerve activity (RSNA) during hemorrhage (indicated by gray box) and subsequent recovery in rats treated with ascorbic acid (control) and 5,7-DHT (lesion) delivered to the cerebroventricles. Number of subjects in control group given saline (A) is 9 for MAP and HR and 7 for RSNA. Number of subjects in

lesion group given saline is 8 for MAP and HR and 6 for RSNA. Number of subjects in control group given 8-OH-DPAT is 10 for MAP and HR and 9 for RSNA (B). Number of subjects in lesion group given 8-OH-DPAT is 10 for MAP and HR and 8 for RSNA. Data are group mean ± S.E.M. Data were analyzed by 3-way ANOVA with repeated measures using Lesion, Drug and Time as factors. Between-group differences were compared using Newman-Keuls post hoc tests. Group n are indicated in parentheses. $^{*,**}P<0.05$, 0.01 between control and lesion saline groups. $^{+,++}P<0.05$, 0.01 between control-saline and control-8-OH-DPAT groups. $^{\#,\#\#}P<0.05$, 0.01 between lesion-saline and lesion-8-OH-DPAT groups.

A 3-way ANOVA with repeated measures examining the effect of Lesion, Drug, and Time on MAP showed a Lesion x Time interaction [$F(3,264) = 2.08$, $P<0.05$]. The source of the interaction was not apparent except for the slight reduction in BP recovery among lesioned rats given saline. A follow up ANOVA that included only saline-treated groups failed to demonstrate a significant effect of Lesion. Likewise, an ANOVA in which control and lesioned animals were pooled across drug treatment and compared also failed to show a significant difference between groups. The only apparent explanation is that the slight reduction in MAP during recovery in the lesioned group treated with saline was similar to the slight reduction in MAP recovery seen in both groups given 8-OH-DPAT. The combination of the two lesion groups having reduced recovery may have reduced

the variability enough that there was a small difference between lesion and control at a few time points that led to an interaction, but no main effect of Lesion. A Drug x Time interaction [F (3,264) = 13.90, $P<0.01$] was also found due to the significant presser response to 8-OH-DPAT in both control and lesioned animals over time. A main effect of Time [F (3,264) = 81.54, $P<0.01$] was also observed due to the change in BP over the course of hemorrhage.

A 3-way ANOVA with repeated measures examining the effect of Lesion, Drug, and Time on the HR response showed a Drug x Time interaction [F (3,264) = 6.52, $P<0.01$] due to the tachycardia response to 8-OH-DPAT injection in both control and lesioned rats. A main effect of Time [F (3,264) = 36.20, $P<0.01$] was due to the changes of HR over the course of hemorrhage.

A 3-way ANOVA with repeated measures examining the effect of Lesion, Drug, and Time on RSNA showed a Lesion x Drug interaction [F (3,208) = 4.48, $P<0.05$] due to the attenuated recovery of sympathetic activity in lesioned rats that was masked by 8-OH-DPAT injection. A Lesion x Time interaction [F (3,208) = 2.39, $P<0.05$] was also found due to the attenuation of sympathetic activity in saline-injected animals subjected to lesion. A Drug x Time interaction [F (3,208) = 6.61, $P<0.01$] was also found due to the sympathetic excitatory effect to 8-OH-DPAT in both control and lesioned rats. A main effect of Drug [F (3,208) = 17.36, $P<0.01$] was due to the large sympathoexcitatory effect of drug in both lesioned

and control groups. A main effect of Time [F (3,208) = 12.91, $P<0.01$] was due to the variation of RSNA over the course of hemorrhage in both groups.

Table 7. Spontaneous baroreflex gain, heart rate and blood pressure variability in lesion and control rats

		Up Sequences (ms/mmHg)	Down Sequences (ms/mmHg)	All Sequences (ms/mmHg)	Alpha (LF)	Alpha (HF)	LF power ($mmHg^2$)	BP SDNN	LF/HF
Control (19)	SBP	2.05 ± 0.18	1.61 ± 0.16	1.91 ± 0.15	0.75 ± 0.07	2.11 ± 0.20	9.88 ± 1.00	3.91 ± 0.16	0.76 ± 0.15
	MBP	2.52 ± 0.24	2.44 ± 0.21	2.49 ± 0.21	0.82 ± 0.09	2.88 ± 0.30	8.26 ± 0.71	3.51 ± 0.13	
	DBP	2.42 ± 0.19	2.22 ± 0.19	2.33 ± 0.18	0.86 ± 0.10	2.76 ± 0.27	7.73 ± 0.67	3.43 ± 0.12	
Lesion (18)	SBP	2.29 ± 0.33	1.89 ± 0.27	2.15 ± 0.32	0.93 ± 0.13	2.02 ± 0.35	7.51 ± 1.19	3.49 ± 0.23	0.79 ± 0.12
	MBP	2.67 ± 0.41	2.55 ± 0.35	2.63 ± 0.37	1.03 ± 0.14	2.70 ± 0.46	5.82 ± 0.71 *	3.02 ± 0.19 *	
	DBP	2.53 ± 0.30	2.33 ± 0.22	2.46 ± 0.26	1.07 ± 0.15	2.48 ± 0.34	5.31 ± 0.59 **	2.95 ± 0.24 *	

Spontaneous baroreflex gain was determined by the sequence method using ascending only (up), descending (down), or all sequences that met criteria outlined in the text. Values are group means ± SEM. Group n are indicated in parentheses. Gain was determined by the sequence method using systolic blood pressure (SBP), mean blood pressure (MBP), and diastolic blood pressure (DBP). Spectral coherence between IBI and pressure variability are reported as coherence in the low frequency domain (alpha LF) or high frequency domain (alpha HF). Power of BP variability in the low frequency domain (LF power) and in the time domain (BP SDNN) and the ratio of low frequency to high frequency HR variability (LF/HF) are also included in the analysis.

Spontaneous baroreflex gain did not differ between groups. Coherence of variability in IBI and BP variability as determined by alpha LF or the alpha HF did not differ regardless of whether SBP, MBP or DBP was used in the analysis.

Power of BP variability in the LF domain was lower in lesioned rats when both MBP [df = 35, t = -2.60, $P<0.05$] and DBP [df = 35, t = -2.87, $P<0.01$] were used. Blood pressure SDNN were lower in lesioned rats when MAP [df = 35, t = -2.34, $P<0.05$] and DBP [df = 35, t = -2.27, $P<0.05$] were used.

Discussion

We recently showed that rats subjected to selective lesion of the caudal hindbrain serotonin neurons have an attenuated recovery of sympathetic activity during the second compensatory phase following hypotensive hemorrhage. However, the initial depressor response to blood loss was not affected. These data contradict several lines of evidence that suggest serotonin contributes to the sympatholytic response to hemorrhage. However, it could be argued that serotonin cells in the midbrain raphe regions contribute to the depressor response to hemorrhage. Therefore, the present study was carried out to determine if midbrain serotonergic neurons were involved in the depressor response to blood loss during sympatholytic phase in conscious rats. We also determined whether 5-HT_{1A} autoreceptors mediate the sympathoexcitatory effect of 8-OH-DPAT in hypovolemic rats. Results from the present study further confirmed that serotonin neurons within the brain likely do not contribute to the depressor response to blood loss during the sympatholytic phase in conscious rats. Nor does the sympathoexcitatory effect of 8-OH-DPAT in hypovolemic rats depend on 5-HT_{1A} autoreceptors. In the present study, cerebroventricular administration of neurotoxin destroyed up to 60% of the TPH-ir cells in all serotonin-rich nuclei including those in the midbrain, but had no effect on the depressor and sympatholytic responses to blood loss. However, as seen in our previous study, serotonin cell destruction attenuated the secondary compensation following hemorrhage (Kung et al., 2010).

The C1 region of the RVLM contains pre-sympathetic neurons that regulate sympathetic output. The cells also receive projections from raphe neurons in the midbrain. Dean and Bago demonstrated that unilateral blockade of 5-TH_{1A} receptors in the C1 region of the RVLM prevented the sympatholytic response to hypotensive hemorrhage in anesthetized rats, suggesting that the syncopal response is mediated, in part, by serotonin projections to the RVLM. Earlier, these same investigators noted that stimulation of the vlPAG produced sympatholysis and hypotension that was blocked by 5-HT_{1A} receptor antagonist administration in the RVLM. These investigators also noted that a small population of serotonergic cells of the vlPAG project to the pressor region of the RVLM. Therefore it seemed reasonable to suggest that serotonergic projections from the vlPAG to the RVLM might contribute to the sympatholytic response to hemorrhage.

In the present study, however, we found that greater than 65% depletion of serotonin neurons in the vlPAG had no effect on the sympatholytic response to blood loss in conscious rat. It has been argued that greater than 80% depletion of modulatory monoamine neurons is necessary to observe a significant physiological effect given the propensity of healthy neurons remaining after lesion to send collateral projections to denervated terminal fields (Marshall, 1979; Zigmond and Stricker, 1973). However, in our prior study we noted that neurotoxin targeted to the caudal hindbrain destroyed approximately 50% of the serotonin positive cell bodies, but eliminated over 80% of terminal field

innervation of the RVLM. Nevertheless, the sympatholytic phase remained intact. In these latter studies it is possible that loss of RVLM innervation by serotonergic cells was so extensive because the neurotoxin was injected very close to the region and so nerve terminal loss may have been due to both loss of cell bodies within the caudal raphe that project to the RVLM, as well as to degeneration of nerve terminals within the RVLM that directly took up the toxin. At the time that these studies were completed we had not yet perfected methods to quantify terminal field innervation by serotonin and the tissue was no longer available after the technique was perfected. Therefore, it is impossible to determine whether the cerebroventricular injections of neurotoxin produced as thorough a nerve terminal loss in the RVLM as did the caudal raphe injection. However, very thorough denervation of the RVLM in prior studies did not delay the sympatholytic response to hemorrhage, likely ruling out a role for vlPAG innervation of the RVLM as a potential source for the sympatholytic response in conscious rats. The current study extends these earlier findings by further indicating that serotonergic cells of the vlPAG that project elsewhere also probably do not mediate the sympatholytic response to hemorrhage in awake animals.

Given the lack of an observable effect of 5,7-DHT on the sympatholytic response to hemorrhage found in the present study, it was not surprising that the sympathoexcitatory effect of 8-OH-DPAT was independent of intact serotonin cells. We posited that if serotonin cells of the CNS were important in the

sympatholytic phase during hemorrhage in the unanaesthetized animal, then suppression of serotonin neuronal activity by activation of autoreceptors by 5-HT_{1A}-receptor agonists should have terminated or rapidly reversed the response. As demonstrated, 8-OH-DPAT, a potent 5-HT_{1A}-receptor agonist, continued to produce sympathoexcitation in hemorrhaged animals subjected to wide-spread global serotonin lesion. These data suggest that 8-OH-DPAT and other 5-HT_{1A}-receptor agonists with similar sympathoexcitatory effects in hypovolemic animals mediate their effects independently of serotonin neurons, either by activating post-synaptic 5-HT_{1A} receptors present on non-serotonergic neurons or by activating other serotonergic or non-serotonergic receptor subtypes on non-serotonergic neurons (Osei-Owusu and Scrogin, 2004; Scrogin, 2003).

In previous work, pre-treatment with the relatively selective 5-HT_{1A}-receptor antagonist, WAY-100635, dose dependently reversed the increase in blood volume withdrawal necessary to initiate the sympatholytic response following administration of 8-OH-DPAT in conscious rats (Scrogin et al., 2000). These results, together with those of the present study suggest that 8-OH-DPAT mediates its autonomic effects via post-synaptic 5-HT_{1A} receptors expressed on non-serotonergic neurons. However, 8-OH-DPAT has also been shown to have appreciable agonist activity at 5-HT_7 receptors and α1-adrenergic receptors that could account for its pressor effects in hemorrhage animals (Bard et al., 1993; Castillo et al., 1993; Damaso et al., 2007). Indeed, we have noted a significant direct agonist effect of 8-OH-DPAT on α1-adrenergic receptors that contributes,

in part, to vasoconstriction in hemorrhaged animals (Osei-Owusu and Scrogin, 2004; Tiniakov and Scrogin, 2006). However, we also noted that a similar sympathoexcitatory effect of the 5-HT_{1A}-receptor agonist, buspirone, was preserved after administration of the α1-adrenergic receptor antagonist, prazosin, as was a portion of its pressor effects (Osei-Owusu and Scrogin, 2004). These data indicate that 5-HT_{1A}-receptor agonists mediate their pressor effects in hemorrhaged animals through both direct α1-adrenergic mediated vasoconstriction as well as through non-α1-adrenergic receptors that are responsive to increased sympathetic drive. Indeed blockade of α2-adrenergic receptors significant reduced the prolonged pressor effect of 8-OH-DPAT in rats subjected to hypovolemic shock.

To date the role of 5-HT_7-receptors in the hemodynamic response to hemorrhage has not be studied. However, recent evidence indicates that 8-OH-DPAT activates both 5-HT_{1A}- and 5-HT_7-receptors to provide a positive modulatory effect on glutamatergic activation of sympathetic nerves innervating brown adipose fat (Madden and Morrison, 2008). Though such sympathetic activation is not thought to contribute substantially to BP control, it remains to be seen whether a parallel activation of 5-HT_{1A} and 5-HT_7 receptors might account for the hemodynamic effects of 8-OH-DPAT in hemorrhaged animals.

The most surprising aspect of the present studies are the parallel effects of 8-OH-DPAT and endogenous serotonin in hypovolemic animals. Both mediate the secondary compensatory sympathetic recovery after the sympatholytic

response to hemorrhage. The observation that the sympathoexcitatory effect of 8-OH-DPAT is not attenuated by serotonin cell loss suggests the intriguing possibility that post-synaptic 5-HT_{1A}-receptors mediate sympathetic compensation to both 8-OH-DPAT and endogenous serotonin release. Thus, exogenous administration of 5-HT_{1A}-receptor agonists may act downstream of serotonin neurons to accelerate a component of the secondary compensatory response that is normally dependent on serotonin neurons. Proof of this concept will require identification of the projection sites that mediate the excitatory effects of serotonin neurons in hypovolemic animals.

Recent work has indicated that 8-OH-DPAT produces a robust increase in venous tone and cardiac output in rats subjected to hypovolemic shock (Tiniakov et al., 2007). This effect appears to be mediated by a preferential increase in sympathetic-dependent venous tone, since total peripheral resistance is unaffected. Presently, it is not known whether endogenous serotonin neurons in the hindbrain promote a selective sympathetic-dependent venoconstriction during hypovolemia as does 8-OH-DPAT. However, the BP and HR responses of animals subjected to global serotonin lesion were not different from sham-lesioned animals subjected to hemorrhage despite a dramatic attenuation of sympathetic recovery. These data suggest that an alternative means of raising BP must compensate for the lack of serotonin-dependent sympathetic activation. The most likely means of raising perfusion pressure in the absence of sympathetic activation is through release of vasoactive hormones. However,

vasoactive hormones tend to act predominantly on the arterial side of the vasculature and may promote excessive arterial resistance to preserve perfusion pressure (Hernandez et al., 1991; Tiniakov and Scrogin, 2006). This presents the intriguing possibility that serotonin neurons are activated during hypovolemia in order to mobilize venous pools of blood and thus preserve cardiac output and peripheral blood flow and consequently oxygenation of peripheral tissue.

The sympathoexcitatory effect of 8-OH-DPAT and other 5-HT_{1A} agonists in hypovolemic animals is somewhat paradoxical given their profound sympathoinhibitory effect in euvolemic animals. Serotonin 5-HT_{1A} receptors are primarily coupled to Gαi and Gαo proteins that inhibit production of cAMP, open K+ channels, or inhibit calcium influx (Fargin et al., 1989; Innis et al., 1988; Penington and Kelly, 1990). As such, their activation results almost exclusively in membrane hyperpolarization and reduced neurotransmitter release (Pan et al., 1993). In accord, 5-HT_{1A} agonists produce profound sympathoinhibitory effects by inhibition of pre-motor sympathetic neurons of the RVLM in euvolemic animals (Fozard et al., 1987; Laubie et al., 1989; Nosjean and Guyenet, 1991; Osei-Owusu and Scrogin, 2004). Thus, our data suggest that the sympathoexcitatory effects of 5-HT_{1A}-receptor agonists likely result from disinhibition of some sympathoexcitatory pathway that is normally not active in the euvolemic animal or that is suppressed during hypotensive hemorrhage. 8-OH-DPAT acts as a full agonist in behavioral and biochemical assessment within several regions of the brain including the brainstem and so should produce the same functional effect

via 5-HT_{1A} receptors as the endogenous ligand serotonin (Dabrowska and Brylinski, 2006). Therefore, it seems reasonable to suggest that endogenous serotonin release and 5-HT_{1A} receptor activation disinhibits cells that can activate sympathetic drive through an alternative pathway than the RVLM. Such alternative pathways could include direct projections of the parvocellular neurons of the paraventricular nucleus of the hypothalamus to the pre-ganglionic sympathetic cells in the spinal cord (Caverson et al., 1984; Ootsuka and Blessing, 2005). In any event, the mechanisms by which 5-HT_{1A}-receptor agonists and endogenous serotonin increase sympathetic activity in hypovolemic animals remain unknown. Results herein appear to rule out a role for 5-HT_{1A}-receptor-mediated inhibition of serotonin cell activity.

As indicated by our previous finding, it is not likely that loss of serotonin neurons inhibited sympathetic recovery following hemorrhage by disrupting the baroreflex (Kung et al., 2010). Instead, our data indicate that serotonin lesion increases BRS. Reduced low frequency fluctuations in BP suggest that sympathetic baroreflex control of vasomotor tone was enhanced in lesioned animals. Interestingly, lesion of caudal raphe serotonin neurons did not affect LF variation in BP but did influence baroreflex gain assessed by the sequence method. This latter method also reflects the vagal component of the reflex to a greater degree then does LF BP variability. It is possible that parenchymal injections of neurotoxin targeted to the caudal hindbrain leads to a loss of serotonin fibers that innervate structures involved in cardiovagal control, while

the more diffuse application of neurotoxin used here does not adequately lesion these projections. Thus, projections to structures involved in sympathetic baroreflex control may be more vulnerable to neurotoxin exposure given through the cisterna magna such as the structures lining the ventral floor of the 4th ventricle. Although in the current study we did not measure serotonin nerve terminal density in the NTS, it is to be expected that serotonin nerve terminals in the floor of the 4th ventricle would be more severely affected by cisterna magna injections than injections that targeted the more ventral and caudal raphe neurons.

It is unlikely that augmented baroreflex control contributed to the reduced sympathetic compensation observed with hemorrhage in animals subjected to a more global serotonin lesion. Tests of BRS or BP variability cannot reveal whether alterations in baroreflex gain results from changes in sensitivity to increased BP or to baroreceptor unloading. However, a general augmentation of baroreflex control would likely not have caused the loss of sympathetic recovery observed in these studies. Instead a more responsive baroreflex would have produced an exaggerated sympathetic response during baroreceptors unloading as in hypovolemia.

Of interest too are prior findings that indicate that the extent of the sympathoexcitatory response to 8-OH-DPAT is dependent on the integrity of sinoaortic nerves that convey baroreceptor and peripheral chemosensory afferents to the central nervous system (Osei-Owusu and Scrogin, 2006).

Hemorrhaged rats subjected to prior sinoarotic denervation had a dramatically attenuated sympathoexcitatory responses to 8-OH-DPAT (Osei-Owusu and Scrogin, 2006). Here we found that 5-HT_{1A}-receptor agonists administrate accelerated sympathetic recovery after hemorrhage at the same rate and to the same extent whether baroreflex function was augmented or not. Together the data suggest the intriguing possibility that the sympathoexcitatory effects of 8-OH-DPAT may be dependent upon chemosensory afferent activity rather than baroreceptor activity. This hypothesis remains to be confirmed with further tests.

In summary, the current study shows that cerebroventricular administration of neurotoxin successfully destroyed 30-60% of TPH-ir neurons in all serotonin-rich nuclei, including the midbrain serotonergic nuclei. Utilizing this method, we further confirmed that serotonergic neurons in the CNS most likely do not contribute to the sympatholytic depressor response to blood loss in conscious rats. Instead, the present study suggests that 8-OH-DPAT and endogenous serotonin mediate the secondary compensatory phase of sympathetic recovery following hemorrhage. Since serotonin lesion does not affect the sympathoexcitatory effect of 8-OH-DPAT after the sympatholytic phase, it is possible that both endogenous serotonin and 8-OH-DPAT act on post-synaptic 5-HT_{1A}-receptors to mediate this secondary sympathoexcitatory response.

CHAPTER V

Serotonergic neurons activate 5-HT_{1A} receptors in the NTS to stimulate recovery of sympathetic activity after hypotensive hemorrhage in conscious rats

Abstract

Previously we have found that hindbrain serotonin neurons and 5-HT_{1A}-receptor agonists mediate sympathetic recovery during the secondary compensatory phase following hypotensive hemorrhage, and this phenomenon may be related to altered chemoreflex function. Here we tested if serotonin projections to the NTS facilitate sympathetic and respiratory recovery from hypotensive hemorrhage. We also tested whether 5-HT_{1A} receptors in the NTS are responsible for the secondary compensatory response to hypotensive hemorrhage and for the sympathoexcitatory effect of 5-HT_{1A}-receptor agonists observed in hemorrhaged animals.

Blood pressure, HR, RSNA and dEMG activity were recorded during hypotensive hemorrhage in rats subjected to sham (n=8) or selective (n=9) denervation of serotonin nerve terminals in the caudal NTS. Neurotoxin injection reduced serotonin immunoreactivity in the NTS (93%, $P<0.01$), but not in the

pressor region of the RVLM. Lesion reduced the initial sympathoexcitation (36.4 ± 17.5 vs. +153.8 ± 36.6 % baseline, *P*<0.05) during primary compensatory phase, but not the subsequent sympatholytic phase to blood loss. During the secondary compensatory phase, sympathetic and ventilatory recovery was also reduced in lesioned rats (+6.2 ± 13.2 vs. +127.9 ± 48.7 %baseline RSNA, *P*<0.05 and -32.4 ± 4.6 vs. +45.7 ± 18.9 %baseline integrated dEMG 35 min after start of hypotensive hemorrhage, *P*<0.05), while BP and HR were not affected. Lesion also reduced sympathetic and ventilatory responses to peripheral chemoreflex activation (+368 ± 63 vs. +618 ± 140 %baseline RSNA, *P*<0.01; +17 ± 21 vs. +104 ± 26 %baseline ΔTV, *P*<0.01), but increased HR (-4.6 ± 0.3 vs. -3.1 ± 0.3 Δbpm/ΔmmHg, *P*<0.01) and sympathetic (-14.1 ± 2.6 vs. -9.1 ± 1.2 Δ%baseline/ΔmmHg, *P*<0.01) baroreflex gain . These data indicate that serotonin neuronal innervation of the caudal NTS is necessary for normal recovery during hemorrhage and that this effect may be related to the function of the peripheral chemoreflex.

Introduction

Progressive blood loss produces a multiphasic hemodynamic response to blood loss, the mechanisms of which are not well understood. The primary compensation that develops during blood loss is mediated by arterial baroreceptor unloading in unanaesthetized animals (Ludbrook and Ventura, 1996; Schadt and Ludbrook, 1991). Prior work has suggested that serotonin

contributes to the sympatholytic response that initiates the rapid depressor response during blood loss in anesthetized animals (Elam et al., 1985; Morgan et al., 1988). In contrast, we recently found that selective destruction of the majority of caudal hindbrain serotonergic neurons tended to exaggerate the sympatholytic response to blood loss in conscious rats, and, in fact, significantly reduced the secondary compensatory recovery (Kung et al., 2010; Ruszaj et al., 2006). Lactic acidosis was exaggerated in lesioned animals, despite the elevated arterial blood oxygen levels and normal BP recovery (Kung et al., 2010). These data suggest that greater tissue hypoxia develops in lesioned animals subjected to hemorrhage as a consequence of reduced blood delivery to peripheral tissues. Taken together, the evidence further suggests that caudal raphe serotonin neurons help to maintain perfusion pressure by preserving cardiac output during recovery from hypotensive hemorrhage, possibly by facilitating sympathetic-mediated increases in venous tone.

The mechanism by which serotonin facilitates the secondary compensatory response following blood loss is not known. We found that serotonin lesion enhanced indices of cardiac and sympathetic baroreflex control, suggesting that in the intact animal serotonin does not facilitate sympathetic recovery by augmenting responses to baroreceptor unloading. We also noted a significant impairment of sympathetic and ventilatory responses to central chemoreceptor stimulation (i.e., hyperoxic, hypercapnia) in conscious rats subjected to serotonin cell lesion. In hemorrhage studies, we further

demonstrated that arterial $PaCO_2$ rose following the initial hypotensive phase of hemorrhage, precisely when sympathetic activity began to recover in intact rats (Kung et al., 2010). Thus, serotonin may play a role in conveying important sensory information to brainstem nuclei that control appropriate sympathetic and ventilatory responses to blood loss. Our data further suggest that, in the absence of serotonin neurons, BP recovery from hypotensive hemorrhage is mediated by potentially detrimental increases in arterial resistance rather than by beneficial increases in cardiac output. Currently, the central neural pathways that determine how perfusion pressure is maintained (i.e., changes in capacitance vs. resistance) during hypovolemia are largely unknown. Such information could spur the development of adjuvant therapies that positively influence the distribution of volume given during resuscitation from hypovolemic shock.

Recent work has suggested that sympathetic-mediated recovery of perfusion pressure in intact conscious rats is largely dependent upon excitatory glutamatergic projections to the VL-LPBN of the brainstem (Blair and Mickelsen, 2006). The NTS provides the largest glutamatergic projection to the VL-LPBN (Dutschmann et al., 1998). Moreover, the NTS receives significant projections from serotonergic neurons of the caudal medullary raphe (Schaffar et al., 1988; Thor and Helke, 1987). Therefore, we determined if selective destruction of serotonin nerve terminals within regions of the NTS that receive cardiovascular and chemosensory afferents attenuated recovery of renal sympathetic activity

and ventilation following hemorrhage. We further determined whether loss of serotonin nerve terminals in this region altered sympathetic responses to baroreflex and peripheral chemoreflex activation, since both are engaged during hypotensive hemorrhage (Evans et al., 1993a; Henry et al., 1998; Scislo and O'Leary, 1998).

Our work has also shown that administration of the 5-HT_{1A}-receptor agonist, 8-OH-DPAT, given into the cisterna magna produces a very rapid and robust increase in sympathetic activity in animals subjected to hypotensive hemorrhage and improves venous tone and acid base balance in rats subjected to hypovolemic shock (Scrogin, 2003; Tiniakov and Scrogin, 2006). Given our recent evidence demonstrating the importance of serotonin cells in sympathetic recovery and acid base balance during the secondary compensatory phase following hemorrhage, these data suggest that activation of 5-HT_{1A}-receptors on the dorsal surface of the hindbrain would contribute to sympathetic recovery following hemorrhage. To address this question we attempted to determine whether pharmacological blockade of 5-HT_{1A} receptors in the NTS attenuated recovery of sympathetic drive following hypertension and/or the sympathoexcitatory effects of 8-OH-DPAT in hypovolemic animals.

Methods

Animals

Male Sprague-Dawley rats (300 - 350 g, Harlan, Indianapolis, IN) were acclimated to the housing facility while given *ad libitum* access to food and water for at least 1 wk prior to surgery. The facility was maintained at a constant temperature of 22 ± 2°C with a light/dark cycle of 12:12 hrs. All experiments were approved by the Institutional Animal Care and Use committee and were conducted in accordance with the Guide for the Care and Use of Laboratory Animals as adopted and promulgated by the US National Institutes of Health.

Surgery

Neurotoxin Study: Regions of the NTS that receive arterial baro- and peripheral chemoreceptor afferents, i.e. the medial, dorsolateral and commissural subnuclei, were targets for selective serotonin nerve terminal lesion. All rats were pre-treated with the dopamine and norepinephrine re-uptake blocker, nomifensine (15 mg/kg in 20% ß-cyclodextran), at least 30 min prior to neurotoxin injection to prevent toxin-induced destruction of adrenergic cells. Rats were anesthetized with sodium pentobarbital (65 mg/kg, i.p.), intubated with an endotracheal tube, and placed in a stereotaxic apparatus with the nose bar positioned 11 mm below a flat skull position. The back of the skull was exposed, and a small portion of the occipital bone was removed to expose the dorsal surface of the brainstem at the level of calamus scriptorus. The occipital

membrane was incised and a glass micropipette injector, pulled and broken back to an outer diameter of ~20 µm, was centered at the caudal tip of calamus scriptorus. The injector was filled with either 5,7-dihydroxytryptamine (5,7-DHT; 5 mM in 0.1% ascorbic acid) or vehicle. Bilateral 100-nl injections of neurotoxin or vehicle were made 0.5 mm ventral to calamus scriptorus at five rostro-caudal planes along the NTS: 1, 0.5, 0, - 0.5, - 1 mm relative to calamus scriptorus. Injections were made ± 0.7 and 0.35 mm from the midline for the two most rostral injection planes and ± 0.25 mm from the midline for the caudal three injections planes for a total of 10 injections. The neck muscle and skin were closed in separate layers.

NTS cannulation

A single cannula was positioned over the commissural subnucleus of the NTS (comNTS) while the animals were anesthetized under sodium pentobarbital (65 mg/kg). Animals were placed in a stereotaxic apparatus with the nose bar positioned 11 mm below a flat skull position. The back of the skull was exposed and a small portion of the occipital bone was removed to expose the brainstem. The dura and pia mater were then carefully removed and the blunt end of a piece of 23 ga. hypodermic needle (13 mm long) was lowered perpendicularly at the mid-line. The injector was lowered until it touched the caudal tip of calamus scriptorus on the brainstem. The cannula was then secured in place by surrounding it with dental acrylic which in turn surrounded a jeweler's screw that

was secured to the skull. The cannula was fitted with a dummy injector (30 ga., 13 mm long) to prevent occlusion. The skin was stapled closed around the guide cannula.

Catheters and Electrode Implantation:

One week later, all rats were re-anesthetized with sodium pentobarbital (65 mg/kg, i.p.) and implanted with bilaterally femoral arterial catheters (PE-50 heat-welded to a length of PE-10) to enable direct measurement of arterial pressure and simultaneous arterial blood withdrawal. A third catheter was placed unilaterally in the femoral vein for drug injections. Catheters were externalized at the nape of the neck and secured with sutures.

Following catheter implantation, dual recording electrode leads were implanted as described previously to enable measurement of renal sympathetic nerve activity and dEMG (Kung and Scrogin., 2009; Kung et al., 2010; Scrogin, 2003). A short segment of a sympathetic fiber bundle from the aorticorenal ganglion was exposed through a left flank incision, isolated and placed on a stainless steel, Teflon-coated wire (bare diameter =.005 in., A-M Systems Inc., Everett, WA). The electrode connector was externalized at the nape of the neck with the vascular catheters. Viability of the nerve preparation was determined by auditory assessment of the bursting activity, after which the preparation was embedded in a quick drying, lightweight silicon (Kwik sil, World Precision Instruments). The flank incision was sutured closed in two layers with the

electrode leads coiled within the subcutaneous space. A second set of lead wires were tied into the abdominal side of the diaphragm through a 2 cm lateral laparotomy using 6-0 nylon. The leads wires that exited from the abdominal muscle layer were coiled in the subcutaneous space. The incisions were closed in layers. Animals were allowed to recover overnight prior to the experiment.

Data Acquisition

Arterial pressure, HR, RSNA and dEMG were recorded on a Macintosh G4 Powerbook computer using PowerLab data acquisition software (Chart v. 5.2.1, ADinstruments, Colorado Springs, CO). Arterial pressure was measured with a disposable pressure transducer (Transpac® IV, Abbott Labs, North Chicago, IL) and a PowerLab bridge amplifier (ADinstruments, CO). Heart rate was calculated using peak-to-peak detection of the pulse pressure wave. Sympathetic activity and dEMG were sampled (4,000 Hz) and amplified (10-20,000x) with PowerLab Bioamplifiers (ADinstruments, CO). The recorded neurograms were filtered (1-1000 Hz), rectified and integrated over a 20-ms time constant. Background noise in the RSNA recordings was determined at the end of each experiment by measuring the remaining signal following ganglionic blockade (hexamethonium chloride, 30 mg/kg, iv.). Background noise was subtracted from nerve activity values to provide a measurement of RSNA. Background noise in the dEMG was determined during expiration, when phrenic motor nerve activity was absent. Measurements of RSNA and dEMG obtained

during the experiment were normalized to basal nerve activity, and dEMG determined over a 10 min period directly prior to the start of interventions. Only RSNA and dEMG data from animals with greater than a 2:1 signal to noise ratio in the respective neurograms were included in the data analysis. Respiratory rate was determined by peak to peak detection of the integrated dEMG signal.

Spontaneous BRS was determined from 5-min segments of BP and HR determined prior to hemorrhage. Data were analyzed with Nevrokard SA-BRS software v.3.2.4 to determine BRS by the sequence method (Osei-Owusu P & Scorgin K 2006). Gain was determined as the average slope of linear regressions obtained from a minimum of 3 sequences that satisfied the following constraints: 3 or more consecutive IBI with variation in the same direction that was >0.5 ms and correlated (r^2 >0.85) with systolic, diastolic or mean arterial BP variations of >0.5 mmHg, with a 3 beat delay. These parameters were chosen based on prior analyses from our lab demonstrating that they retrieved the most sequences with the highest gain in normal Sprague-Dawley rats of approximately the same age as the rats used in the present study (Henze M et al 2008). Cross-spectral analyses were performed on IBI and BP data using a 128-point fast Fourier transformation with a smoothed Hamming window. Coherence between IBI and BP variability was determined as the square root of the ratio of the IBI and BP power spectra with, 50% overlap, and zero padding of 8. Values are reported as the alpha index in the low (0.06 - 0.6 Hz) and high frequency (0.6 - 3.0 Hz) domains. In addition, BP variability was determined in the low frequency

domain (LF power) and in the time domain, the latter of which was determined as the standard deviation of BP between normal beats (BP SDNN). Heart rate variability in the frequency domains was also determined using the IBI power spectra criteria described above. Heart rate variability was determined as the power in the LF domain divided by that in the HF domain (LF/HF). Frequency domains were defined as described above for the alpha indices.

Protocols

Protocol 1: Peripheral chemoreflex testing

On the day of the experiment, one of the rat's arterial catheters was connected to the BP transducer through saline-filled polyethylene tubing via an overhead swivel system to enable recordings while the rat rested in its home cage. The RSNA and dEMG leads were connected to the appropriate amplifiers via lead wires extending from the same swivel. The rats were allowed to rest, unrestrained in their home cage for at least 1 hr after connection to the recording instruments. Increasing doses (3, 30 and 100 μg/kg) of KCN were given at 40 to 50 min intervals while all variables were measured continuously. Ten to 15 min after connecting the drug-filled catheter, drug was injected over 30 sec. After 10 minutes, the tubing was changed and the rat allowed to rest prior to the next injection.

Protocol 2 : Hypotensive hemorrhage

At least 24 hrs after chemoreflex testing, the same group of rats were again connected to a withdrawal pump and an arterial pressure transducer through an overhead swivel system. After 1 hr of habituation arterial blood was withdrawn using an automated withdrawal pump set at a rate of 3.2 ml/min/kg for 6 min and adjusted to a slower withdrawal rate of 0.52 ml/min for 4 additional minutes. Data acquisition was begun 15 min prior to the experiment and continued throughout hemorrhage and for an additional 50 min following termination of hemorrhage. At the end of the experiment rats were given hexamethonium chloride (30 mg/kg, iv.) for determination of background noise in the sympathetic recording. Animals were then rapidly anesthetized with sodium pentobarbital (65 mg/kg, iv.) and quickly perfused transcardially with 90 ml of sodium nitrite (50 mM) in 0.1 mM phosphate buffered saline (PBS) followed by 90 ml 4% of formaldehyde. The brains were removed and post-fixed for 1 hour. The brainstem was blocked and post-fixed for an additional hour and subsequently dehydrated in 30% sucrose. Brains sections were cut in 40 μm sections and collected serially into 6 wells. Sections were saved in cryoprotectant (30 % sucrose + 30 % ethylene glycol in phosphate buffered saline) and stored at -20°C for immunohistochemical verification of serotonin lesion.

Protocol 3: Baroreflex control of HR and RSNA

Separate groups of rats prepared as described in the surgical methods were connected to the recording instruments as described in the above protocols. An additional length of PE-50 tubing was connected to the venous catheter for drug administration. After at least 1 hr of habituation BP, HR, RSNA and dEMG were measured during a variable infusion of sodium nitroprusside (3-25 μg/sec) to produce a ramp BP decrease from baseline to 50-60 mmHg over 3 minutes. The drug was cleared from the tubing after which the rats were allowed to rest for at least 1hr. A variable infusion of phenylephrine (3 – 13 μl/min, iv.) was given to produce a smooth ramp increase in BP from baseline to 160 mmHg over 3 minutes. At the end of the experiment rats were given hexamethonium chloride (30 mg/kg, iv.) for determination of background noise in the sympathetic recording. The rats were then anesthetized with sodium pentobarbital (65 mg/kg, iv.) and perfused transcardially as described at the end of protocol 2 to enable collection of brain tissue for immunohistochemical verification of serotonin lesion.

Protocol 4: Hypotensive hemorrhage and 5-HT_{1A} receptor manipulation

Rats were implanted with the NTS cannula as described above. One week after cannula placement, rats were instrumented with catheters and a dual recording electrode as describe above. The next day, they were connected to the recording instruments via an overhead swivel to allow for recording of MAP, HR, RSNA and dEMG while they rested unrestrained in their home cage. After

at least one hour habituation, hemorrhage was initiated as described previously (Kung et al., 2010). Seven minutes after the start of hemorrhage an injector needle (30 ga. 14 mm long) connected to tubing with the appropriate drug or saline was inserted into the NTS guide cannula such that the injector tip extended 1 mm below the end of the guide cannula to reach the caudal NTS. Animals were injected with the selective 5-HT_{1A}-receptor antagonist, WAY-100635 (0.1 nmol) or saline (100 nl), at the rate of 1 µl/min. The 5-HT_{1A}-receptor agonist 8-OH-DPAT (30 nmol/kg) or saline was then administered iv. at the end of blood withdrawal (i.e., 10 minutes after the start of hemorrhage). At the end of the experiment rats were given hexamethonium chloride (30 mg/kg, iv.) for determination of background noise in the sympathetic recording electrode. At least one hour after the end of the experiment, the excitatory amino acid, D,L-homocysteic acid, DLH (10 nmol), was injected into the NTS at the rate of 1 µl/min to determine whether the injector location targeted areas involved in primarily baroreflex or chemoreflex responses, the former of which is characterized by sympathoinhibition and BP decreases and the latter by sympathetic activation and bradycardia. Lastly, 250 nl of fluorescent latex beads (0.05-0.2 µm) were injected through the guide cannula at a rate of 0.5 µl/min to verify the location of injection. At the end of experiment, rats were perfused as described above and the brains were sectioned and mounted in order to visualize the injection sites.

Immunohistochemistry

Serotonin nerve terminal density was determined by quantifying the percent area of interest occupied by serotonin immunoreactivity in brains of rats subjected to sham or real serotonin cell lesion. Quantification was performed in coronal sections obtained from 5 rostral-caudal planes through the portion of the NTS where the majority of baro- and chemosensory afferents terminate. Nerve terminal density was also determined in the underlying dorsomedial nucleus of the vagus (DMX) at the same 5 planes. Additional measurements were taken in 3 planes or the C1 region of the RVLM.

Rabbit anti-serotonin antibody (1:200,000, Immunostar) was pre-incubated with 6 mM reduced L-glutathione (Sigma) in 1mM tris-EDTA buffer (pH 8) for 1 hr at room temperature prior to incubation with tissue. One in six sections from lesioned- and sham-lesioned rats was incubated in 0.2% Triton X and the primary antibody for 48 hr at 4°C. Sections were then washed and incubated in 6% donkey serum, 0.2%Triton X, donkey anti-rabbit Dylight 649 (1:200, Jackson ImmunoResearch) for 2 hr. Sections were rinsed in PBS, mounted on gel-coated slides and immediately coverslipped with fluoromount (Sigma). Sections were stored at 4°C for 7 days prior to microscopy.

Additional NTS sections were double-labeled for serotonin- and TH-ir to qualitatively assess adrenergic cell density and morphology in regions where the serotonin lesion was effective. In this case the above protocol was followed except that mouse anti-TH antibody (1:2500 Chemicon) was used in the primary

incubation step and donkey anti-mouse Cy3 (1:200, Jackson ImmunoResearch) was used in the second incubation.

Brain sections from rats subjected to protocols 1, 2 and 3 were also processed to expose TPH-ir in order to verify that retrograde degeneration of nerve terminals that took up toxin in the NTS did not extend to the cell bodies and thus affect collateral innervation of other terminal fields. In this case, one of every six sections was incubated with sheep anti-TPH primary antibody (1:1000, Chemicon) over night at room temperature. Sections were then incubated with biotinylated goat anti-sheep IgG (1:1000, Vector) for 1 hr at room temperature followed by incubation with avidin-biotin complex (Vector) for 50 min. Immunoreactivity was exposed with nickel ammonium sulfate-intensified 3, 3'–diaminobenzadine tetrhydrochloride (DAB) chromagen to produce a black nuclear label. To quantify noradrenergic neurons, one of every six sections was incubated in mouse-anti-TH (1:1000, Chemicon). Sections were washed and incubated in the appropriate biotinylated IgG made in goat for 1 hr and incubated with avidin-biotin complex as described above. The specificity of the primary antibodies was verified by characteristic labeling of known serotonergic and adrenergic cell groups of the brain stem. Omission of the primary antibodies completely prevented cell labeling.

Microscopy

Tryptophan hydroxylase immunoreactivity in lesion studies

Tryptophan hydroxylase-ir cells were counted in every 6th section throughout the anatomical extent of those serotonin-rich nuclei known to project to the comNTS. These regions included the RM, the RO, and the RP (Schaffar et al., 1988; Thor and Helke, 1987)

Serotonin immunoreactivity in NTS/DMX terminal fields

Tissue from equal numbers of lesioned and control rats were processed in parallel in two separate cohorts. All images were acquired at the same exposure length, exactly 7 days after tissue processing. Serotonin immunoreactive fiber content in the NTS was determined unilaterally at the level of the medial and commissural subnuclei at 5 rostral-caudal planes situated approximately 13.1, 13.3, 13.6, 13.8, and 14.1 mm ±120 μm caudal to Bregma. Serotonin immunoreactive fiber content was also determined in the RVLM at 3 levels; 11.8, 12.2 and 12.8 mm ±120 μm caudal to Bregma.

Immunoreactive fiber content was determined as described previously with modifications (Kung et al., 2010). Briefly, images were taken with an Olympus inverted IX81 epifluorescence microscope with a motor driven stage and a 10x objective. Measurements were determined from composite images of thirty 1 μm deconvolved optical sections taken from each tissue section. Deconvolution was performed with Vaytek Microtome software using the rapid

nearest neighbor method within each image. Background intensity of the composite image, i.e., the intensity of unlabeled neuropil was averaged from at least 4 different brains, and was subtracted from each image. Threshold intensity was set approximately 1.5 times background and was held constant for each region measured. An area of interest (AOI) was outlined in all 5 levels of NTS and DMX regions as describe above using the selection tools in NIH Image J software. Serotonin immunoreactive fiber content was also determined in the RVLM at 3 levels as described above. For measurements in the RVLM, an AOI 900 pixels in width and 800 pixels in height was placed 450 pixels from the midline such that the right lower corner touched the right ventrolateral subependymal surface of the section. Using this method, AOIs were consistently centered over the pressor region of the RVLM as determined previously by the density and orientation of PNMT-positive cells which make up the C1 bulbospinal neurons that project to pre-ganglionic sympathetic cells of the spinal cord (Kung et al., 2010). The percent area of the thresholded image that was occupied by thresholded signal was then determined.

Tyrosine hydroxylase immunoreactivity in lesion studies

The numbers of TH-ir cells were counted in every 6th section throughout the rostro-caudal extent of the A2 adrenergic nucleus bilaterally.

NTS cannula injection location

The brains from animals subjected to protocol 3 were sectioned (40μm), mounted and immediately coverslipped with fluoromount (sigma). Sections were photographed for evaluation of injection site.

Data Analysis

Blood pressure, HR, RSNA, integrated dEMG (used as an index of minute ventilation), and RR were averaged into 30 sec bins and compared between groups at 5 min intervals from the start of blood withdrawal through the 50 min post-hemorrhage period using 2-way ANOVA with repeated measures. Serotonin immunoreactive nerve terminal fiber content was determined in each plane as described above under microscopy and compared between groups by 2-way ANOVA with repeated measures. The effect of neurotoxin injection on TH-ir and TPH-ir cell numbers was compared through the anatomical extent of the relevant nuclei by 2-way ANOVA with repeated measures. Significant interactions and main effects were followed up with Newman-Keuls post-hoc tests.

Baroreflex

Heart rate and RSNA data from phenylephrine and nitroprusside exposure were combined and sorted into ascending order of BP. The resulting data were subjected to curve fitting to a 4 parameter logistical equation: $HR = A/[1 + e^{B(MAP-}$

$^{C)}$] + D, where A is the range of HR or RSNA over the resulting sigmoidal curve, B is a gain parameter, C is MAP at the inflection point of the resulting curve, and D is the asymptotic minimum. The resulting parameters were used to determine maximal gain, (-B)(A)/4.56 as described by Howe et al (Howe et al., 1989). Parameters were compared between groups by Student's t-test. Instantaneous gain (*Y*) over the range of MAP was determined by taking the first derivative of each curve. Gain at baseline BP, i.e., set point gain, was determined for each animal by solving for *Y* at baseline BP in the best fit of the derivative curve according to the Gaussian expression $Y = (k/s)e^{[(x-m)/s\text{^}2]}$, where *Y* is instantaneous gain, *X* is the set point BP, k is kurtosis, s is skewness, and m is MAP at midrange (MAP_{50}).

Peripheral Chemoreflex

Maximal depressor, pressor and bradycardic responses were determined during the initial biphasic hemodynamic response to KCN injection. Sympathetic and respiratory responses were somewhat variable in time of onset. However, KCN injection produced a consistent transient apneic response that was followed by increased dEMG and sympathetic activity at all doses tested. Therefore, two sets of RSNA data points were collected: responses were averaged over 2.5 sec prior to the termination of apnea (apneic period) and 3.0 sec after termination of apnea. These time frames were chosen based on the average duration of apnea in control animals and in an effort to minimize the contribution of baroreflex

unloading on the post apneic measurements. Such baroreflex effects were clearly evident beyond 3 sec after the post-apneic period. For ventilatory parameters, the area under the curve of the integrated dEMG signal was determined for the 3-4 largest breaths and averaged to provide a measure of tidal volume (TV). Tidal volume of the 3-4 largest breaths taken during the post apneic period were averaged and compared to a 3 sec average TV determined prior to drug injection. The percent difference was taken as the change in TV in response to drug. The RR was determined from the breathing period and multiplied by the TV to provide an index of minute ventilation (MVI). The change in MVI during the post-apneic period was determined as % change from baseline.

Results

Rats subjected to sham lesion showed a typical biphasic response during hemorrhage characterized by a short normotensive primary compensatory phase during which sympathetic activity and HR increased, followed by a sympatholytic phase which included rapid falls in BP, HR and sympathetic activity (Figure 20). After reaching their nadir between 6 and 8 minutes after the start of blood withdrawal, all three variables began to enter the secondary compensatory phase and reached a steady state within 20 minutes of hemorrhage termination. The respiratory response was characterized by tachypnea during blood withdrawal and recovery to baseline during the secondary compensatory phase. The

integrated dEMG response was somewhat variable. In general, it rose during the initial blood withdrawal and declined back to baseline in parallel with the fall in BP. Ventilation (i.e., dEMG) subsequently remained at baseline for the next 15 min after which it began to increase and remained elevated for the remainder of the secondary compensatory recovery period.

Neurotoxin lesion in the NTS did not significantly affect BP or HR responses to hemorrhage or during the secondary compensatory phase. Qualitatively, baseline sympathetic burst frequency or amplitude did not appear different between groups (data not shown). The maximal rise in sympathetic activity during blood withdrawal was significantly lower in lesioned rats (153.8 ± 36.5 vs. 36.4 ± 17.5 %baseline, $P<0.01$). Though the primary sympathoexcitatory response was attenuated in lesion rats, the nadir of the sympatholytic response was not different between groups. Sympathetic activity also recovered to a lower steady state in lesioned rats ($P<0.01$). Integrated dEMG of lesioned animals declined from the start of hemorrhage and remained below baseline and below that of control rats during the secondary compensatory phase ($P<0.01$). Respiratory rate did not differ between groups.

Potassium cyanide (KCN) injection in sham-lesioned rats produced immediate bradycardia and apneic responses accompanied by a biphasic BP response (Figure 21). The BP response was characterized by an immediate depressor response followed quickly by a pressor response, with the pressor response being most obvious at the highest dose tested. The pressor response

was accompanied by a transient burst of increased sympathetic activity. Sympathetic activation occurred simultaneously with increased ventilation characterized by a more rapid pace and larger TV. Lesioned rats subjected to KCN injection exhibited a significantly attenuated depressor response regardless of dose and a slightly lower pressor response at the highest dose (P<0.01). Lesioned animals also showed a significant smaller increase in TV (P<0.01) and MVI at the highest doses (P<0.01). Lesion did not affect the magnitude of the bradycardic response or the RR response to KCN (Figures 22).

Average spontaneous baroreflex gain of the HR reflex did not differ between groups when assessed with the sequence and spectral methods (Table 8). However, the power of BP variability in the low frequency domain was significantly lower in lesioned animals when either systolic (P<0.01), mean (P<0.05) or diastolic pressure (P<0.05) were assessed. However, BP variability in the time domain was not different when either systolic, mean or diastolic pressures were assessed. The LF/HF ratio of HR variability was also significantly lower in lesioned rats (P<0.05).

Maximal gain of both HR and RSNA baroreflex curves generated using pharmacological manipulations of BP were significantly elevated in lesioned animal (p<0.05) (Figure 23). In addition, HR baroreflex gain at the set point (or baseline MAP) was significantly higher in lesioned animals (P<0.05). The HR range was significantly lower in lesioned animals (P<0.01), while the lower plateau was elevated (P<0.01) (Table 9). Diaphragmatic EMG activity was found

to increase with decreasing pressure in sham-lesioned rats, while ventilatory rate decreased slightly but not significantly (Figure 24). Diaphragmatic EMG decreased only slightly when BP was increased above baseline. Lesioned animals showed no change in ventilation with either increasing or decreasing pressure.

Neurotoxin injected into the NTS resulted in large reductions in the content of serotonin-ir fibers throughout the medial and commissural subnuclei of the NTS and the neighboring region of the DMX (Figure 25-26A, B). However, the NTS neurotoxin injection did not affect serotonin-ir fiber content in the RVLM (Figure 25-26C). Lesion did not affect TPH-ir cell number in the serotonin-rich nuclei in the caudal raphe that have been shown to project to the NTS (Figure 27 A-H). Tyrosine hydroxylase immunoreactive cells in the A2 region showed no apparent difference in morphology following treatment with the neurotoxin (Figure 27, I and J). Likewise, TH-ir cell number in the A2 region was not affected by neurotoxin injection (Figure 27).

Representative sections showing NTS cannula placement are shown in Figure 28 along with the responses to DLH injection in one rat treated with vehicle in the NTS and saline iv. Responses from 2 additional rats treated with saline in the NTS and 8-OH-DPAT systemically are also shown. Rarely did DLH produce the expected chemoreflex-like response, suggesting that the drug was not reaching chemosensitive neurons. Contrary to results shown in Chapter IV,

systemic injection of 8-OH-DPAT had no sympathoexcitatory effect whether given after the 5-HT_{1A}-receptor antagonist or saline in the NTS (Figure 29).

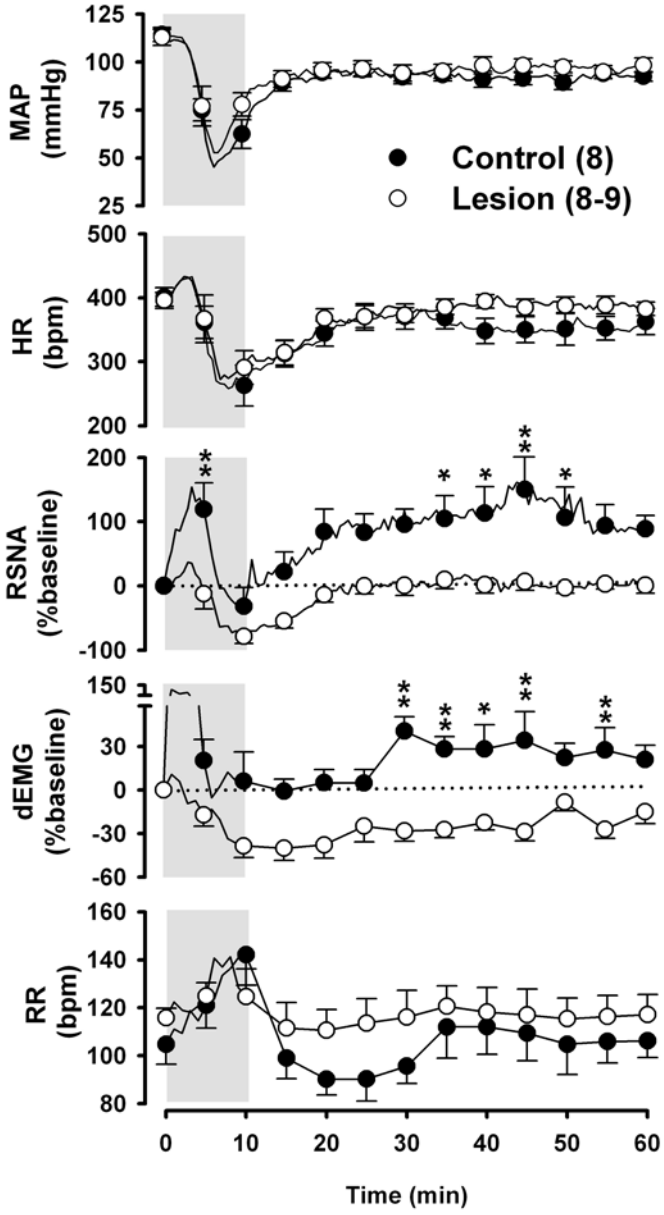

Figure 20. Mean arterial pressure (MAP), heart rate (HR), renal sympathetic nerve activity (RSNA), integrated diaphragmatic EMG (dEMG) and respiratory rate (RR) during hemorrhage (gray shaded region) and subsequent recovery in rats treated with vehicle (Control) and 5,7-dihydroxytryptamine (Lesion) targeted

to the NTS. Number of subjects in control group is 8 for all parameters. Number of subjects in lesion group is 8 for AP, HR and RSNA and 9 for DEMG and RR.

Data were analyzed by 2-way ANOVA with repeated measures using Lesion and Time as factors. Main effects and significant interactions were followed up with between-group comparisons using Newman-Keuls post hoc tests. Data are group mean ± S.E.M. *, ** $P<0.05$, <0.01 compare between groups.

Overall 2-way ANOVA with repeated measures examining the effect of Lesion and Time on MAP showed a main effect of Time [$F(1,156) = 17.43$, $P<0.01$] due to the decline and recovery of MAP over the course of hemorrhage and the secondary compensatory phase. There was no effect of Lesion on the MBP response to hemorrhage.

Overall 2-way ANOVA with repeated measures examining the effect of Lesion and Time on HR showed a main effect of Time [$F(1,156) = 10.94$, $P<0.01$] due to the decline and recovery of HR over the course of hemorrhage and the secondary compensatory phase. There was no effect of Lesion on the HR response to hemorrhage.

An overall 2-way ANOVA with repeated measures examining the effect of Lesion and Time on RSNA showed a main effect of Lesion [$F(1,168) = 14.32$, $P<0.01$]

due to an overall attenuation of sympathetic activity in lesioned animals. A main effect of Time [F (1,168) = 6.05, $P<0.01$] was due to the decline and recovery of RSNA over the course of hemorrhage and the secondary compensatory phase.

An overall 2-way ANOVA with repeated measures examining the effect of Lesion and Time on dEMG activity showed a Lesion x Time interaction [F (1,180) = 1.84, $P<0.05$] due to the attenuation of dEMG activity in lesioned rats that remained low throughout the experiment, while sham-lesioned animals showed a dramatic rise initially with hemorrhage that subsided with hypotension and rose again in the end of the secondary compensatory phase. A main effect of Lesion [F (1,180) = 35.05, $P<0.05$] was due to an overall attenuation of dEMG activity in lesioned rats. A main effect of Time [F (1,180) = 2.09, $P<0.05$] was due to the change in RSNA over the course of hemorrhage and the secondary compensatory phase.

An overall 2-way ANOVA with repeated measures examining the effect of Lesion and Time on RR showed a main effect of Time [F (1,180) = 4.40, $P<0.01$] due to the fluctuation of RR throughout the course of hemorrhage. There was no main effect of Lesion on RR response to hemorrhage.

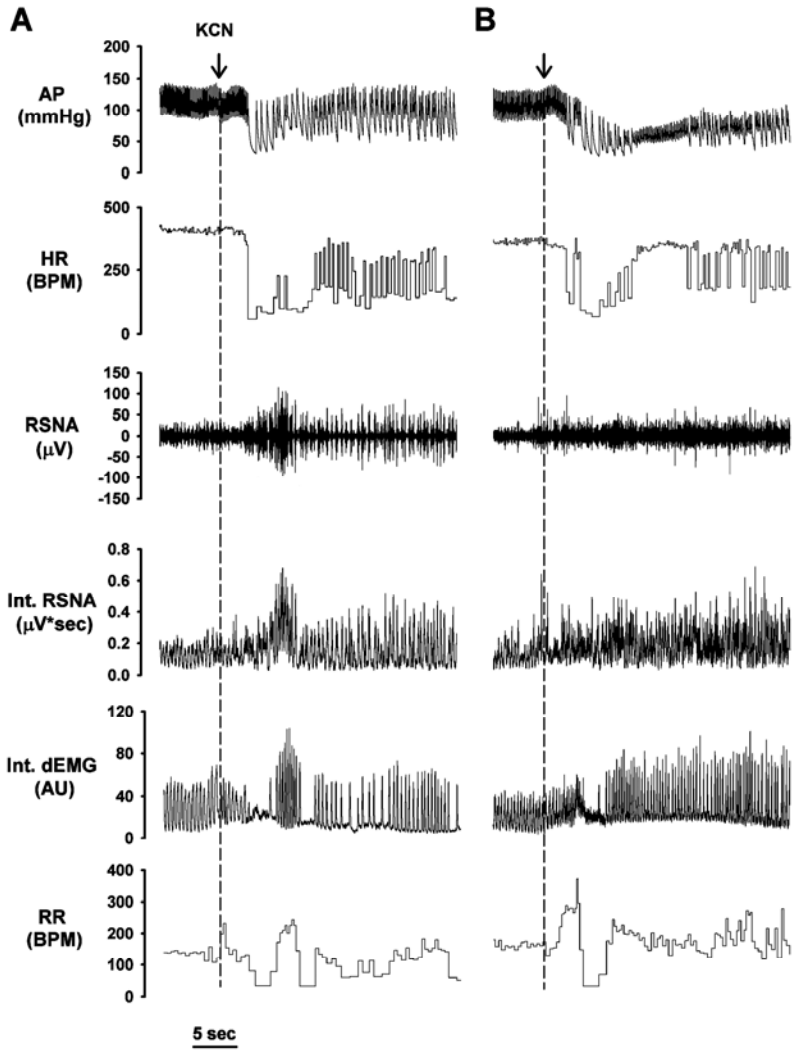

Figure 21. Representative recordings of arterial pressure, heart rate (HR), renal sympathetic activity (RSNA), integrated renal sympathetic activity (int. RSNA), integrated diaphragmatic EMG (int. dEMG) and respiratory rate (RR) during exposure to KCN 30 μg/kg (at arrows) in rats subjected to sham-lesioned (A) or serotonin nerve terminal lesion in the NTS (B).

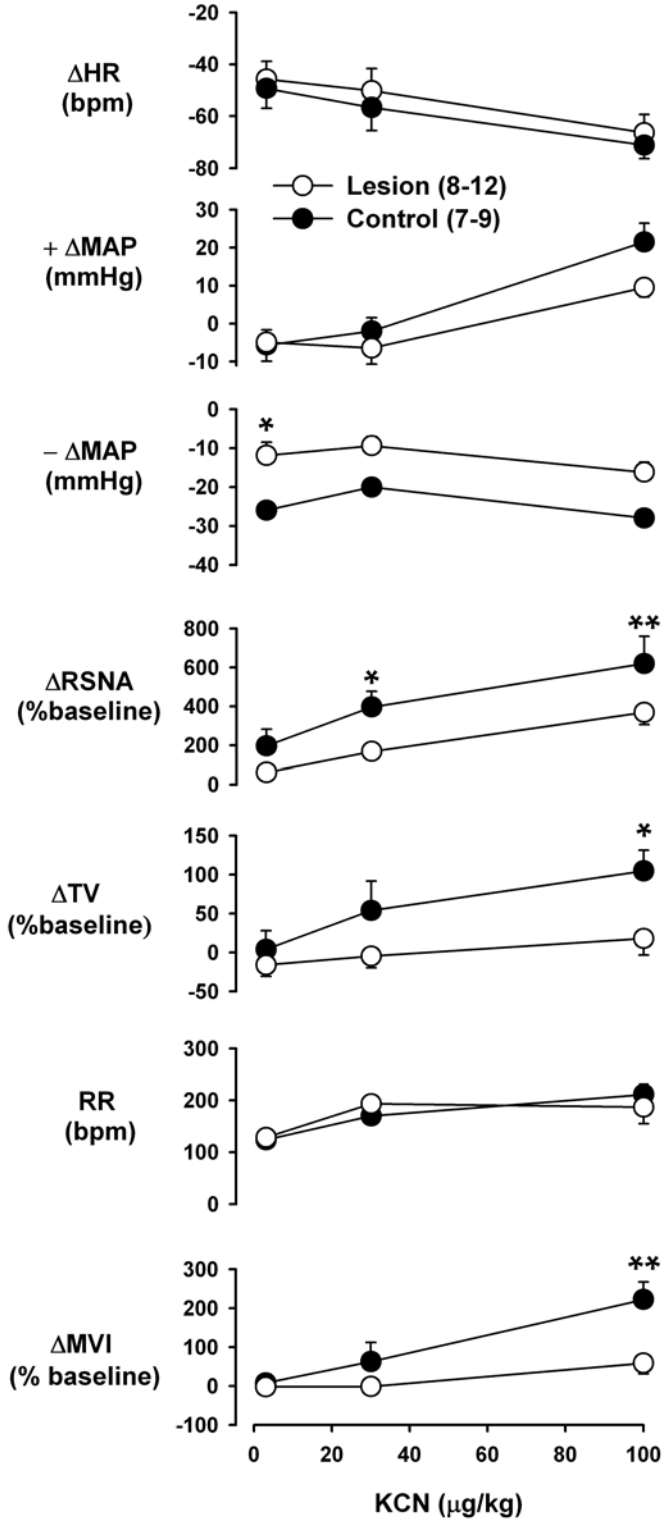
ΔHR
(bpm)
-20
-40
-60
-80
Lesion (8-12)
Control (7-9)
+ ΔMAP
(mmHg)
30
20
10
0
-10
– ΔMAP
(mmHg)
0
-10
-20
-30
-40
*
ΔRSNA
(%baseline)
800
600
400
200
0
*
**
ΔTV
(%baseline)
150
100
50
0
-50
*
RR
(bpm)
300
200
100
0
ΔMVI
(% baseline)
300
200
100
0
-100
**
0
20
40
60
80
100
KCN (μg/kg)

Figure 22. Summary data of change in MAP for both pressor (+∆MAP) and depressor (-∆MAP) responses, heart rate (HR), renal sympathetic nerve activity (RSNA), tidal volume (TV), absolute respiratory rate (RR) and change in minute ventilation index (MVI) in response to increasing doses of KCN (3, 30 and 100 µg/kg iv.) in rats treated with vehicle (control) or 5,7-dihydroxytryptamine (lesion) targeted to the NTS. Subject n in the control group was 9 for HR and MAP, and 8 for all other parameters. Number of subjects in the lesion group was 12 for MAP and HR, 8 for RSNA, and 7 for TV, RR and MVI.

Data were analyzed by 2-way ANOVA with repeated measures using Lesion and Dose of KCN as factors. Main effects and significant interactions were followed up with between-group comparisons using Newman-Keuls post hoc tests. Data are group mean ± S.E.M. *, ** $P<0.05$, <0.01 compare between groups.

An overall 2-way ANOVA with repeated measures examining the effect of Lesion and Dose on the presser response to KCN showed a main effect of Dose [$F(1,38) = 25.35$, $P<0.01$] due to the dose-dependent increase in the presser response to KCN.

An overall 2-way ANOVA with repeated measures examining the effect of Lesion and Dose on HR showed a main effect of Dose [$F(1,38) = 11.01$, $P<0.01$] due to the larger bradycardic effect with increasing dose.

An overall 2-way ANOVA with repeated measures examining the effect of Lesion and Dose on the depressor response showed a main effect of Lesion [F (1,38) = 18.53, *P*<0.01] due to the overall smaller depressor response over the range of the doses, though the difference between groups was only significant at the lowest dose.

An overall 2-way ANOVA with repeated measures examining the effect of Lesion and Dose on RSNA showed significant main effects of Lesion [F (1,34) = 4.79, *P*<0.05] and Dose [F (1,34) = 25.20, *P*<0.01]. A main effect of Lesion was due to overall attenuation of the sympathetic response in the post-apneic period in lesioned animals. The main effect of Dose was due to a larger post-apneic increase in activity with increasing dose.

An overall 2-way ANOVA with repeated measures examining the effect of Lesion and Dose on TV showed a Lesion x Dose interaction [F (1,26) = 8.09, *P*<0.01] due to a significant attenuation of TV in lesioned animals at the highest dose tested, but not at the lower doses. A main effect of Lesion [F (1,28) = 5.37, *P*<0.05] was due to the smaller increase in TV during the post-apneic period in lesioned animals. A main effect of Dose [F (1,28) = 4.74, *P*<0.05] was due to an overall increase in TV during the post-apneic period in both groups with increasing dose.

An overall 2-way ANOVA with repeated measures examine the effects of Lesion and Dose on RR showed no main effects or interaction.

An overall 2-way ANOVA with repeated measures examining the effect of Lesion and Dose on MVI showed a Lesion x Dose interaction [$F(1,28) = 5.31$, $P<0.01$] due to a significant attenuation of MVI in lesioned animals at the highest dose tested, but not at the lower doses. A main effect of Lesion [$F(1,28) = 4.54$, $P<0.05$] was due to the smaller increase in MVI during the post-apneic period in lesioned animals. A main effect of Dose [$F(1,28) = 18.45$, $P<0.01$] was due to an overall increase in MVI with increasing doses.

Table 8. Spontaneous baroreflex gain, heart rate and blood pressure variability in lesion and control rats

		Up Sequences (ms/mmHg)	Down Sequences (ms/mmHg)	All Sequences (ms/mmHg)	Alpha (LF)	Alpha (HF)	LF power ($mmHg^2$)	BP SDNN	LF/HF
Control (13)	SBP	2.13 ± 0.19	2.03 ± 0.26	2.12 ± 0.20	0.71 ± 0.10	2.39 ± 0.40	14.11 ± 2.11	4.50 ± 0.29	
	MBP	2.32 ± 0.15	2.79 ± 0.31	2.60 ± 0.21	0.82 ± 0.12	3.18 ± 0.56	10.61 ± 1.65	3.83 ± 0.22	0.91 ± 0.20
	DBP	2.33 ± 0.20	2.50 ± 0.25	2.45 ± 0.22	0.88 ± 0.13	2.73 ± 0.36	9.35 ± 1.52	3.49 ± 0.18	
Lesion (14)	SBP	2.28 ± 0.23	2.18 ± 0.37	2.24 ± 0.25	0.72 ± 0.10	2.52 ± 0.54	7.73 ± 0.67 **	3.78 ± 0.23	
	MBP	2.85 ± 0.25	2.95 ± 0.40	2.92 ± 0.31	0.80 ± 0.11	3.25 ± 0.47	6.50 ± 0.58 *	3.33 ± 0.24	0.71 ± 0.16 *
	DBP	2.70 ± 0.27	2.49 ± 0.24	2.56 ± 0.26	0.84 ± 0.12	3.00 ± 0.40	6.04 ± 0.56 *	3.27 ± 0.27	

Spontaneous baroreflex gain was determined from the sequence method using ascending only (up) descending only (down) or all sequences that met criteria outlined in the text. Values are group means ± SEM. Group n are indicated in parentheses. Gain was determined by the sequence method using systolic blood pressure (SBP), mean blood pressure (MBP), diastolic blood pressure (DBP). Spectral coherence between IBI and BP variability are reported as coherence in the low frequency domain (alpha LF) or high frequency domain (alpha HF). Power of BP variability in the low frequency

domain (LF power) and in the time domain (BP SDNN) and the ratio of LF to HF heart rate variability (LF/HF) are also included in the analysis.

All variables were compared between groups by Student's t-test. *, ** $P<0.05$, $P<0.01$, lesioned vs. sham-lesioned animals.

Power of BP variability in the LF power and LF/HF were lower in the lesioned group when MBP and DBP were assessed. Significant differences between groups were found in LF power and LF/HF ratio using Student's t-test. LF power in SBP [df = 25, t = 2.95, $P<0.05$], MBP [df = 25, t = 2.40, $P<0.05$] and DBP [df = 25, t = 2.09, $P<0.05$] were significantly lower in lesioned animals. LF/HF ratio [df = 25, t = 2.37, $P<0.05$] was also lower in lesioned animals.

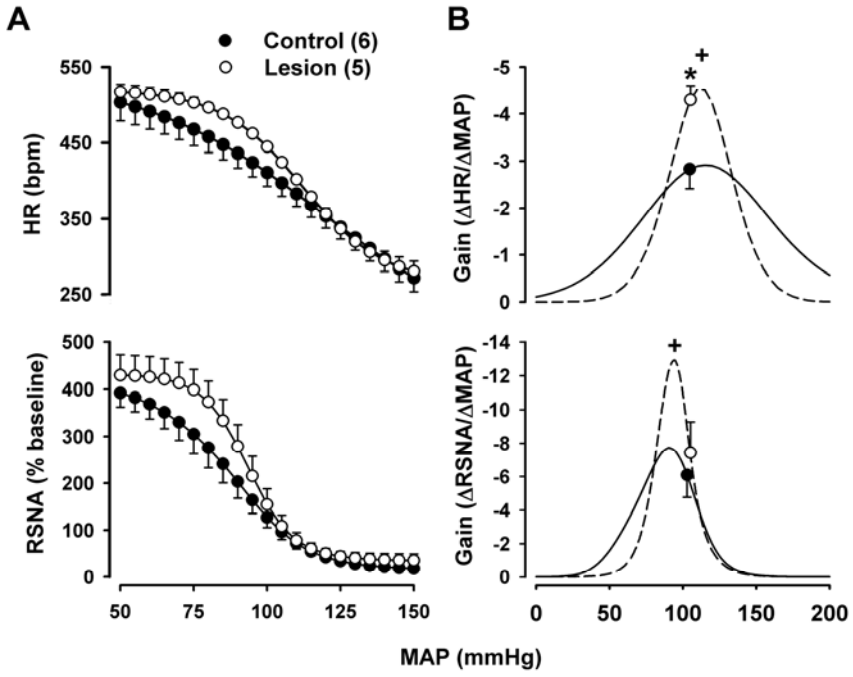

Figure 23. Heart rate (HR) and renal sympathetic nerve activity (RSNA) baroreflex responses to pharmacological BP manipulations in vehicle-treated and lesioned rats. Average of fitted curves for HR and RSNA baroreflex are shown for vehicle-treated (control) and lesioned rats (A). Average instantaneous gain of HR and RSNA are shown in vehicle-treated (control) and lesioned rats (B).

Student's t-tests were performed to test the difference of baseline and maximal gain of HR and RSNA baroreflex between lesioned and control animals. Data are group mean ±SEM. Group n are indicated in parentheses. *P<0.05 vs. control at set-point gain. $^{+}$$P$<0.05 vs. control at maximum gain.

Both maximal [df = 9, t = 3.10, $P<0.05$] and baseline gain [df = 9, t = 2.75, $P<0.05$] of the HR response were elevated in lesioned animals. Maximal gain [df = 9, t = 1.82, $P<0.05$] of RSNA reflex was also elevated in lesioned rats.

Table 9. HR and RSNA baroreflex parameters

	Range (bpm)	Maximal gain (Δbpm/ ΔmmHg)	MAP_{50} (mmHg)	Lower plateau (bpm)	Set point gain (Δbpm/ ΔmmHg)
Control HR (6)	342 ± 31	-3.1 ± 0.3	120 ± 7	189 ± 15	-2.83 ± 0.41
Lesion HR (5)	255 ± 9 **	-4.6 ± 0.3 *	112 ± 2	264 ± 16 **	-4.29 ± 0.30 *
	Range (%baseline)	Maximal gain (Δ%baseline/ ΔmmHg	MAP_{50} (%baseline)	Lower plateau (%baseline)	Set point gain (Δ%baseline/ ΔmmHg)
Control RSNA (6)	398 ± 30	-9.1 ± 1.2	88 ± 4	14 ± 6	-6.06 ± 1.35
Lesion RSNA (5)	396 ± 43	-14.1 ± 2.6 *	93 ± 2	34 ± 14	-7.40 ± 1.80

Between group differences in range, maximum gain, lower plateau and set point gain of HR and sympathetic baroreflex responses were determined using Student's t-tests. Values are group means ± SEM. *, **P<0.05, 0.01 vs. control in HR and RSNA. Group n are indicated in parentheses. MAP_{50} = mean arterial pressure at mid-range of the curve. The range of HR was smaller [df = 9, t = 2.42, P<0.05] in lesioned animals. Maximum gain [df = 9, t = 3.10, P<0.05] of HR was elevated with lesion. Heart rate plateau [df = 9, t = -3.28, P<0.01] and the set point gain [df = 9, t = 2.75, P<0.05] was higher in lesioned rats. Maximum gain [df = 9, t = 1.82, P<0.05] of the RSNA baroreflex response was significantly higher in lesioned rats. There was no difference found in MAP_{50} for both HR and

RSNA baroreflex. There was no difference found in range, lower plateau and set point gain for RSNA baroreflex.

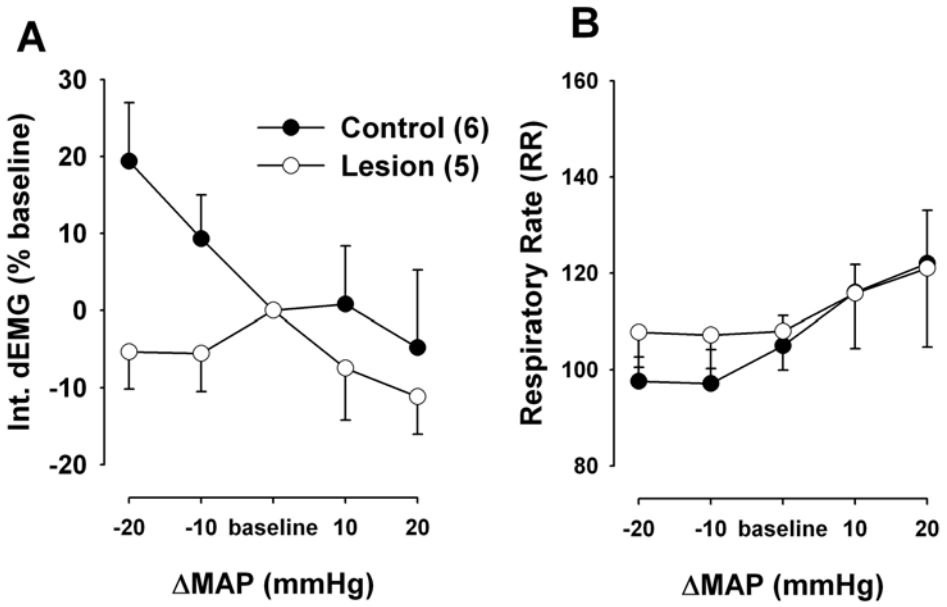

Figure 24. Integrated dEMG and respiratory rate (RR) changes during pharmacological BP manipulations (i.e., baroreflex testing) of vehicle-treated and lesioned rat. Averages of dEMG (A) and RR (B) at baseline, ±10 and ±20 mmHg are shown for sham-lesioned and neurotoxin-injected animals.

Data were analyzed by 2-way ANOVA with repeated measures using Lesion and ΔMAP as factors. Main effects and significant interactions were followed up with between-group comparisons using Newman-Keuls post hoc tests. Data are group mean ± S.E.M. Group n are indicated in parentheses.

Two-way ANOVA with repeated measure used to examine the effect of NTS serotonin Lesion and ΔMAP on change in dEMG showed a main effect of Lesion

[F (1,36) = 15.21, $p<0.01$] due to the significant decrease of dEMG in lesioned rats particularly at the lowest BP.

A 2-way ANOVA with repeated measure preformed to examine the effect of NTS serotonin Lesion and ∆MAP on RR showed no main effects or interaction.

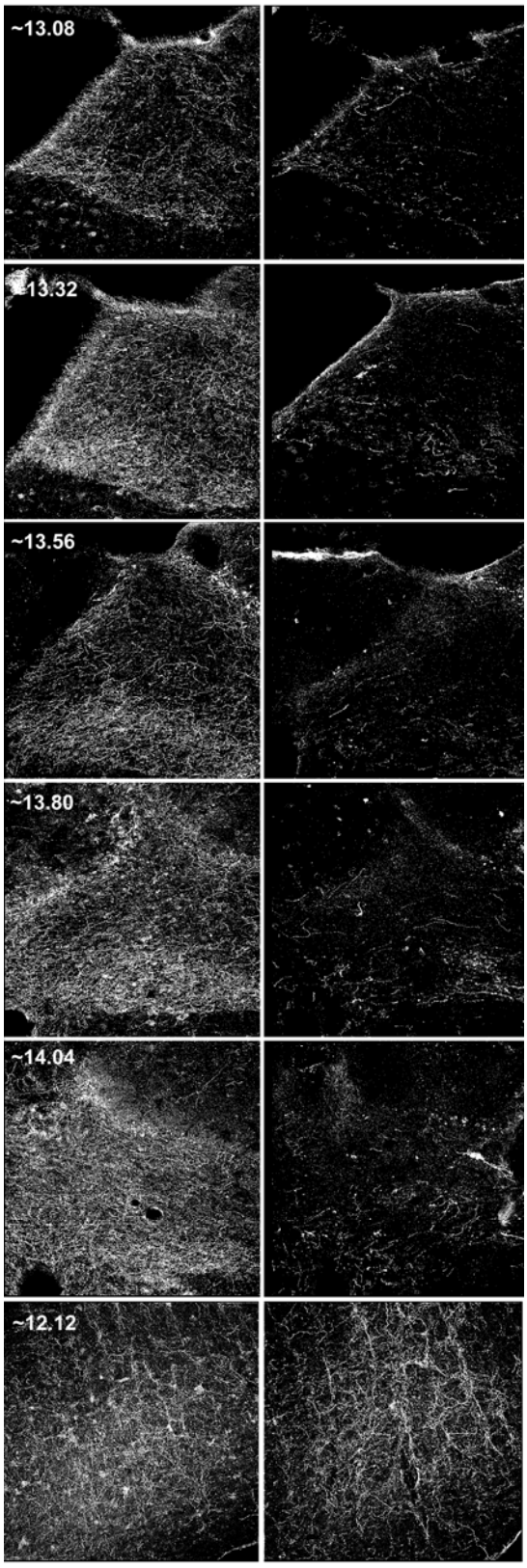
~13.08
~13.32
~13.56
~13.80
~14.04
~12.12

Figure 25. Representative examples of serotonin immunoreactivity in 5 coronal planes of the NTS and DMX. The location of each section in relationship to Bregma is indicated in the left images (caudal to Bregma in mm). Images on the left were obtained from a representative sham-lesioned animal. Images on the right were taken from a representative lesioned animal at approximately the same coronal planes as the images on the left. The first 5 pairs of images are of the NTS/DMX region. The last image pair shows the C1 region of the RVLM.

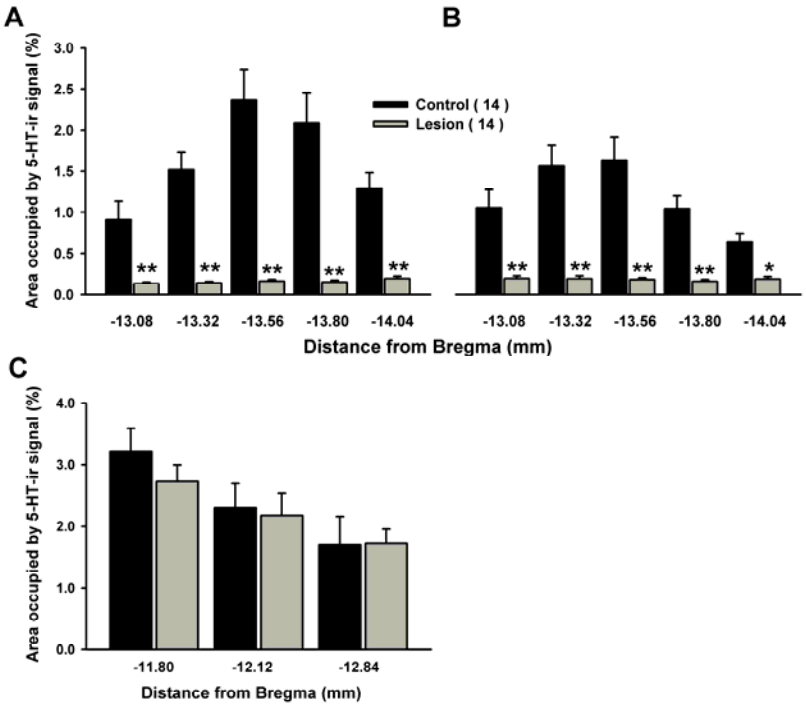

Figure 26. Quantification of serotonin nerve terminal content of vehicle-treated and lesioned rats from the 5 rostral-caudal coronal planes of the NTS (A) and DMX (B). The 5-HT-ir nerve terminal content is also shown in 3 rostral-caudal planes within the C1 region of the RVLM (C).

Data were analyzed by 2-way ANOVA with repeated measures using Lesion and Distance from Bregma as factors. Main effects and significant interactions were followed up with between-group comparisons using Newman-Keuls post hoc tests. Data are group mean ± S.E.M. Group n are indicated in parentheses. *, ** $P<0.05$, $P<0.01$ between groups.

An overall 2-way ANOVA with repeated measures examining the effect Lesion and Distance from Bregma on 5-HT-ir nerve terminal content in the NTS showed a Lesion x Distance from Bregma interaction [F (1,104) =9.31, $P<0.001$] due to the more extensive lesion of 5-HT-ir nerve terminals in the central regions of the caudal NTS where nerve terminal content was greatest in sham-lesioned rats. A main effect of Lesion [F (1,104) = 53.62, $P<0.01$] was due to the lower 5-HT-ir serotonin nerve terminal content in lesioned animals. A main effect of Distance from Bregma [F (1,104) = 9.30, $P<0.01$] was due to the change of 5-HT-ir nerve terminal content in both groups throughout the NTS.

An overall 2-way ANOVA with repeated measures examining the effect of Lesion and Distance from Bregma on the 5-HT-ir nerve terminal content in the DMX showed a Lesion x Distance from Bregma interaction [F (1,104) = 6.22, $p<0.01$] due to the more extensive lesion in the more rostral central region of the nucleus where 5-HT-ir nerve terminal density is normally highest. A main effect of Lesion [F (1,104) = 40.35, $P<0.01$] was due to the lower 5-HT-ir nerve terminal content in lesioned animals. A main effect of Distance from Bregma [F (1,104) = 6.25, $P<0.01$] was due to the variation of 5-HT-ir nerve terminal content in both groups over the extent of the DMX.

An overall 2-way ANOVA with repeated measures examining the effect of Lesion and Distance from Bregma on the 5-HT-ir nerve terminal content in the RVLM region showed no effect of lesion.

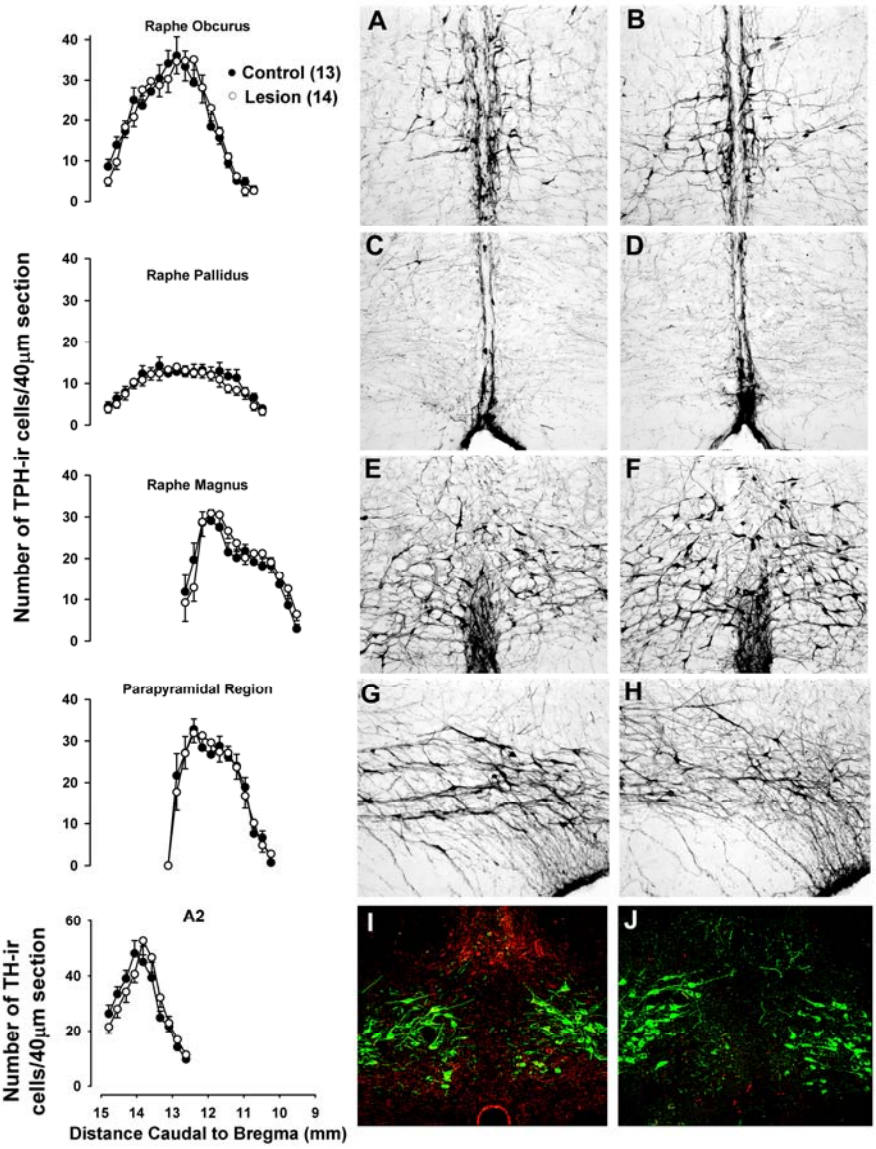

Figure 27. Cell profiles of TPH-ir cell number are shown for the serotonin-rich nuclei that provide major projections to the NTS. Cell profiles of TH-ir cells are shown for the A2 region throughout the extent of the nucleus. Examples of TPH-ir cells are shown for vehicle-treated (control) (A,C,E,G) and lesioned rats (B,D,F,H) in the serotonin-rich nuclei known to project to the NTS including the raphe obscurus (A-B), raphe pallidus (C-D), raphe magnus (E-F) and

parapyramidal region (G-H). Examples of the A2 region of the NTS showing TH-ir cells (green) and serotonin-ir fibers (red) are shown for control (I) and lesioned (J) rats.

Data were analyzed by 2-way ANOVA with repeated measures using Lesion and Distance from Bregma as factors. Main effects and significant interactions were followed up with between-group comparisons using Newman-Keuls post hoc tests. Data are group mean ± S.E.M. Group n are indicated in parentheses.

Overall 2-way ANOVA with repeated measures was preformed to examine the effect of Lesion and Distance from Bregma of TPH-ir cell numbers in each serotonin-rich nucleus and TH-ir cell number in the A2 region. There was no significant difference found between groups.

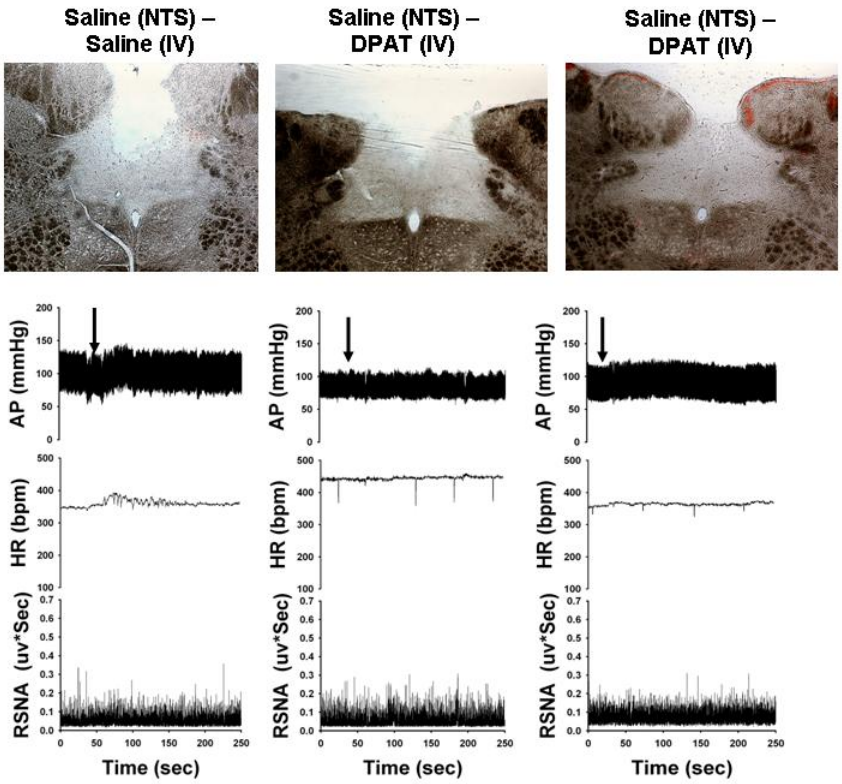

Figure 28. Three representative histology pictures of NTS injection sites are shown (top). Their respective DLH responses of arterial pressure, heart rate (HR) and renal sympathetic nerve activity (RSNA) are shown below. Arrows indicated DLH injection. There was no obvious DLH response even with correct placement of cannula in the NTS.

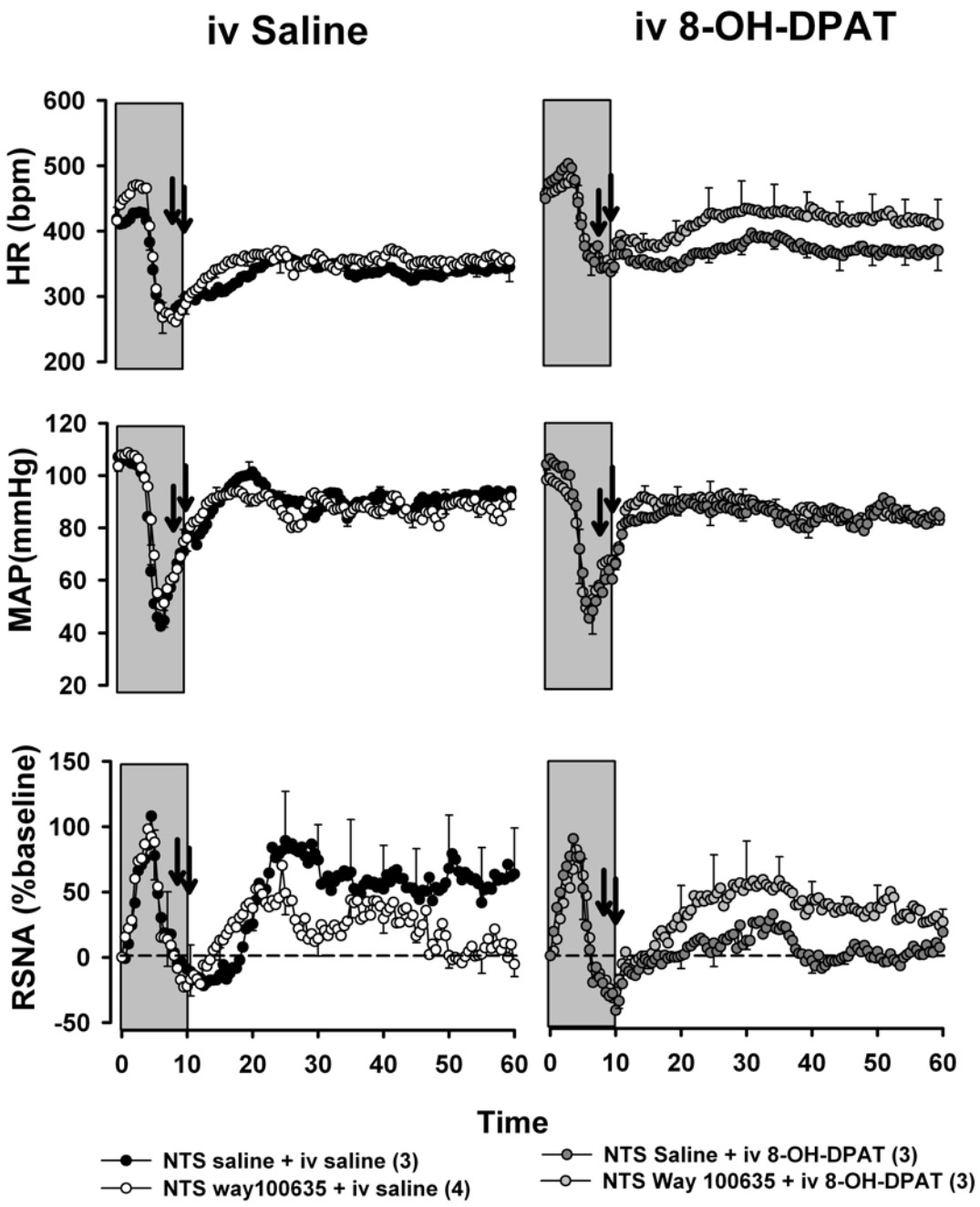

Figure 29. Mean arterial pressure (MAP), heart rate (HR), renal sympathetic nerve activity (RSNA) during hemorrhage and subsequent recovery in rats injected with saline or Way-100635 in the NTS (first arrow) followed by

hemorrhage and subsequent systemic injection of saline or 8-OH-DPAT (second arrow). Data are group means ± S.E.M. Group n are indicated in parentheses. Three way-ANOVA used to examine the effects of 5-HT_{1A} receptor blockade, 8-OH-DPAT and Time on HR, MAP and RSNA showed a main effect of Time on HR [$F(1,108) = 16.82$, $P<0.01$], MAP [$F(1,108) = 21.74$, $P<0.01$] and RSNA [$F(1,108) = 16.07$, $P<0.01$] due to variation of the two variables in all four groups over time.

Discussion

Selective lesion of serotonin nerve terminals in the caudal aspect of the dorsomedial brainstem, where arterial baro- and chemoreceptors projections terminate, attenuated compensatory sympathetic and ventilatory responses to blood loss. The same lesion augmented HR and sympathetic arterial baroreflex gain but attenuated ventilatory responses to lower pressure. Sympathetic and ventilatory responses to acute arterial chemoreceptor stimulation with KCN were also attenuated by the lesion. These findings indicate that serotonergic axon terminals in the NTS and/or surrounding region release neurotransmitters critical for normal ventilatory and sympathetic responses to hypovolemia. The data further suggest that the attenuated sympathetic and ventilatory responses to blood loss in animals with reduced serotonin innervation of the dorsomedial medulla may be related to deficient processing of peripheral chemoreceptor afferent input in the NTS.

The NTS receives serotonin-positive projections from multiple sites, including the nodose ganglia, the DR, as well as the caudal raphe nuclei including the RO, RM and RP (Schaffar et al., 1988; Thor and Helke, 1987). In addition, 5-HT-ir positive cell soma have been detected in the AP and mediolateral portions of the NTS itself (Calza et al., 1985). In a prior study, we found virtually the same pattern of suppressed ventilatory and sympathetic responses during recovery from hemorrhage in rats subjected to lesion of caudal raphe serotonin cells that we also observed here after a more discrete lesion of

serotonin nerve terminals in the NTS (Kung et al., 2010). As such, it seems most likely that caudal hindbrain serotonergic projections to the NTS or surrounding regions contribute to normal ventilatory and sympathetic responses after hemorrhage. It remains to be determined if altered arterial baroreflex and chemoreflex responses observed with NTS serotonin nerve terminal lesions are mediated by loss of axonal projections from the caudal raphe.

Selective lesion of serotonin-producing cells in the nodose ganglia using 5,7-DHT results in transient hypertension and a persistent increase in BP variability, suggesting that these cells facilitate baroreflex control of BP (Orer et al., 1991). In contrast, others have found that BP is normal and that BP variability is reduced 2 weeks after injection of 5,7-DHT directly into the NTS (Itoh et al., 1992). The data suggest that 5-HT-ir nerve terminals in the NTS that originate from cells in the nodose ganglion may facilitate baroreflex control, while serotonin projections from cells within the AP/NTS region or caudal raphe may instead suppress baroreflex gain. In preliminary studies we found that by 10-12 days after NTS injection of 5,7-DHT, TPH-ir positive cell bodies in the caudal raphe began to degenerate (data not shown). Serotonergic cells of the caudal raphe send collaterals to a wide range of targets. Thus, it is unclear whether prior studies performed 2 weeks after neurotoxin injection in the NTS faithfully assessed a specific role for NTS serotonergic projections in baroreflex control.

In the current study, both HR and RSNA baroreflex gain was increased 7 days after neurotoxin injection in the NTS. These findings were observed in the

absence of any evidence of caudal raphe serotonin cell loss, or loss of 5-HT-ir nerve terminal density in the C1 region of the RVLM, the latter of which contains or lies near to important serotonergic targets that control ventilatory rhythm generation as well as pre-motor neurons of the sympathetic nervous system. Because of this it is unlikely that increased baroreflex gain after NTS lesion was the result of degeneration of serotonin cell bodies and subsequent loss of collateral projections outside the NTS to alternative sites involved in arterial baroreflex control.

In our previous study, we noted that caudal raphe serotonin cell lesion also enhanced baroreflex control of HR (Kung et al., 2010). Indices of improved baroreflex control included a greater average increase in the gain of fluctuations in HR interval in response to spontaneous changes in BP. In the current study, a serotonin nerve terminal lesion limited to the NTS and its immediate surrounding region did not affect spontaneous baroreflex gain, but instead reduced BP variability in the LF domain. Assessments of spontaneous baroreflex gain reflect the activity of both the vagal and sympathetic components of baroreflex control (Cerutti et al., 1991; Japundzic et al., 1990; Pagani et al., 1986). In contrast, low frequency BP oscillations result primarily from the baroreflex-mediated waxing and waning of sympathetic vasoconstriction. The reduced power of low frequency BP oscillations observed with NTS lesion reflects a greater precision in sympathetic BP control, i.e., BP deflections away from the set-point produce a more robust sympathetic correction leading to reduced maximum and minimum

BP deviations. Taken together the data suggest that serotonin nerve terminals in the NTS may have a greater effect on the sympathetic control of BP, while caudal raphe derived serotonin innervation of other regions may suppress other targets that influence cardiovagal control of BP.

Enhanced arterial baroreflex function was probably not responsible for deficits in the sympathetic secondary compensation in NTS-lesioned animals. Indeed, the primary sympathetic compensatory response to blood loss that is presumed to be mediated by baroreceptor unloading was almost completely abolished by the lesion. Surprisingly, BP was maintained during the primary compensatory phase despite the absence of significant sympathetic compensation. In prior studies, we noted that sinoaortic denervation and the commensurate loss of sympathetic compensation during blood loss resulted in a slightly earlier onset of hypotension (Osei-Owusu and Scrogin, 2006). In the present study, it is likely that alternative vasoconstrictor mechanisms mediated by the intact baroreflex, such as vasoconstrictor hormone release, helped to maintain BP in the absence of sympathoexcitation. Alternatively, it is plausible that serotonin nerve terminals in the NTS selectively influence renal sympathetic drive during baroreflex activation and that changes in RSNA may not accurately reflect sympathetic-dependent increases in vascular resistance that maintain BP during baroreceptor unloading with hemorrhage. However, this seems unlikely since lesioned rats showed a robust increase in RSNA during baroreceptor unloading with nitroprusside.

The attenuated sympathetic compensation observed during the initial phase of blood withdrawal was paralleled by a similar absence of ventilatory response in lesioned rats. The attenuation of sympathetic compensatory responses during the primary compensatory phase may have been due, in part, to a deficit in respiratory drive that normally develops during the early phase of hemorrhage. This possibility is supported by observations that NTS lesion attenuated the post-apneic sympathetic and ventilatory responses to KCN in the same animals. Suppressed chemoreflex sensitivity commonly accompanies increased baroreflex function in many models. (Gao et al., 2004; Haider et al., 2009; Wang et al., 2006). Thus, it is possible that increased BRS suppressed sympathetic responses to chemoreflex activation in lesioned rats. However, we observed that the ventilatory response to baroreceptor unloading during nitroprusside infusion was virtually abolished by the NTS lesion. As such there appears to be a primary deficit in the ability to increase ventilation following serotonin lesion in the NTS that is independent of sympathetic baroreflex responses.

Serotonin has been implicated in a wide range of roles in ventilatory function. However, little is known about its role in arterial chemoreflex control at the level of the NTS. Contrary to our findings, corroborating reports indicate that the bradycardic response to peripheral chemoreceptor activation is inhibited by either serotonin or 5-HT_3 receptor agonist injection into the comNTS (Sevoz et al., 1997). This effect appears to be selective for the cardiovagal component of

the reflex since neither ventilatory nor sympathetic responses to KCN injection or infiltration of the carotid body with CO_2 were influenced by local application of serotonin or 5-HT_3 receptor agonists in the NTS. In the present study there was no effect of serotonin nerve terminal lesion on the bradycardic response to chemoreflex stimulation. In our studies the bradycardic response was profound even at the lowest dose tested. Thus, the effects of serotonin nerve terminal lesion on the HR component of the chemoreflex response may have been obscured by the very large effect at the doses tested. Alternatively, the endogenous serotonin release that occurs within the NTS during chemoreceptor activation may not be sufficient to activate a 5-HT_3 receptor-dependent inhibition of the bradycardic reflex. In any case, these data further confirm that sympathetic activity and ventilation are tightly coupled during reflex activation of ventilatory response, while the bradycardic response to chemosensory afferent stimulation is somehow modulated differently.

Additional evidence suggests that serotonin released from the caudal raphe may actually have an inhibitory effect on ventilatory responses to hypoxia rather than a facilitatory effect as our data suggest. For instance chemical stimulation of the RM region suppressed activation of chemosensitive NTS neurons during systemic KCN injection in anesthetized rats (Netzer et al., 2009). A second study showed no effect of caudal raphe suppression on ventilatory responses to hypoxia in awake rats (Taylor et al., 2005). In the latter study, dialysis of the 5-HT_{1A}-receptor agonist, 8-OH-DPAT, into various regions of the

caudal raphe successfully attenuated ventilatory responses to central chemoreflex activation with hyperoxic hypercapnia, presumably by selectively inhibiting serotonin neurons via 5-HT_{1A} autoreceptors. However, the same strategy had no effect on minute ventilation during 60 min of hypoxia, suggesting that caudal raphe serotonin cells do not contribute to peripheral chemoreflex responses. However, drug diffusion during dialysis may have also activated inhibitory 5-HT_{1A}-receptors expressed on non-serotonergic cells in regions that regulate motoric responses to chemosensory reflex information. Thus, it is still not entirely clear how the high density of serotonin innervation of the comNTS influences afferent input from chemosensory afferents. It remains to be determined whether disruption of chemoreflex sensitivity directly contributes to the loss of sympathetic and ventilatory compensation during both the early phase of active blood loss or to the deficit in compensation after blood loss is terminated.

In our prior studies, we noted that the initial sympathoexcitatory response to hemorrhage was truncated in rats subjected to caudal hindbrain serotonin cell lesion, while the early ventilatory response to active blood withdrawal was abolished. In these studies, 5-HT-ir nerve terminal content in the comNTS was decreased by 50-60%. In the present study, both sympathetic and ventilatory responses to early hemorrhage were completely abolished when 5-HT-ir nerve terminal content in the NTS was reduced by over 90%. These data support the view that loss of serotonin innervation of the NTS region was responsible for the

attenuated sympathetic response to hemorrhage after lesion of serotonin cells in the caudal raphe. The data also suggest that separate pathways may activate the initial ventilatory and sympathetic responses to blood loss but that an underlying coupling between ventilatory drive and sympathetic activity also contributes to the primary compensatory phase. In this scenario, the ventilatory response appears to be more sensitive to loss of serotonin innervation in the NTS than the sympathetic response. However, more thorough loss of serotonin innervation in the NTS may suppress ventilation to such a degree that the coupling between sympathetic activity and ventilation overcomes the baroreflex-mediated sympathetic response to blood loss.

These findings further support the view that loss of peripheral chemoreflex responses may contribute to deficits in sympathetic compensation during hemorrhage. In anesthetized dogs, hemorrhage produces a local decrease in carotid body PaO_2 that stimulates carotid sinus afferents during the sympatholytic phase of blood loss (Schertel et al., 1994). With continued blood loss or prolonged hypovolemia ventilatory responses normally increase PaO_2. However, reduced blood flow may continue to compromise delivery of O_2 to the carotid body and thus prolong chemoreceptor activation. Moreover, the development of metabolic acidosis may provide an additional stimulus to activate the carotid sinus nerves. In our prior studies, animals subjected to the same hemorrhage procedure as performed in the current study showed evidence of increased lactate within 10 minutes of blood withdrawal (Kung et al., 2010). At the same

time ventilation began to increase despite lower $PaCO_2$ and higher PaO_2. Together these data suggest that peripheral chemoreceptor activation in response to metabolic acidosis may contribute to ventilatory and sympathetic recovery following hemorrhage in intact animals, and that loss of serotonin in the NTS may interfere with the ability of the peripheral chemoreflex to elicit appropriate compensatory responses.

Serotonin nerve terminals contain multiple neurotransmitters that may facilitate chemoreflex responses to hypoxia. For instance substance P is co-localized in a subset of serotonin-containing cells within the NTS (Thor and Helke, 1987). Substance P is also released in the NTS in response to hypoxia in conscious animals (Abdala et al., 2006). However, administration of a substance P antagonist in the NTS does not affect either BP or HR responses to KCN (Zhang et al., 2000). Thyrotropin releasing hormone is also co-localized in serotonin neurons and has also been implicated in ventilatory function (Hedner et al., 1981). As yet, it is not possible to determine whether the attenuation of compensatory responses to hemorrhage or chemosensory activation in response to serotonin nerve terminals is due to loss of serotonin *per se*.

In our prior study, animals subjected to serotonin cell lesion developed more severe tissue hypoxia following hemorrhage despite their having higher PaO2 compared to sham-lesioned animals (Kung et al., 2010). As in the present study, lesioned animals also exhibited normal BP. Together with the evidence from the current study, these findings suggest that serotonin nerve terminals in

the NTS may be critical for appropriate distribution of blood volume during acute hypovolemic states. In the absence of such innervation, the animal defends perfusion pressure by increasing peripheral resistance, which in turn contributes to exaggerated tissue hypoxia. The presence of serotonin in the NTS may help the animals defend perfusion pressure through a sympathetic-mediated increase in venous tone and or cardiac output and thereby facilitate perfusion of peripheral tissue. It remains to be determined whether serotonin innervation of the NTS mediates these effects by altering sympathetic responses to peripheral chemoreflex activation.

We have shown previously that endogenous serotonin and 8-OH-DPAT act on 5-HT_{1A} receptors located at the postsynaptic non-serotonergic neurons to positively mediate the sympathetic activity during the secondary compensatory phase following blood loss. In the current study, animals subjected to NTS cannulation did not respond to iv. injection of 8-OH-DPAT. These data were intriguing and further implicate the NTS as a potential site of action for systemically administered 8-OH-DPAT. Specifically, it is plausible that NTS cannula placement may have compromised blood flow to the area, thus reducing the delivery of systemic 8-OH-DPAT to its site of action. Future experiments that effectively knock down 5-HT_{1A} receptors in the NTS region will help to further clarify the role of 5-HT_{1A} receptors in the sympathetic, ventilatory responses during hypoxia and the secondary compensatory phase of hypotensive hemorrhage.

Chapter VI

General Discussion

Our studies contradict several earlier studies suggesting that serotonin contributes to the sympatholytic phase of hemorrhage (Dean and Woyach, 2004; Elam et al., 1985; Morgan et al., 1988) and suggest instead that serotonin contributes to the secondary compensatory sympathoexcitation that develops with circulatory shock.

The contradictory results may be due to the fact that anesthesia was used in the majority of prior studies. The confounding effect of anesthesia is a vexing problem when conducting studies examining sympathetic and ventilatory reflex responses, since reflex regulation of both is highly influenced by GABA neurotransmission. Several of the most common anesthetic types have effects on GABA neurotransmission and so can lead to suppression or even abolishment of the reflex responses normally seen in unanaesthetized preparations. Anesthesia can sometimes result in completely different reflex responses in awake and anesthetized animals (Bloms-Funke et al., 1999; Heym et al., 1984; Montgomery et al., 1982; Seyde et al., 1985).

Nevertheless, these are the first studies to show evidence that serotonin neurons are necessary for normal sympathetic recovery from hypotensive

hemorrhage. Moreover, these studies provide the first evidence that central serotonin neurons may be important in protecting perfusion pressure during hypovolemia by maintaining cardiac output rather than by promoting potentially damaging increases in peripheral resistance. Serotonin-dependent maintenance of cardiac output is paralleled by sympathetic recovery, suggesting that sympathetic nerves may increase cardiac output. This could be due to either stimulation of cardiac contractility or to increases in venous return. Though studies in this dissertation did not specifically test either possibility, serotonin lesion did not affect HR, suggesting that sympathetic drive to the heart was probably normal. Thus it seems more likely that serotonin activates a sympathetic-dependent increase in venous return. This possibility is particularly intriguing given prior evidence from our lab that the 5-HT_{1A}-receptor agonist 8-OH-DPAT raises cardiac output in hemorrhaged animals by selectively increasing venoconstriction (Tiniakov et al., 2007). Evidence in the present study also demonstrated that the sympathoexcitatory effect of 8-OH-DPAT was most likely due to activation of 5-HT_{1A}-receptors on non-serotonergic neurons, which further suggests the possibility that endogenous serotonin acts on 5-HT_{1A}-receptor to mediate the secondary compensatory sympathetic recovery following hemorrhage.

Indeed, we have observed several parallels between serotonin-dependent sympathoexcitation and the sympathetic excitation produced by 8-OH-DPAT in hemorrhaged animals. Both are associated with reductions in lactate

accumulate, which indicates improved tissue oxygenation. Both are related to increases in cardiac output. Furthermore studies from our laboratory also suggest that 8-OH-DPAT increases venous tone (Tiniakov and Scrogin, 2006), which coincides with evidence that serotonin improves tissue perfusion without further raising BP or HR.

Our evidence now brings to light a novel possibility that serotonin acts on receptors in the NTS to mediate sympathoexcitation following hemorrhage. This finding is consistent with the possibility that the effects are mediated by 5-HT_{1A} receptors, since studies from our laboratory indicate that 8-OH-DPAT injections in the IVth cerebroventricle produce the most rapid and robust increase in sympathetic activity compared to other injections sites in more rostral portions of the cerebroventricular system (Scrogin, 2003). The IVth ventricle injections were made just rostral to portions of the NTS that control cardiorespiratory function. Injections given here were able to initiate sympathoexcitatory responses within 20 sec of drug administration. It is highly unlikely that the drug could have diffused down the spinal column to act directly within the spinal cord to produce sympathoexcitation to promote such a rapid response.

Furthermore, our studies demonstrated that disruption of the integrity of the NTS was sufficient to prevent normal sympathoexcitatory responses to 8-OH-DPAT given into the systemic circulation. Specifically, rats implanted with NTS cannula and subsequently injected with saline had almost no response to systemic 8-OH-DPAT. Though these results were inconclusive, they do suggest

the possibility that placement of the guide cannula somehow disrupted normal circulatory perfusion of the area such that systemic administration of 8-OH-DPAT was not able to reach the site of action in the NTS. Future studies utilizing more sophisticated methods, such as specific knock-down 5-HT_{1A} receptors, will be needed to determine whether systemic 8-OH-DPAT administration must reach the NTS to mediate its sympathoexcitatory effect in hypovolemic animals.

Studies in this thesis support the view that serotonin facilitates both peripheral and central chemoreflex responses to promote sympathetic activation during hemorrhage. The importance of caudal raphe serotonin neurons in central chemoreception in awake animals is now well established. Our studies extend these findings by demonstrating the importance of these neurons in determining the distribution of blood volume in hypovolemia. It remains to be determined if appropriate central chemoreception is necessary for beneficial hemodynamic responses to hemorrhage. This question can be answered by lesioning caudal serotonergic neurons then subjecting rats to hypotensive hemorrhage and measurement of cardiac output during recovery.

Findings from this study that serotonin may facilitate responses to peripheral chemoreflex activation are highly novel. Previous data suggests that serotonin neurons either have no effect on ventilatory responses to hypoxia or that they are inhibitory (Herman et al., 2000; Olson, 1987; Sevoz et al., 1997). The explanation for this disagreement with the literature is not evident. However, most prior studies have manipulated serotonin levels in the NTS by activation or

inhibition of caudal raphe neurons, which not only project to the NTS, but also send collateral projections to a myriad of other targets that, could interfere with the expression of the chemoreflex response. Ours is the sole study to examine peripheral chemoreflex sensitivity after selectively manipulating serotonin nerve terminals at the level of the NTS and its immediate surrounding area. Our immunohistochemical data suggest that serotonergic projections to other targets were not impaired following NTS lesion. However, direct measures of serotonin release, possibly through microdialysis would be required to confirm this assumption.

An anatomical substrate for serotonin's facilitation of peripheral chemoreflex responses and subsequent improvement of the hemodynamic response to hypovolemia has not so far been described. Our studies have shown that the sympathoexcitatory effects of 8-OH-DPAT are dependent upon intact sinoaortic innervation. The carotid sinus and aortic arch both give rise to chemo and baroreceptor afferents that convey sensory input to the NTS. Evidence that these sensory afferents are required for the full expression of the sympathoexcitatory effect of 8-OH-DPAT is intriguing, given evidence that serotonin also acts in the NTS to facilitate chemoreflex responses. Additional future studies that selectively denervate carotid bodies then measure sympathetic and ventilatory recovery after 8-OH-DPAT injection during hemorrhage will be necessary to further clarify and separate out the role of chemo or baroreceptor afferents during hemorrhage.

Also significant are findings that 8-OH-DPAT promotes a profound sympathoinhibition in euvolemic animals. This effect is most likely due to activation of 5-HT_{1A} receptors in the RVLM. In fact, 5-HT_{1A} receptors are coupled to Gαi and Gαo proteins of the heterotrimeric G-protein complex, and their activation promotes membrane hyperpolarization (Albert et al., 1996; Boess and Martin, 1994). Together the evidence suggests that during hemorrhage 8-OH-DPAT likely disinhibits a sympathoexcitatory process that is activated by hypovolemia through carotid sinus and/or aortic arch afferents. Recent evidence has actually shown that the inhibitory neurotransmitter GABA is released into the comNTS during exposure to hypoxia (Tabata et al., 2001). This effect is dependent upon intact carotid bodies. Thus, our evidence coupled with findings in the literature has led us to propose a model by which endogenous serotonin and exogenous 5-HT_{1A}-receptor agonists may mediate sympathoexcitation following blood loss. In this model Figures 30 and 31, the carotid bodies are activated by either reduced carotid body blood flow or the metabolic acidemia that accompanies hypotensive hemorrhage or hemorrhagic shock. Subsequent activation of second order NTS neurons promotes sympathoexcitation and increased ventilation. As peripheral chemoreceptor activation persists, GABA neurons in the NTS are activated, which suppress the chemoreflex response. Serotonin release in the NTS could act on 5-HT_{1A} receptors expressed on GABA neurons to attenuate this inhibition, allowing for greater sympathoexcitation to continue. In the hypovolemic animal, the 5-HT_{1A} receptor dependent

sympathoexcitation promotes selective venoconstriction. However, in the absence of 5-HT_{1A} receptor-dependent sympathoexcitation, the organism attempts to defend arterial pressure by increasing vasoconstrictor hormones that act primarily on the arterial side of the vasculature, promoting a potentially detrimental hemodynamic response to hypovolemia that could exacerbate ischemia. Thus, exogenous 5-HT_{1A}-receptor agonists may be useful as adjuvant treatment of hypovolemic shock by helping to facilitate appropriate sympathetic and hemodynamic responses to hemorrhage. Future studies that examine the role of GABA in unanaesthetized rats can utilize the working heat-brainstem preparation to measure single unit extracellular recording of the chemosensitive cells in the comNTS and determine whether they are sensitive to direct exposure to serotonin or 5-HT_{1A} agonist.

Important Implication

Our findings have significant implications for the current treatment of hypovolemic shock for obvious reasons. 5-HT_{1A} agonists giving during blood loss may provide a thermodynamically beneficial way to improve perfusion pressure when given as an adjuvant to volume resuscitation. However, it is possible that only a subset of the population may be responsive to this treatment.

Patients treated chronically with selective serotonin reuptake inhibitors show a desensitization of 5-HT_{1A} autoreceptors 5-HT_{1A} receptors on the non-serotonergic neurons as well (Stahl, 1998). Therefore, therapeutically 5-HT_{1A}

receptors may not work well and may not be able to exert their sympathoexcitatory effect during blood loss in those patients.

Sudden infant death syndrome is postulated to result from abnormalities in brainstem control of autonomic function and breathing during a critical developmental period. It is also reported that abnormalities of serotonin receptor binding in serotonin-rich nuclei may promote the abnormal peripheral and central- chemosensitivity that has been described in infants with apnea (Duncan et al., 2010; Gdovin et al., 2010; Liu and Wong-Riley, 2010). Serotonin has also been implicated in obstructive sleep apnea that results in increased sensitivity of the peripheral chemoreflex and potentially detrimental increases in sympathetic drive to the heart (Ling, 2008; Phillips et al., 2009). Therefore, manipulation of serotonin neuronal transmission from caudal raphe nuclei to the NTS could provide improved therapeutic treatments to modulate sympathetic and ventilation activities in these devastating pathologies.

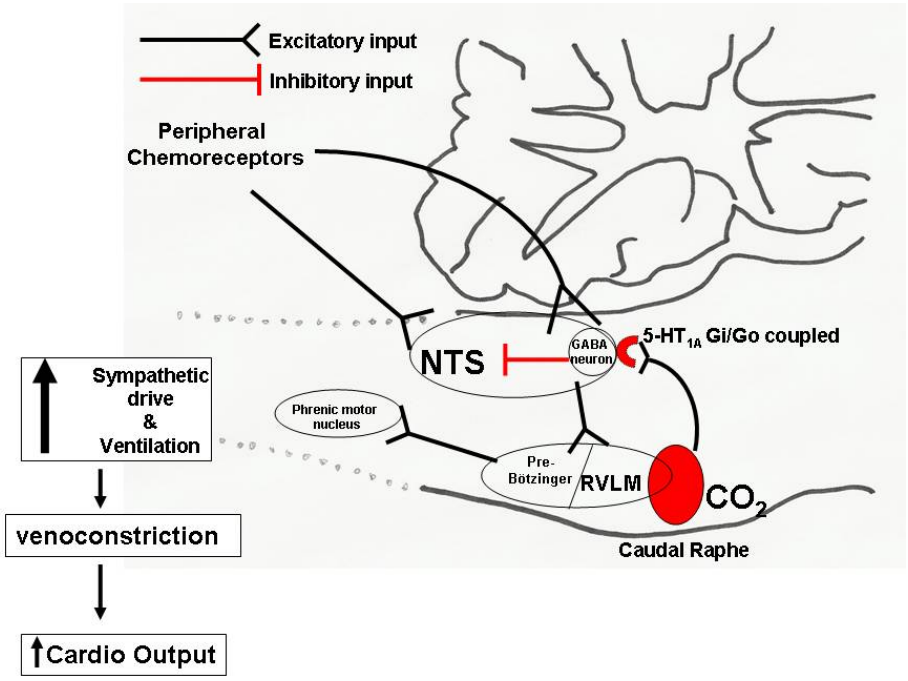

Figure 30. Hypothetical model to explain the effects of peripheral- and central-chemoreflex activation and modulation of sympathetic and ventilatory drive during hypotension hemorrhage.

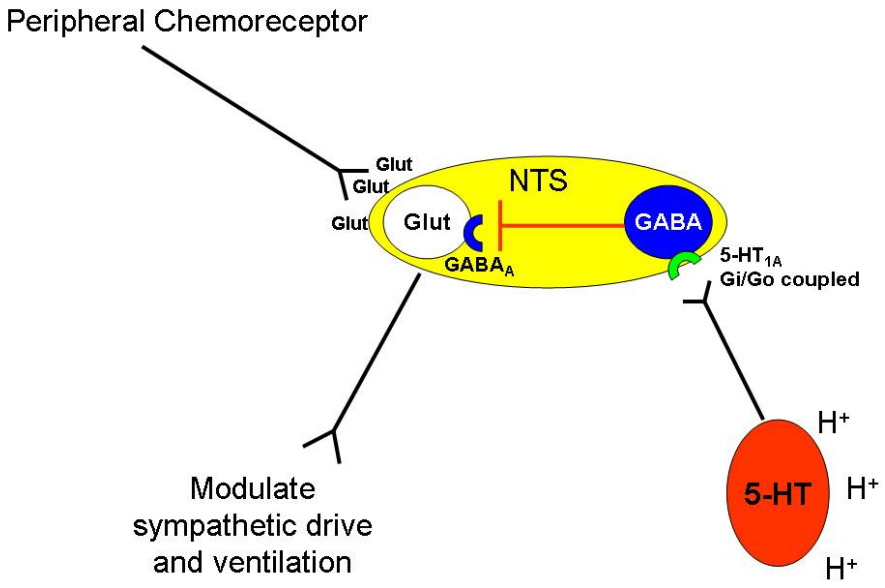

Figure 31. Detailed NTS circuitry within the hypothetical model. During hemorrhage, glutamate is released from peripheral chemoreflex afferent terminals and acts on receptors in the NTS to increase sympathetic and ventilatory drives. With continued hypoxia GABA neurons are stimulated by chemoreceptor afferents which suppresses the ventilatory and sympathetic response to hemorrhage. When CO_2 and H^+ concentration increase, serotonin is released from caudal raphe neurons and acts on 5-HT_{1A} receptors in the NTS. These receptors are Gi/Go coupled and thus may disinhibit GABA release. Therefore, during hemorrhage both central- and peripheral- chemoreflexes may modulate sympathetic drive and ventilation during hypotension hemorrhage.

REFERENCE LIST

Abdala, A. P., G. H. Schoorlemmer, and E. Colombari, 2006, Ablation of NK1 receptor bearing neurons in the nucleus of the solitary tract blunts cardiovascular reflexes in awake rats: Brain Res, v. 1119, p. 165-73.

Aitken, A. R., and I. Tork, 1988, Early development of serotonin-containing neurons and pathways as seen in wholemount preparations of the fetal rat brain: J Comp Neurol, v. 274, p. 32-47.

Alayash, A. I., 1999, Hemoglobin-based blood substitutes: oxygen carriers, pressor agents, or oxidants?: Nat Biotechnol, v. 17, p. 545-9.

Albert, P. R., P. Lembo, J. M. Storring, A. Charest, and C. Saucier, 1996, The 5-HT1A receptor: signaling, desensitization, and gene transcription: Neuropsychopharmacology, v. 14, p. 19-25.

Arnaud, F., M. Hammett, L. Asher, N. Philbin, J. Rice, F. Dong, B. Pearce, W. S. Flournoy, C. Nicholson, R. McCarron, and D. Freilich, 2005, Effects of bovine polymerized hemoglobin on coagulation in controlled hemorrhagic shock in swine: Shock, v. 24, p. 145-52.

Averill, D. B., A. M. Scher, and E. O. Feigl, 1983, Angiotensin causes vasoconstriction during hemorrhage in baroreceptor-denervated dogs: Am J Physiol, v. 245, p. H667-73.

Bago, M., and C. Dean, 2001, Sympathoinhibition from ventrolateral periaqueductal gray mediated by 5-HT(1A) receptors in the RVLM: Am J Physiol Regul Integr Comp Physiol, v. 280, p. R976-84.

Bago, M., L. Marson, and C. Dean, 2002, Serotonergic projections to the rostroventrolateral medulla from midbrain and raphe nuclei: Brain Res, v. 945, p. 249-58.

Ballantyne, D., and P. Scheid, 2001, Central chemosensitivity of respiration: a brief overview: Respir Physiol, v. 129, p. 5-12.

Balogh, Z., B. A. McKinley, C. S. Cocanour, R. A. Kozar, C. S. Cox, and F. A. Moore, 2003a, Patients with impending abdominal compartment syndrome

do not respond to early volume loading: Am J Surg, v. 186, p. 602-7; discussion 607-8.

Balogh, Z., B. A. McKinley, C. S. Cocanour, R. A. Kozar, A. Valdivia, R. M. Sailors, and F. A. Moore, 2003b, Supranormal trauma resuscitation causes more cases of abdominal compartment syndrome: Arch Surg, v. 138, p. 637-42; discussion 642-3.

Barcroft, H., and O. G. Edholm, 1945, On the vasodilatation in human skeletal muscle during post-haemorrhagic fainting: J Physiol, v. 104, p. 161-75.

Bard, J. A., J. Zgombick, N. Adham, P. Vaysse, T. A. Branchek, and R. L. Weinshank, 1993, Cloning of a novel human serotonin receptor (5-HT7) positively linked to adenylate cyclase: J Biol Chem, v. 268, p. 23422-6.

Barnes, N. M., and T. Sharp, 1999, A review of central 5-HT receptors and their function: Neuropharmacology, v. 38, p. 1083-152.

Bedard, P., H. Barbeau, G. Barbeau, and M. Filion, 1979, Progressive increase of motor activity induced by 5-HTP in the rat below a complete secretion of the spinal cord: Brain Res, v. 169, p. 393-7.

Bedard, P., and C. J. Pycock, 1977, "Wet-dog" shake behaviour in the rat: a possible quantitative model of central 5-hydroxytryptamine activity: Neuropharmacology, v. 16, p. 663-70.

Bereiter, D. A., A. M. Zaid, and D. S. Gann, 1984, Adrenocorticotropin response to graded blood loss in the cat: Am J Physiol, v. 247, p. E398-404.

Berger, A. J., 1979, Distribution of carotid sinus nerve afferent fibers to solitary tract nuclei of the cat using transganglionic transport of horseradish peroxidase: Neurosci Lett, v. 14, p. 153-8.

Bishop, V., A. Malliani, and P. Thoren, 1983, Cardiac mechanoreceptors., in *Handbook of physiology, sect 2; The cardiovascular system-peripheral circulation and organ blood flow*: American Physiology society, Bethesda, Md.

Blair, M. L., and D. Mickelsen, 2006, Activation of lateral parabrachial nucleus neurons restores blood pressure and sympathetic vasomotor drive after hypotensive hemorrhage: Am J Physiol Regul Integr Comp Physiol, v. 291, p. R742-50.

Bloms-Funke, P., M. Gernert, U. Ebert, and W. Loscher, 1999, Extracellular single-unit recordings of piriform cortex neurons in rats: influence of

different types of anesthesia and characterization of neurons by pharmacological manipulation of serotonin receptors: J Neurosci Res, v. 55, p. 608-19.

Blum, P. S., and J. A. Spath, Jr., 1986, Interaction between naloxone and serotonin in the control of the cardiovascular system in hemorrhaged cats: Eur J Pharmacol, v. 123, p. 99-108.

Boess, F. G., and I. L. Martin, 1994, Molecular biology of 5-HT receptors: Neuropharmacology, v. 33, p. 275-317.

Bowker, R. M., K. N. Westlund, and J. D. Coulter, 1981, Origins of serotonergic projections to the spinal cord in rat: an immunocytochemical-retrograde transport study: Brain Res, v. 226, p. 187-99.

Bradley, S. R., V. A. Pieribone, W. Wang, C. A. Severson, R. A. Jacobs, and G. B. Richerson, 2002, Chemosensitive serotonergic neurons are closely associated with large medullary arteries: Nat Neurosci, v. 5, p. 401-2.

Brizzee, B. L., R. D. Russ, and B. R. Walker, 1991, Role of vasopressin in acutely altered baroreflex sensitivity during hemorrhage in rats: Am J Physiol, v. 261, p. R677-85.

Brooks, V. L., and D. C. Hatton, 1991, Hypotension during vasopressin receptor blockade: role of V2 receptors and sympathetic nervous system: Am J Physiol, v. 260, p. H1878-87.

Brunner, M. J., M. S. Sussman, A. S. Greene, C. H. Kallman, and A. A. Shoukas, 1982, Carotid sinus baroreceptor reflex control of respiration: Circ Res, v. 51, p. 624-36.

Calza, L., L. Giardino, R. Grimaldi, M. Rigoli, H. W. Steinbusch, and M. Tiengo, 1985, Presence of 5-HT-positive neurons in the medial nuclei of the solitary tract: Brain Res, v. 347, p. 135-9.

Castillo, C., M. Ibarra, J. A. Marquez, R. Villalobos-Molina, and E. Hong, 1993, Pharmacological evidence for interactions between 5-HT1A receptor agonists and subtypes of alpha 1-adrenoceptors on rabbit aorta: Eur J Pharmacol, v. 241, p. 141-8.

Caverson, M. M., J. Ciriello, and F. R. Calaresu, 1984, Paraventricular nucleus of the hypothalamus: an electrophysiological investigation of neurons projecting directly to intermediolateral nucleus in the cat: Brain Res, v. 305, p. 380-3.

Cerutti, C., M. P. Gustin, C. Z. Paultre, M. Lo, C. Julien, M. Vincent, and J. Sassard, 1991, Autonomic nervous system and cardiovascular variability in rats: a spectral analysis approach: Am J Physiol, v. 261, p. H1292-9.

Chalmers, J. P., P. I. Korner, and S. W. White, 1967, The effects of haemorrhage in the unanaesthetized rabbit: J Physiol, v. 189, p. 367-91.

Chaudry, I. H., A. Ayala, W. Ertel, and R. N. Stephan, 1990, Hemorrhage and resuscitation: immunological aspects: Am J Physiol, v. 259, p. R663-78.

Chen, J., S. L. Zeng, Z. R. Rao, and J. W. Shi, 1992, Serotonergic projections from the midbrain periaqueductal gray and nucleus raphe dorsalis to the nucleus parafascicularis of the thalamus: Brain Res, v. 584, p. 294-8.

Cocchi, M. N., E. Kimlin, M. Walsh, and M. W. Donnino, 2007, Identification and resuscitation of the trauma patient in shock: Emerg Med Clin North Am, v. 25, p. 623-42, vii.

Cornish, K. G., J. P. Gilmore, and T. McCulloch, 1988, Central blood volume and blood pressure in conscious primates: Am J Physiol, v. 254, p. H693-701.

Currie, P. J., and D. V. Coscina, 1998, 5-Hydroxytryptaminergic receptor agonists: effects on neuropeptide Y potentiation of feeding and respiratory quotient: Brain Res, v. 803, p. 212-7.

Dabrowska, J., and M. Brylinski, 2006, Stereoselectivity of 8-OH-DPAT toward the serotonin 5-HT1A receptor: biochemical and molecular modeling study: Biochem Pharmacol, v. 72, p. 498-511.

Dahlstrom, A., and K. Fuxe, 1964, Localization of monoamines in the lower brain stem: Experientia, v. 20, p. 398-9.

Damaso, E. L., L. G. Bonagamba, D. O. Kellett, D. Jordan, A. G. Ramage, and B. H. Machado, 2007, Involvement of central 5-HT7 receptors in modulation of cardiovascular reflexes in awake rats: Brain Res, v. 1144, p. 82-90.

Darlington, D. N., J. Shinsako, and M. F. Dallman, 1986, Responses of ACTH, epinephrine, norepinephrine, and cardiovascular system to hemorrhage: Am J Physiol, v. 251, p. H612-8.

Dean, C., 2005, Sympathoinhibition from ventrolateral periaqueductal gray mediated by the caudal midline medulla: Am J Physiol Regul Integr Comp Physiol, v. 289, p. R1477-81.

Dean, C., and M. Bago, 2002, Renal sympathoinhibition mediated by 5-HT(1A) receptors in the RVLM during severe hemorrhage in rats: Am J Physiol Regul Integr Comp Physiol, v. 282, p. R122-30.

Dean, C., and V. L. Woyach, 2004, Serotonergic neurons of the caudal raphe nuclei activated in response to hemorrhage in the rat: Brain Res, v. 1025, p. 159-68.

DeMaria, E. J., M. P. Lilly, and D. S. Gann, 1989, Aldosterone secretion following non-hypotensive hemorrhage is potentiated by prior blood loss: J Trauma, v. 29, p. 1183-90; discussion 1191-2.

Dempsher, D. P., and D. S. Gann, 1983, Increased cortisol secretion after small hemorrhage is not attributable to changes in adrenocorticotropin: Endocrinology, v. 113, p. 86-93.

Dias, M. B., T. B. Nucci, L. O. Margatho, J. Antunes-Rodrigues, L. H. Gargaglioni, and L. G. Branco, 2007, Raphe magnus nucleus is involved in ventilatory but not hypothermic response to CO2: J Appl Physiol, v. 103, p. 1780-8.

Duncan, J. R., D. S. Paterson, J. M. Hoffman, D. J. Mokler, N. S. Borenstein, R. A. Belliveau, H. F. Krous, E. A. Haas, C. Stanley, E. E. Nattie, F. L. Trachtenberg, and H. C. Kinney, 2010, Brainstem serotonergic deficiency in sudden infant death syndrome: Jama, v. 303, p. 430-7.

Dutschmann, M., A. Guthmann, and H. Herbert, 1998, NMDA receptor subunit NR1-immunoreactivity in the rat pons and brainstem and colocalization with Fos induced by nasal stimulation: Brain Res, v. 809, p. 221-30.

Elam, R., F. Bergmann, and G. Feuerstein, 1985, The use of antiserotonergic agents for the treatment of acute hemorrhagic shock of cats: Eur J Pharmacol, v. 107, p. 275-8.

Erickson, J. T., and D. E. Millhorn, 1994, Hypoxia and electrical stimulation of the carotid sinus nerve induce Fos-like immunoreactivity within catecholaminergic and serotoninergic neurons of the rat brainstem: J Comp Neurol, v. 348, p. 161-82.

Essadki, A., and J. Atkinson, 1981, Renin release by renin-depleted rats following hypotensive haemorrhage and anesthetics: Pflugers Arch, v. 392, p. 46-50.

Evans, R. G., I. P. Hayes, J. Ludbrook, and S. Ventura, 1993a, Factors confounding blockade of cardiac afferents by intrapericardial procaine in conscious rabbits: Am J Physiol, v. 264, p. H1861-70.

Evans, R. G., J. M. Haynes, and J. Ludbrook, 1993b, Effects of 5-HT-receptor and alpha 2-adrenoceptor ligands on the haemodynamic response to acute central hypovolaemia in conscious rabbits: Br J Pharmacol, v. 109, p. 37-47.

Evans, R. G., V. Kapoor, and J. Ludbrook, 1992, A CNS serotonergic mechanism in acute central hypovolemia in conscious rabbits?: J Cardiovasc Pharmacol, v. 19, p. 1009-17.

Everitt, B. J., T. Hokfelt, L. Terenius, K. Tatemoto, V. Mutt, and M. Goldstein, 1984, Differential co-existence of neuropeptide Y (NPY)-like immunoreactivity with catecholamines in the central nervous system of the rat: Neuroscience, v. 11, p. 443-62.

Fargin, A., J. R. Raymond, J. W. Regan, S. Cotecchia, R. J. Lefkowitz, and M. G. Caron, 1989, Effector coupling mechanisms of the cloned 5-HT1A receptor: J Biol Chem, v. 264, p. 14848-52.

Fitzpatrick, C. M., K. L. Biggs, B. Z. Atkins, F. J. Quance-Fitch, P. S. Dixon, S. A. Savage, D. H. Jenkins, and J. D. Kerby, 2005, Prolonged low-volume resuscitation with HBOC-201 in a large-animal survival model of controlled hemorrhage: J Trauma, v. 59, p. 273-81; discussion 281-3.

Fox, I. J., D. A. Gerasch, and J. J. Leonard, 1977, Left ventricular mechanoreceptors: a haemodynamic study: J Physiol, v. 273, p. 405-25.

Fozard, J. R., A. K. Mir, and D. N. Middlemiss, 1987, Cardiovascular response to 8-hydroxy-2-(di-n-propylamino) tetralin (8-OH-DPAT) in the rat: site of action and pharmacological analysis: J Cardiovasc Pharmacol, v. 9, p. 328-47.

Francis, R. C., C. Hohne, G. Kaczmarczyk, and W. Boemke, 2004, Effect of angiotensin II and endothelin-1 receptor blockade on the haemodynamic and hormonal changes after acute blood loss and after retransfusion in conscious dogs: Acta Physiol Scand, v. 180, p. 319-28.

Fujisawa, Y., A. Miyatake, Y. Hayashida, Y. Aki, S. Kimura, T. Tamaki, and Y. Abe, 1994, Role of vasopressin on cardiovascular changes during hemorrhage in conscious rats: Am J Physiol, v. 267, p. H1713-8.

Gao, L., Z. Zhu, I. H. Zucker, and W. Wang, 2004, Cardiac sympathetic afferent stimulation impairs baroreflex control of renal sympathetic nerve activity in rats: Am J Physiol Heart Circ Physiol, v. 286, p. H1706-11.

Garner, S. J., F. L. Eldridge, P. G. Wagner, and R. T. Dowell, 1989, Buspirone, an anxiolytic drug that stimulates respiration: Am Rev Respir Dis, v. 139, p. 946-50.

Garrison, R. N., A. A. Conn, P. D. Harris, and R. Zakaria el, 2004, Direct peritoneal resuscitation as adjunct to conventional resuscitation from hemorrhagic shock: a better outcome: Surgery, v. 136, p. 900-8.

Gaudin-Chazal, G., P. Portalier, M. C. Barrit, and J. J. Puizillout, 1982, Serotonin-like immunoreactivity in paraffin-sections of the nodose ganglia of the cat: Neurosci Lett, v. 33, p. 169-72.

Gautier, H., M. Bonora, S. A. Schultz, and J. E. Remmers, 1987, Hypoxia-induced changes in shivering and body temperature: J Appl Physiol, v. 62, p. 2477-84.

Gdovin, M. J., D. A. Zamora, C. R. Ravindran, and J. C. Leiter, 2010, Serotonergic modulation of respiratory rhythmogenesis and central chemoreception: Ethn Dis, v. 20, p. S1-39-44.

Glasgow, J., L.-H. Kung, J. Vantrease, and K. Scrogin, 2009, Anatomical Study of Serotonergic Involvement in Cardiovascular Compensation Following Hypotensive Hemorrhage: FASEB v. 23.

Gray, P. A., W. A. Janczewski, N. Mellen, D. R. McCrimmon, and J. L. Feldman, 2001, Normal breathing requires preBotzinger complex neurokinin-1 receptor-expressing neurons: Nat Neurosci, v. 4, p. 927-30.

Gray, P. A., J. C. Rekling, C. M. Bocchiaro, and J. L. Feldman, 1999, Modulation of respiratory frequency by peptidergic input to rhythmogenic neurons in the preBotzinger complex: Science, v. 286, p. 1566-8.

Greenway, C. V., and A. E. Lawson, 1966, The effects of adrenaline and noradrenaline on venous return and regional blood flows in the anaesthetized cat with special reference to intestinal blood flow: J Physiol, v. 186, p. 579-95.

Greer, J. J., Z. al-Zubaidy, and J. E. Carter, 1996, Thyrotropin-releasing hormone stimulates perinatal rat respiration in vitro: Am J Physiol, v. 271, p. R1160-4.

Haggendal, E., M. Lindfors, and D. Lundberg, 1976, Haemodynamic effects of massive doses of hydrocortisone and the interaction with phenoxybenzamine in controlled haemorrhagic shock in the dog: Acta Anaesthesiol Scand, v. 20, p. 285-95.

Haider, T., G. Casucci, T. Linser, M. Faulhaber, H. Gatterer, G. Ott, A. Linser, I. Ehrenbourg, E. Tkatchouk, M. Burtscher, and L. Bernardi, 2009, Interval hypoxic training improves autonomic cardiovascular and respiratory control in patients with mild chronic obstructive pulmonary disease: J Hypertens, v. 27, p. 1648-54.

Haljamae, H., 1984, Microcirculation and hemorrhagic shock: Am J Emerg Med, v. 2, p. 100-7.

Hamed, A. T., J. Z. Ginos, R. D. Ekas, Jr., B. S. Jandhyala, and M. F. Lokhandwala, 1983, Renal hemodynamics in hemorrhagic hypotension: studies on the effects of pre- and postjunctional dopamine receptor agonists: J Cardiovasc Pharmacol, v. 5, p. 207-12.

Hasser, E. M., and J. C. Schadt, 1992, Sympathoinhibition and its reversal by naloxone during hemorrhage: Am J Physiol, v. 262, p. R444-51.

Haxhiu, M. A., F. Tolentino-Silva, G. Pete, P. Kc, and S. O. Mack, 2001, Monoaminergic neurons, chemosensation and arousal: Respir Physiol, v. 129, p. 191-209.

Hedner, T., J. Hedner, J. Jonason, and D. Lundberg, 1981, Evidence suggesting a role for substance P in central respiratory regulation in the rat: Acta Physiol Scand, v. 112, p. 487-9.

Hellman, A., E. Haggendal, and D. Lundberg, 1982, Hemodynamic effects of massive doses of dexamethasone in controlled hypovolemic shock in the dog: Acta Anaesthesiol Scand, v. 26, p. 222-4.

Henderson, L. A., K. A. Keay, and R. Bandler, 2000a, Caudal midline medulla mediates behaviourally-coupled but not baroreceptor-mediated vasodepression: Neuroscience, v. 98, p. 779-92.

Henderson, R. A., M. E. Whitehurst, K. R. Morgan, and R. G. Carroll, 2000b, Reduced oxygen consumption precedes the drop in body core temperature caused by hemorrhage in rats: Shock, v. 13, p. 320-4.

Hendricks, T. J., D. V. Fyodorov, L. J. Wegman, N. B. Lelutiu, E. A. Pehek, B. Yamamoto, J. Silver, E. J. Weeber, J. D. Sweatt, and E. S. Deneris, 2003, Pet-1 ETS gene plays a critical role in 5-HT neuron development and is

required for normal anxiety-like and aggressive behavior: Neuron, v. 37, p. 233-47.

Henry, R. A., I. L. Lu, L. A. Beightol, and D. L. Eckberg, 1998, Interactions between CO2 chemoreflexes and arterial baroreflexes: Am J Physiol, v. 274, p. H2177-87.

Hensel, H., 1973, Neural processes in thermoregulation: Physiol Rev, v. 53, p. 948-1017.

Henze, M., D. Hart, A. Samarel, J. Barakat, L. Eckert, and K. Scrogin, 2008, Persistent alterations in heart rate variability, baroreflex sensitivity, and anxiety-like behaviors during development of heart failure in the rat: Am J Physiol Heart Circ Physiol, v. 295, p. H29-38.

Herman, J. K., K. D. O'Halloran, and G. E. Bisgard, 2000, Serotonin and the hypoxic ventilatory response in awake goats: Adv Exp Med Biol, v. 475, p. 559-69.

Hernandez, I., A. C. Ingles, J. M. Pinilla, T. Quesada, and L. F. Carbonell, 1991, Cardiocirculatory responses to AII and AVP in conscious rats: J Cardiovasc Pharmacol, v. 17, p. 916-22.

Heron, M., D. Hoyert, S. Murphy, J. Xu, K. Kochanek, and B. Tejada-Vera, 2009, National Vital Statistics Reports. Deaths: Final Data for 2006: National center for Health Statistics, v. 57.

Heslop, D. J., K. A. Keay, and R. Bandler, 2002, Haemorrhage-evoked compensation and decompensation are mediated by distinct caudal midline medullary regions in the urethane-anaesthetised rat: Neuroscience, v. 113, p. 555-67.

Hess, J. R., and M. J. Thomas, 2003, Blood use in war and disaster: lessons from the past century: Transfusion, v. 43, p. 1622-33.

Heym, J., G. F. Steinfels, and B. L. Jacobs, 1984, Chloral hydrate anesthesia alters the responsiveness of central serotonergic neurons in the cat: Brain Res, v. 291, p. 63-72.

Heymans, C., 1968, Regulation of blood pressure and hypertension: Nord Med, v. 79, p. 79-82.

Hokfelt, T., J. O. Kellerth, G. Nilsson, and B. Pernow, 1975, Substance p: localization in the central nervous system and in some primary sensory neurons: Science, v. 190, p. 889-90.

Holtman, J. R., Jr., 1988, Immunohistochemical localization of serotonin- and substance P-containing fibers around respiratory muscle motoneurons in the nucleus ambiguus of the cat: Neuroscience, v. 26, p. 169-78.

Horn, A. S., H. G. Baumgarten, and H. G. Schlosserberger, 1973, Inhibition of the uptake of 5-hydroxytryptamine, noradrenaline and dopamine into rat brain homogenates by various hydroxylated tryptamines: J Neurochem, v. 21, p. 233-6.

Howe, P. R., P. F. Rogers, and G. A. Head, 1989, Limited baroreflex control of heart rate in young stroke-prone spontaneously hypertensive rats: J Hypertens, v. 7, p. 69-75.

Hoyer, D., D. E. Clarke, J. R. Fozard, P. R. Hartig, G. R. Martin, E. J. Mylecharane, P. R. Saxena, and P. P. Humphrey, 1994, International Union of Pharmacology classification of receptors for 5-hydroxytryptamine (Serotonin): Pharmacol Rev, v. 46, p. 157-203.

Innis, R. B., E. J. Nestler, and G. K. Aghajanian, 1988, Evidence for G protein mediation of serotonin- and GABAB-induced hyperpolarization of rat dorsal raphe neurons: Brain Res, v. 459, p. 27-36.

Itoh, H., R. H. Alper, and R. D. Bunag, 1992, Baroreflex changes produced by serotonergic or catecholaminergic lesions in the rat nucleus tractus solitarius: J Pharmacol Exp Ther, v. 261, p. 225-33.

Itoh, H., and R. D. Bunag, 1991, Cardiovascular and sympathetic effects of injecting serotonin into the nucleus tractus solitarius in rats: J Pharmacol Exp Ther, v. 256, p. 1147-53.

Jacobs, B. L., and E. C. Azmitia, 1992, Structure and function of the brain serotonin system: Physiol Rev, v. 72, p. 165-229.

Jacobs, B. L., and C. A. Fornal, 1997, Serotonin and motor activity: Curr Opin Neurobiol, v. 7, p. 820-5.

Jansen, A. S., X. V. Nguyen, V. Karpitskiy, T. C. Mettenleiter, and A. D. Loewy, 1995, Central command neurons of the sympathetic nervous system: basis of the fight-or-flight response: Science, v. 270, p. 644-6.

Japundzic, N., M. L. Grichois, P. Zitoun, D. Laude, and J. L. Elghozi, 1990, Spectral analysis of blood pressure and heart rate in conscious rats: effects of autonomic blockers: J Auton Nerv Syst, v. 30, p. 91-100.

Jeggo, R. D., D. O. Kellett, Y. Wang, A. G. Ramage, and D. Jordan, 2005, The role of central 5-HT3 receptors in vagal reflex inputs to neurones in the nucleus tractus solitarius of anaesthetized rats: J Physiol, v. 566, p. 939-53.

Johnson, J. V., G. W. Bennett, and R. Hatton, 1988, Central and systemic effects of a vasopressin V1 antagonist on MAP recovery after haemorrhage in rats: J Cardiovasc Pharmacol, v. 12, p. 405-12.

Johnson, M. D., 1994, Synaptic glutamate release by postnatal rat serotonergic neurons in microculture: Neuron, v. 12, p. 433-42.

Johnson, P. L., J. H. Hollis, R. Moratalla, S. L. Lightman, and C. A. Lowry, 2003, A panicogenic stimulus (acute hypercapnia) increases c-fos immunoreactivity in subpopulations of midbrain serotonergic neurons.: Society of Neuroscience, v. Abstr. 29, 712.5

Jorgensen, H. S., 2007, Studies on the neuroendocrine role of serotonin: Dan Med Bull, v. 54, p. 266-88.

Julien, C., Z. Q. Zhang, and C. Barres, 1995, How sympathetic tone maintains or alters arterial pressure: Fundam Clin Pharmacol, v. 9, p. 343-9.

Kadekaro, M., J. Y. Summy-Long, M. L. Terrell, H. Lekan, H. E. Gary, Jr., and H. M. Eisenberg, 1990, Cerebral metabolic and hormonal activations during hemorrhage in sinoaortic-denervated rats: Am J Physiol, v. 259, p. R305-12.

Kalia, M., and R. V. Welles, 1980, Brain stem projections of the aortic nerve in the cat: a study using tetramethyl benzidine as the substrate for horseradish peroxidase: Brain Res, v. 188, p. 23-32.

Kaneko, T., and T. P. Hicks, 1990, GABA(B)-related activity involved in synaptic processing of somatosensory information in S1 cortex of the anaesthetized cat: Br J Pharmacol, v. 100, p. 689-98.

Kasting, N. W., 1988, Simultaneous and independent release of vasopressin and oxytocin in the rat: Can J Physiol Pharmacol, v. 66, p. 22-6.

Kasting, N. W., and M. F. Wilkinson, 1987, Vasopressin functions as an endogenous antipyretic in the newborn: Biol Neonate, v. 51, p. 249-54.

Kellum, J. A., and M. R. Pinsky, 2002, Use of vasopressor agents in critically ill patients: Curr Opin Crit Care, v. 8, p. 236-41.

Kenney, M. J., D. E. Claassen, R. J. Fels, and C. S. Saindon, 1999, Cold stress alters characteristics of sympathetic nerve discharge bursts: J Appl Physiol, v. 87, p. 732-42.

Kheck, N. M., P. J. Gannon, and E. C. Azmitia, 1995, 5-HT1A receptor localization on the axon hillock of cervical spinal motoneurons in primates: J Comp Neurol, v. 355, p. 211-20.

Kung, L.-H., and K. Scrogin., 2009, Serotonin (5-HT) innervation of the nuclerus tractus solitariius (NTS) is necessary for sympathetic recovery following hypotensive hemorrhage FASEB J. , v. 23.

Kung, L. H., J. Glasgow, A. Ruszaj, T. Gray, and K. E. Scrogin, 2010, Serotonin neurons of the caudal raphe nuclei contribute to sympathetic recovery following hypotensive hemorrhage: Am J Physiol Regul Integr Comp Physiol.

Laguzzi, R., D. J. Reis, and W. T. Talman, 1984, Modulation of cardiovascular and electrocortical activity through serotonergic mechanisms in the nucleus tractus solitarius of the rat: Brain Res, v. 304, p. 321-8.

Lambert, G. A., E. Friedman, E. Buchweitz, and S. Gershon, 1978, Involvement of 5-hydroxytryptamine in the central control of respiration, blood pressure and heart rate in the anaesthetized rat: Neuropharmacology, v. 17, p. 807-13.

Larnicol, N., F. Wallois, P. Berquin, F. Gros, and D. Rose, 1994, c-fos-like immunoreactivity in the cat's neuraxis following moderate hypoxia or hypercapnia: J Physiol Paris, v. 88, p. 81-8.

Laubie, M., M. Drouillat, H. Dabire, C. Cherqui, and H. Schmitt, 1989, Ventrolateral medullary pressor area: site of hypotensive and sympatho-inhibitory effects of (+/-)8-OH-DPAT in anaesthetized dogs: Eur J Pharmacol, v. 160, p. 385-94.

Laycock, J. F., W. Penn, D. G. Shirley, and S. J. Walter, 1979, The role of vasopressin in blood pressure regulation immediately following acute haemorrhage in the rat: J Physiol, v. 296, p. 267-75.

Leppaniemi, A., R. Soltero, D. Burris, E. Pikoulis, C. Waasdorp, J. Ratigan, H. Hufnagel, and D. Malcolm, 1996, Fluid resuscitation in a model of uncontrolled hemorrhage: too much too early, or too little too late?: J Surg Res, v. 63, p. 413-8.

Li, Y. Q., H. G. Jia, Z. R. Rao, and J. W. Shi, 1990, Serotonin-, substance P- or leucine-enkephalin-containing neurons in the midbrain periaqueductal gray and nucleus raphe dorsalis send projection fibers to the central amygdaloid nucleus in the rat: Neurosci Lett, v. 120, p. 124-7.

Li, Y. W., S. L. Wesselingh, and W. W. Blessing, 1992, Projections from rabbit caudal medulla to C1 and A5 sympathetic premotor neurons, demonstrated with phaseolus leucoagglutinin and herpes simplex virus: J Comp Neurol, v. 317, p. 379-95.

Liard, J. F., 1988, V1 vs. combined V1+V2 vasopressin blockade after hemorrhage in conscious dogs: Am J Physiol, v. 255, p. H1325-9.

Liard, J. F., 1990, Interaction between V1 and V2 effects in hemodynamic response to vasopressin in dogs: Am J Physiol, v. 258, p. H482-9.

Lighton, C., C. A. Marsden, and G. W. Bennett, 1984, The effects of 5,7-dihydroxytryptamine and p-chlorophenylalanine on thyrotrophin-releasing hormone in regions of the brain and spinal cord of the rat: Neuropharmacology, v. 23, p. 55-60.

Ling, L., 2008, Serotonin and NMDA receptors in respiratory long-term facilitation: Respir Physiol Neurobiol, v. 164, p. 233-41.

Little, R. A., H. W. Marshall, M. I. Reynolds, and H. B. Stoner, 1980, Effect of changes in baroreceptor input on the intensity of shivering in the anaesthetised cat: Pflugers Arch, v. 384, p. 261-5.

Liu, L. M., J. A. Ward, and M. A. Dubick, 2003, Hemorrhage-induced vascular hyporeactivity to norepinephrine in select vasculatures of rats and the roles of nitric oxide and endothelin: Shock, v. 19, p. 208-14.

Liu, Q., and M. T. Wong-Riley, 2010, Postnatal changes in the expressions of serotonin 1A, 1B, and 2A receptors in ten brain stem nuclei of the rat: implication for a sensitive period: Neuroscience, v. 165, p. 61-78.

Loeschcke, H. H., 1982, Central chemosensitivity and the reaction theory: J Physiol, v. 332, p. 1-24.

Loeschcke, H. H., R. A. Mitchell, B. Katsaros, J. F. Perkins, and A. Konig, 1963, Interaction of intracranial chemosensitivity with peripheral afferents to the respiratory centers: Ann N Y Acad Sci, v. 109, p. 651-60.

Loewy, A. D., 1981, Raphe pallidus and raphe obscurus projections to the intermediolateral cell column in the rat: Brain Res, v. 222, p. 129-33.

Loewy, A. D., and S. McKellar, 1981, Serotonergic projections from the ventral medulla to the intermediolateral cell column in the rat: Brain Res, v. 211, p. 146-52.

Lorang, D., S. G. Amara, and R. B. Simerly, 1994, Cell-type-specific expression of catecholamine transporters in the rat brain: J Neurosci, v. 14, p. 4903-14.

Lovick, T. A., 1997, The medullary raphe nuclei: a system for integration and gain control in autonomic and somatomotor responsiveness?: Exp Physiol, v. 82, p. 31-41.

Ludbrook, J., and S. Ventura, 1994, The decompensatory phase of acute hypovolaemia in rabbits involves a central delta 1-opioid receptor: Eur J Pharmacol, v. 252, p. 113-6.

Ludbrook, J., and S. Ventura, 1996, Roles of carotid baroreceptor and cardiac afferents in hemodynamic responses to acute central hypovolemia: Am J Physiol, v. 270, p. H1538-48.

Madden, C. J., and S. F. Morrison, 2008, Brown adipose tissue sympathetic nerve activity is potentiated by activation of 5-hydroxytryptamine (5-HT)1A/5-HT7 receptors in the rat spinal cord: Neuropharmacology, v. 54, p. 487-96.

Maley, B., and R. Elde, 1982, The ultrastructural localization of serotonin immunoreactivity within the nucleus of the solitary tract of the cat: J Neurosci, v. 2, p. 1499-506.

Manaker, S., and H. M. Verderame, 1990, Organization of serotonin 1A and 1B receptors in the nucleus of the solitary tract: J Comp Neurol, v. 301, p. 535-53.

Marshall, J. F., 1979, Somatosensory inattention after dopamine-depleting intracerebral 6-OHDA injections: spontaneous recovery and pharmacological control: Brain Res, v. 177, p. 311-24.

Martel, M. J., K. J. MacKinnon, M. Y. Arsenault, E. Bartellas, M. C. Klein, C. A. Lane, A. E. Sprague, and A. K. Wilson, 2002, Hemorrhagic shock: J Obstet Gynaecol Can, v. 24, p. 504-20; quiz 521-4.

Mason, P., 2001, Contributions of the medullary raphe and ventromedial reticular region to pain modulation and other homeostatic functions: Annu Rev Neurosci, v. 24, p. 737-77.

Mathai, M. L., G. L. Pennington, and M. J. McKinley, 1997, The effect of angiotensin AT1 receptor blockade in the brain on the maintenance of blood pressure during haemorrhage in sheep: Acta Physiol Scand, v. 161, p. 495-502.

McDermott, B. J., B. C. Millar, and H. M. Piper, 1993, Cardiovascular effects of neuropeptide Y: receptor interactions and cellular mechanisms: Cardiovasc Res, v. 27, p. 893-905.

Meier-Hellmann, A., K. Reinhart, D. L. Bredle, M. Specht, C. D. Spies, and L. Hannemann, 1997, Epinephrine impairs splanchnic perfusion in septic shock: Crit Care Med, v. 25, p. 399-404.

Mendelson, W. B., J. V. Martin, and D. M. Rapoport, 1990, Effects of buspirone on sleep and respiration: Am Rev Respir Dis, v. 141, p. 1527-30.

Merahi, N., H. S. Orer, and R. Laguzzi, 1992, 5-HT2 receptors in the nucleus tractus solitarius: characterisation and role in cardiovascular regulation in the rat: Brain Res, v. 575, p. 74-8.

Messier, M. L., A. Li, and E. E. Nattie, 2004, Inhibition of medullary raphe serotonergic neurons has age-dependent effects on the CO2 response in newborn piglets: J Appl Physiol, v. 96, p. 1909-19.

Miura, M., J. Okada, and M. Kanazawa, 1998, Topology and immunohistochemistry of proton-sensitive neurons in the ventral medullary surface of rats: Brain Res, v. 780, p. 34-45.

Montgomery, S. B., P. A. Jose, and G. M. Eisner, 1982, The role of anesthesia and catecholamines in the renal response to mild hemorrhage: Circ Shock, v. 9, p. 433-44.

Moore, F. A., B. A. McKinley, and E. E. Moore, 2004, The next generation in shock resuscitation: Lancet, v. 363, p. 1988-96.

Moreira, T. S., A. C. Takakura, E. Colombari, and P. G. Guyenet, 2006, Central chemoreceptors and sympathetic vasomotor outflow: J Physiol, v. 577, p. 369-86.

Morgan, D. A., P. Thoren, E. A. Wilczynski, R. G. Victor, and A. L. Mark, 1988, Serotonergic mechanisms mediate renal sympathoinhibition during severe hemorrhage in rats: Am J Physiol, v. 255, p. H496-502.

Morris, M., V. Kapoor, and J. Chalmers, 1987, Plasma neuropeptide Y concentration is increased after hemorrhage in conscious rats: relative

contributions of sympathetic nerves and the adrenal medulla: J Cardiovasc Pharmacol, v. 9, p. 541-5.

Morrison, S. F., A. F. Sved, and A. M. Passerin, 1999, GABA-mediated inhibition of raphe pallidus neurons regulates sympathetic outflow to brown adipose tissue: Am J Physiol, v. 276, p. R290-7.

Mueller, R. A., A. C. Towle, and G. R. Breese, 1984, Supersensitivity to the respiratory stimulatory effect of TRH in 5,7-dihydroxytryptamine-treated rats: Brain Res, v. 298, p. 370-3.

Mueller, R. A., A. C. Towle, and G. R. Breese, 1985, The role of vagal afferents and carbon dioxide in the respiratory response to thyrotropin-releasing hormone: Regul Pept, v. 10, p. 157-66.

Munzner, R. F., D. G. Ward, and D. S. Gann, 1981, Right atrium mediates a vasomotor reflex: Am J Physiol, v. 241, p. R163-6.

Nakamura, K., K. Matsumura, T. Hubschle, Y. Nakamura, H. Hioki, F. Fujiyama, Z. Boldogkoi, M. Konig, H. J. Thiel, R. Gerstberger, S. Kobayashi, and T. Kaneko, 2004, Identification of sympathetic premotor neurons in medullary raphe regions mediating fever and other thermoregulatory functions: J Neurosci, v. 24, p. 5370-80.

Nattie, E. E., and A. Li, 2002a, CO2 dialysis in nucleus tractus solitarius region of rat increases ventilation in sleep and wakefulness: J Appl Physiol, v. 92, p. 2119-30.

Nattie, E. E., and A. Li, 2002b, Substance P-saporin lesion of neurons with NK1 receptors in one chemoreceptor site in rats decreases ventilation and chemosensitivity: J Physiol, v. 544, p. 603-16.

Nattie, E. E., A. Li, G. B. Richerson, and D. A. Lappi, 2004, Medullary serotonergic neurones and adjacent neurones that express neurokinin-1 receptors are both involved in chemoreception in vivo: J Physiol, v. 556, p. 235-53.

Neiberger, R. E., and J. C. Passmore, 1979, Effects of dopamine on canine intrarenal blood flow distribution during hemorrhage: Kidney Int, v. 15, p. 219-26.

Netzer, F., N. Mandjee, A. J. Verberne, J. F. Bernard, M. Hamon, R. Laguzzi, and C. Sevoz-Couche, 2009, Inhibition of the bradycardic component of the von Bezold-Jarisch reflex and carotid chemoreceptor reflex by

periaqueductal gray stimulation: involvement of medullary receptors: Eur J Neurosci, v. 29, p. 2017-28.

Nicholas, A. P., V. A. Pieribone, U. Arvidsson, and T. Hokfelt, 1992, Serotonin-, substance P- and glutamate/aspartate-like immunoreactivities in medullo-spinal pathways of rat and primate: Neuroscience, v. 48, p. 545-59.

Nosjean, A., C. Compoint, C. Buisseret-Delmas, H. S. Orer, N. Merahi, J. J. Puizillout, and R. Laguzzi, 1990, Serotonergic projections from the nodose ganglia to the nucleus tractus solitarius: an immunohistochemical and double labeling study in the rat: Neurosci Lett, v. 114, p. 22-6.

Nosjean, A., B. Franc, and R. Laguzzi, 1995, Increased sympathetic nerve discharge without alteration in the sympathetic baroreflex response by serotonin3 receptor stimulation in the nucleus tractus solitarius of the rat: Neurosci Lett, v. 186, p. 41-4.

Nosjean, A., and P. G. Guyenet, 1991, Role of ventrolateral medulla in sympatholytic effect of 8-OHDPAT in rats: Am J Physiol, v. 260, p. R600-9.

Nucci, T. B., L. G. Branco, and L. H. Gargaglioni, 2008, 5-HT1A, but not 5-HT2 and 5-HT7, receptors in the nucleus raphe magnus modulate hypoxia-induced hyperpnoea: Acta Physiol (Oxf), v. 193, p. 403-14.

Oliver, K. R., A. M. Kinsey, A. Wainwright, and D. J. Sirinathsinghji, 2000, Localization of 5-ht(5A) receptor-like immunoreactivity in the rat brain: Brain Res, v. 867, p. 131-42.

Olson, E. B., Jr., 1987, Ventilatory adaptation to hypoxia occurs in serotonin-depleted rats: Respir Physiol, v. 69, p. 227-35.

Ootsuka, Y., and W. W. Blessing, 2005, Activation of slowly conducting medullary raphe-spinal neurons, including serotonergic neurons, increases cutaneous sympathetic vasomotor discharge in rabbit: Am J Physiol Regul Integr Comp Physiol, v. 288, p. R909-18.

Orer, H. S., N. Merahi, A. Nosjean, C. M. Fattaccini, and R. Laguzzi, 1991, Cardiovascular effects of the local injection of 5,7-dihydroxytryptamine into the nodose ganglia and nucleus tractus solitarius in awake freely moving rats: Brain Res, v. 553, p. 123-8.

Osborn, J. W., and G. D. Fink, 2009, Region-specific changes in sympathetic nerve activity in angiotensin II-salt hypertension in the rat: Exp Physiol, v. 95, p. 61-8.

Osei-Owusu, P., and K. Scrogin, 2006, Role of the arterial baroreflex in 5-HT1A receptor agonist-mediated sympathoexcitation following hypotensive hemorrhage: Am J Physiol Regul Integr Comp Physiol, v. 290, p. R1337-44.

Osei-Owusu, P., and K. E. Scrogin, 2004, Buspirone raises blood pressure through activation of sympathetic nervous system and by direct activation of alpha1-adrenergic receptors after severe hemorrhage: J Pharmacol Exp Ther, v. 309, p. 1132-40.

Oskutyte, D., D. Jordan, and A. G. Ramage, 2009, Evidence that 5-hydroxytryptamine(7) receptors play a role in the mediation of afferent transmission within the nucleus tractus solitarius in anaesthetized rats: Br J Pharmacol, v. 158, p. 1387-94.

Ottersen, O. P., and J. Storm-Mathisen, 1984, Glutamate- and GABA-containing neurons in the mouse and rat brain, as demonstrated with a new immunocytochemical technique: J Comp Neurol, v. 229, p. 374-92.

Padley, J. R., D. H. Overstreet, P. M. Pilowsky, and A. K. Goodchild, 2005, Impaired cardiac and sympathetic autonomic control in rats differing in acetylcholine receptor sensitivity: Am J Physiol Heart Circ Physiol, v. 289, p. H1985-92.

Pagani, M., F. Lombardi, S. Guzzetti, O. Rimoldi, R. Furlan, P. Pizzinelli, G. Sandrone, G. Malfatto, S. Dell'Orto, E. Piccaluga, and et al., 1986, Power spectral analysis of heart rate and arterial pressure variabilities as a marker of sympatho-vagal interaction in man and conscious dog: Circ Res, v. 59, p. 178-93.

Pan, Z. Z., M. W. Wessendorf, and J. T. Williams, 1993, Modulation by serotonin of the neurons in rat nucleus raphe magnus in vitro: Neuroscience, v. 54, p. 421-9.

Pazos, A., R. Cortes, and J. M. Palacios, 1985, Quantitative autoradiographic mapping of serotonin receptors in the rat brain. II. Serotonin-2 receptors: Brain Res, v. 346, p. 231-49.

Peitzman, A. B., T. R. Billiar, B. G. Harbrecht, E. Kelly, A. O. Udekwu, and R. L. Simmons, 1995, Hemorrhagic shock: Curr Probl Surg, v. 32, p. 925-1002.

Penington, N. J., and J. S. Kelly, 1990, Serotonin receptor activation reduces calcium current in an acutely dissociated adult central neuron: Neuron, v. 4, p. 751-8.

Perez, H., and S. Ruiz, 1995, Medullary responses to chemoreceptor activation are inhibited by locus coeruleus and nucleus raphe magnus: Neuroreport, v. 6, p. 1373-6.

Peuler, J. D., G. L. Edwards, P. G. Schmid, and A. K. Johnson, 1990, Area postrema and differential reflex effects of vasopressin and phenylephrine in rats: Am J Physiol, v. 258, p. H1255-9.

Phillips, C. L., B. J. Yee, M. I. Trenell, J. S. Magnussen, D. Wang, D. Banerjee, N. Berend, and R. R. Grunstein, 2009, Changes in regional adiposity and cardio-metabolic function following a weight loss program with sibutramine in obese men with obstructive sleep apnea: J Clin Sleep Med, v. 5, p. 416-21.

Pompeiano, M., J. M. Palacios, and G. Mengod, 1994, Distribution of the serotonin 5-HT2 receptor family mRNAs: comparison between 5-HT2A and 5-HT2C receptors: Brain Res Mol Brain Res, v. 23, p. 163-78.

Pratt, G. D., N. G. Bowery, G. J. Kilpatrick, R. A. Leslie, N. M. Barnes, R. J. Naylor, B. J. Jones, D. R. Nelson, J. M. Palacids, P. Slater, and et al., 1990, Consensus meeting agrees distribution of 5-HT3 receptors in mammalian hindbrain: Trends Pharmacol Sci, v. 11, p. 135-7.

Prueckner, S., P. Safar, R. Kentner, J. Stezoski, and S. A. Tisherman, 2001, Mild hypothermia increases survival from severe pressure-controlled hemorrhagic shock in rats: J Trauma, v. 50, p. 253-62.

Putnam, R. W., 2001, Intracellular pH regulation of neurons in chemosensitive and nonchemosensitive areas of brain slices: Respir Physiol, v. 129, p. 37-56.

Quail, A. W., R. L. Woods, and P. I. Korner, 1987, Cardiac and arterial baroreceptor influences in release of vasopressin and renin during hemorrhage: Am J Physiol, v. 252, p. H1120-6.

Qureshi, N. U., E. K. Dayao, S. Shirali, Z. Zukowska-Grojec, and G. J. Hauser, 1998, Endogenous neuropeptide Y mediates vasoconstriction during endotoxic and hemorrhagic shock: Regul Pept, v. 75-76, p. 215-20.

Ramage, A. G., and C. M. Villalon, 2008, 5-hydroxytryptamine and cardiovascular regulation: Trends Pharmacol Sci, v. 29, p. 472-81.

Repine, T. B., J. G. Perkins, D. S. Kauvar, and L. Blackborne, 2006, The use of fresh whole blood in massive transfusion: J Trauma, v. 60, p. S59-69.

Riad, M., S. Garcia, K. C. Watkins, N. Jodoin, E. Doucet, X. Langlois, S. el Mestikawy, M. Hamon, and L. Descarries, 2000, Somatodendritic localization of 5-HT1A and preterminal axonal localization of 5-HT1B serotonin receptors in adult rat brain: J Comp Neurol, v. 417, p. 181-94.

Richerson, G. B., 1995, Response to CO2 of neurons in the rostral ventral medulla in vitro: J Neurophysiol, v. 73, p. 933-44.

Richerson, G. B., 2004, Serotonergic neurons as carbon dioxide sensors that maintain pH homeostasis: Nat Rev Neurosci, v. 5, p. 449-61.

Rogers, A. B., K. S. Cormier, and J. G. Fox, 2006, Thiol-reactive compounds prevent nonspecific antibody binding in immunohistochemistry: Lab Invest, v. 86, p. 526-33.

Ruszaj, A., L.-H. K. ., and K. Scrogin., 2006, Hindbrain serotonergic neurons facilitate recovery from hypotensive hemorrhage.: FASEB, v. 20, p. A773.

Sabharwal, R., E. J. Johns, and S. Egginton, 2004, The influence of acute hypothermia on renal function of anaesthetized euthermic and acclimatized rats: Exp Physiol, v. 89, p. 455-63.

Sander-Jensen, K., J. Mehlsen, N. H. Secher, F. W. Bach, P. Bie, J. Giese, T. W. Schwartz, J. Trap-Jensen, and J. Warberg, 1987, Progressive central hypovolaemia in man--resulting in a vasovagal syncope? Haemodynamic and endocrine variables during venous tourniquets of the thighs: Clin Physiol, v. 7, p. 231-42.

Saper, C. B., T. C. Chou, and T. E. Scammell, 2001, The sleep switch: hypothalamic control of sleep and wakefulness: Trends Neurosci, v. 24, p. 726-31.

Sauaia, A., F. A. Moore, E. E. Moore, K. S. Moser, R. Brennan, R. A. Read, and P. T. Pons, 1995, Epidemiology of trauma deaths: a reassessment: J Trauma, v. 38, p. 185-93.

Sawchenko, P. E., L. W. Swanson, R. Grzanna, P. R. Howe, S. R. Bloom, and J. M. Polak, 1985, Colocalization of neuropeptide Y immunoreactivity in brainstem catecholaminergic neurons that project to the paraventricular nucleus of the hypothalamus: J Comp Neurol, v. 241, p. 138-53.

Schadt, J. C., and J. Ludbrook, 1991, Hemodynamic and neurohumoral responses to acute hypovolemia in conscious mammals: Am J Physiol, v. 260, p. H305-18.

Schaffar, N., J. P. Kessler, O. Bosler, and A. Jean, 1988, Central serotonergic projections to the nucleus tractus solitarii: evidence from a double labeling study in the rat: Neuroscience, v. 26, p. 951-8.

Schertel, E. R., J. D. Brourman, S. M. Kling, L. M. Schmall, T. A. Tobias, and P. D. Myerowitz, 1994, Vagal innervation influences the whole body oxygen consumption-delivery relationship in the dog: Shock, v. 2, p. 127-32.

Schreihofer, A. M., E. M. Stricker, and A. F. Sved, 1994, Chronic nucleus tractus solitarius lesions do not prevent hypovolemia-induced vasopressin secretion in rats: Am J Physiol, v. 267, p. R965-73.

Scislo, T. J., and D. S. O'Leary, 1998, Differential control of renal vs. adrenal sympathetic nerve activity by NTS A2a and P2x purinoceptors: Am J Physiol, v. 275, p. H2130-9.

Scrogin, K. E., 2003, 5-HT1A receptor agonist 8-OH-DPAT acts in the hindbrain to reverse the sympatholytic response to severe hemorrhage: Am J Physiol Regul Integr Comp Physiol, v. 284, p. R782-91.

Scrogin, K. E., A. K. Johnson, and V. L. Brooks, 2000, Methysergide delays the decompensatory responses to severe hemorrhage by activating 5-HT(1A) receptors: Am J Physiol Regul Integr Comp Physiol, v. 279, p. R1776-86.

Sekizawa, S., J. P. Joad, K. E. Pinkerton, and A. C. Bonham, 2010, Secondhand tobacco smoke exposure differentially alters nucleus tractus solitarius neurons at two different ages in developing non-human primates: Toxicol Appl Pharmacol, v. 242, p. 199-208.

Sevoz, C., J. C. Callera, B. H. Machado, M. Hamon, and R. Laguzzi, 1997, Role of serotonin3 receptors in the nucleus tractus solitarii on the carotid chemoreflex: Am J Physiol, v. 272, p. H1250-9.

Seyde, W. C., L. McGowan, N. Lund, B. Duling, and D. E. Longnecker, 1985, Effects of anesthetics on regional hemodynamics in normovolemic and hemorrhaged rats: Am J Physiol, v. 249, p. H164-73.

Sprouse, J. S., and G. K. Aghajanian, 1987, Electrophysiological responses of serotoninergic dorsal raphe neurons to 5-HT1A and 5-HT1B agonists: Synapse, v. 1, p. 3-9.

Stahl, S. M., 1998, Mechanism of action of serotonin selective reuptake inhibitors. Serotonin receptors and pathways mediate therapeutic effects and side effects: J Affect Disord, v. 51, p. 215-35.

Steinbusch, H. W., 1981, Distribution of serotonin-immunoreactivity in the central nervous system of the rat-cell bodies and terminals: Neuroscience, v. 6, p. 557-618.

Stern, S. A., 2001, Low-volume fluid resuscitation for presumed hemorrhagic shock: helpful or harmful?: Curr Opin Crit Care, v. 7, p. 422-30.

Steward, L. J., K. E. West, G. J. Kilpatrick, and N. M. Barnes, 1993, Labelling of 5-HT3 receptor recognition sites in the rat brain using the agonist radioligand [3H]meta-chlorophenylbiguanide: Eur J Pharmacol, v. 243, p. 13-8.

Stocker, S. D., E. M. Stricker, and A. F. Sved, 2001, Acute hypertension inhibits thirst stimulated by ANG II, hyperosmolality, or hypovolemia in rats: Am J Physiol Regul Integr Comp Physiol, v. 280, p. R214-24.

Strittmatter, R. R., and J. C. Schadt, 2007, Sex differences in the respiratory response to hemorrhage in the conscious, New Zealand white rabbit: Am J Physiol Regul Integr Comp Physiol, v. 292, p. R1963-9.

Struzik, L., J. Duffin, M. Vermani, K. Hegadoren, and M. A. Katzman, 2002, Effects of tryptophan depletion on central and peripheral chemoreflexes in man: Respir Physiol Neurobiol, v. 133, p. 183-95.

Tabata, M., H. Kurosawa, Y. Kikuchi, W. Hida, H. Ogawa, S. Okabe, Y. Tun, T. Hattori, and K. Shirato, 2001, Role of GABA within the nucleus tractus solitarii in the hypoxic ventilatory decline of awake rats: Am J Physiol Regul Integr Comp Physiol, v. 281, p. R1411-9.

Tabatabaie, T., R. N. Goyal, C. L. Blank, and G. Dryhurst, 1993, Further insights into the molecular mechanisms of action of the serotonergic neurotoxin 5,7-dihydroxytryptamine: J Med Chem, v. 36, p. 229-36.

Takakura, A. C., T. S. Moreira, E. Colombari, G. H. West, R. L. Stornetta, and P. G. Guyenet, 2006, Peripheral chemoreceptor inputs to retrotrapezoid nucleus (RTN) CO2-sensitive neurons in rats: J Physiol, v. 572, p. 503-23.

Takasu, A., S. W. Stezoski, J. Stezoski, P. Safar, and S. A. Tisherman, 2000, Mild or moderate hypothermia, but not increased oxygen breathing, increases long-term survival after uncontrolled hemorrhagic shock in rats: Crit Care Med, v. 28, p. 2465-74.

Takasu, A., Y. Yanagawa, T. Sakamoto, and Y. Okada, 2005, Therapeutic hypothermia limited to the resuscitation period does not prolong survival after severe hemorrhagic shock in rats: Resuscitation, v. 67, p. 119-26.

Taylor, N. C., A. Li, and E. E. Nattie, 2005, Medullary serotonergic neurones modulate the ventilatory response to hypercapnia, but not hypoxia in conscious rats: J Physiol, v. 566, p. 543-57.

Teng, Y. D., M. Bingaman, A. M. Taveira-DaSilva, P. P. Pace, R. A. Gillis, and J. R. Wrathall, 2003, Serotonin 1A receptor agonists reverse respiratory abnormalities in spinal cord-injured rats: J Neurosci, v. 23, p. 4182-9.

Thor, K. B., A. Blitz-Siebert, and C. J. Helke, 1992a, Autoradiographic localization of 5HT1 binding sites in autonomic areas of the rat dorsomedial medulla oblongata: Synapse, v. 10, p. 217-27.

Thor, K. B., A. Blitz-Siebert, and C. J. Helke, 1992b, Autoradiographic localization of 5HT1 binding sites in the medulla oblongata of the rat: Synapse, v. 10, p. 185-205.

Thor, K. B., and C. J. Helke, 1987, Serotonin- and substance P-containing projections to the nucleus tractus solitarii of the rat: J Comp Neurol, v. 265, p. 275-93.

Thor, K. B., and C. J. Helke, 1989, Serotonin and substance P colocalization in medullary projections to the nucleus tractus solitarius: dual-colour immunohistochemistry combined with retrograde tracing: J Chem Neuroanat, v. 2, p. 139-48.

Thor, K. B., K. M. Hill, C. Harrod, and C. J. Helke, 1988, Immunohistochemical and biochemical analysis of serotonin and substance P colocalization in the nucleus tractus solitarii and associated afferent ganglia of the rat: Synapse, v. 2, p. 225-31.

Tiniakov, R., P. Osei-Owusu, and K. E. Scrogin, 2007, The 5-hydroxytryptamine1A receptor agonist, (+)-8-hydroxy-2-(di-n-propylamino)-tetralin, increases cardiac output and renal perfusion in rats subjected to hypovolemic shock: J Pharmacol Exp Ther, v. 320, p. 811-8.

Tiniakov, R., and K. E. Scrogin, 2006, The serotonin 5-Hydroxytryptaphan1A receptor agonist, (+)8-hydroxy-2-(di-n-propylamino)-tetralin, stimulates sympathetic-dependent increases in venous tone during hypovolemic shock: J Pharmacol Exp Ther, v. 319, p. 776-82.

Tiniakov, R., and K. E. Scrogin, 2009, The spleen is required for 5-HT1A receptor agonist-mediated increases in mean circulatory filling pressure during hemorrhagic shock in the rat: Am J Physiol Regul Integr Comp Physiol, v. 296, p. R1392-401.

Trulson, M. E., 1985, Simultaneous recording of dorsal raphe unit activity and serotonin release in the striatum using voltammetry in awake, behaving cats: Life Sci, v. 37, p. 2199-204.

Underwood, M. D., M. J. Bakalian, V. Arango, and J. J. Mann, 1995, Effect of chemical stimulation of the dorsal raphe nucleus on cerebral blood flow in rat: Neurosci Lett, v. 199, p. 228-30.

Undesser, K. P., E. M. Hasser, J. R. Haywood, A. K. Johnson, and V. S. Bishop, 1985, Interactions of vasopressin with the area postrema in arterial baroreflex function in conscious rabbits: Circ Res, v. 56, p. 410-7.

van de Kar, L. D., and S. A. Lorens, 1979, Differential serotonergic innervation of individual hypothalamic nuclei and other forebrain regions by the dorsal and median midbrain raphe nuclei: Brain Res, v. 162, p. 45-54.

Van Lieshout, J. J., W. Wieling, J. M. Karemaker, and N. H. Secher, 2003, Syncope, cerebral perfusion, and oxygenation: J Appl Physiol, v. 94, p. 833-48.

Voss, M. D., D. De Castro, J. Lipski, P. M. Pilowsky, and C. Jiang, 1990, Serotonin immunoreactive boutons form close appositions with respiratory neurons of the dorsal respiratory group in the cat: J Comp Neurol, v. 295, p. 208-18.

Wang, W., J. H. Pizzonia, and G. B. Richerson, 1998, Chemosensitivity of rat medullary raphe neurones in primary tissue culture: J Physiol, v. 511 (Pt 2), p. 433-50.

Wang, W., J. K. Tiwari, S. R. Bradley, R. V. Zaykin, and G. B. Richerson, 2001, Acidosis-stimulated neurons of the medullary raphe are serotonergic: J Neurophysiol, v. 85, p. 2224-35.

Wang, W. Z., L. Gao, Y. X. Pan, I. H. Zucker, and W. Wang, 2006, Differential effects of cardiac sympathetic afferent stimulation on neurons in the nucleus tractus solitarius: Neurosci Lett, v. 409, p. 146-50.

Wei, E., S. Sigel, H. Loh, and E. L. Way, 1975, Thyrotrophin-releasing hormone and shaking behaviour in rat: Nature, v. 253, p. 739-40.

Weissheimer, K. V., and B. H. Machado, 2007, Inhibitory modulation of chemoreflex bradycardia by stimulation of the nucleus raphe obscurus is mediated by 5-HT3 receptors in the NTS of awake rats: Auton Neurosci, v. 132, p. 27-36.

WISQARS, 2009, Leading Causes of Death Report 1999-2006: National Center for Injury Prevention and Control.

Wladis, A., R. G. Hahn, H. Hjelmqvist, B. Brismar, and B. T. Kjellstrom, 2001, Acute hemodynamic effects of induced hypothermia in hemorrhagic shock: an experimental study in the pig: Shock, v. 15, p. 60-4.

Wolf, W. A., D. M. Kuhn, and W. Lovenberg, 1981, Blood pressure responses to local application of serotonergic agents in the nucleus tractus solitarii: Eur J Pharmacol, v. 69, p. 291-9.

Zhan, W. Z., H. H. Ellenberger, and J. L. Feldman, 1989, Monoaminergic and GABAergic terminations in phrenic nucleus of rat identified by immunohistochemical labeling: Neuroscience, v. 31, p. 105-13.

Zhang, C., L. G. Bonagamba, and B. H. Machado, 2000, Blockade of NK-1 receptors in the lateral commissural nucleus tractus solitarii of awake rats had no effect on the cardiovascular responses to chemoreflex activation: Braz J Med Biol Res, v. 33, p. 1379-85.

Zigmond, M. J., and E. M. Stricker, 1973, Recovery of feeding and drinking by rats after intraventricular 6-hydroxydopamine or lateral hypothalamic lesions: Science, v. 182, p. 717-20.

Zukowska-grojec, Z., and C. Walestedt, 1993, Origin and action of neuropeptide Y in the cardiovascular system. : The Biology of Neuropeptide Y and Related Peptides, p. 315-388.

VITA

The author, Ling-Hsuan Kung (Theresa), was born on November 8, 1980 in Tainan, Taiwan to Wen-tai Mi and Feng-I Kung. At the age of 15 she relocated to the Philippines. Consequently, she completed of her senior high education in 1999 at Poveda Learning Centre in Manila, Philippines. She entered the University of Colorado at Denver. Theresa graduated with an honor Summa Cum Laude Bachelor of Science degree in Psychology in December of 2003.

In July of 2004, Theresa began her graduate studies in the Neuroscience program in Loyola University of Chicago. In October of 2005, she joined the laboratory of Dr. Karie Scrogin. Her dissertation research focused on the mechanism by which that hindbrain serotonin neurons activate 5-HT_{1A} receptors in the nucleus tractus solitarius (NTS) to modulate sympathetic and ventilatory responses during recovery of hypotensive hemorrhage for which she was awarded a pre-doctoral fellowship from the American Heart Association, Mid-West Affiliate. During her 5 years in Scrogin's Lab, Theresa presented her research at multiple Experimental Biology meetings (2006-2007 and 2009) and at the international symposium on the autonomic nervous system meeting in Hawaii (2008). She also had the opportunity to teach many rotation graduate students, summer college students and high school students.

Theresa met her husband, Fei Han, in Loyola and got married in November 2007. This year April, they had their baby boy, Nathan. Currently, Theresa is looking for a post-doc position to enable her to continue her Neuroscience research career.